

Homogeneous versus Heterogeneous Self-Exchange Electron Transfer Reactions of Metal Complexes: Insights from Pressure Effects

Thomas W. Swaddle*

Department of Chemistry, University of Calgary, Calgary, Alberta T2N 1N4, Canada

Received September 1, 2004

Contents

1. Introduction	2573
2. Experimental Approaches to Electrode Kinetics	2574
2.1. Butler–Volmer (Tafel) Plots	2574
2.2. Forced Convection Methods	2575
2.3. Cyclic Voltammetry	2576
2.4. Alternating Current Voltammetry (AC Polarography)	2576
2.5. Ultramicroelectrodes	2577
2.6. Special Constraints in Experimental Electrode Kinetics	2578
2.7. Electrode Kinetics at Variable Pressure and Temperature	2579
3. Theory and Observation in Electron Transfer Reactions	2581
3.1. Free Energies of Activation	2581
3.2. Preexponential Factors	2583
3.3. Nonadiabaticity	2583
3.4. Solvent Dynamics	2584
3.5. Reactant Size and Shape	2586
3.6. Electrolyte Effects	2587
3.7. Specific Counterion Effects	2588
3.8. Metal Aqua Ions in Aqueous Solution	2591
3.9. Nonaqueous Systems	2592
4. Insights from Pressure Effects	2593
4.1. Pressure Effects on Homogeneous Electron Transfer Kinetics	2593
4.2. “Well-Behaved” Homogeneous Self-Exchange Reactions	2594
4.3. “Anomalous” Homogeneous Self-Exchange Reactions	2596
4.4. Pressure Effects on the Kinetics of Electrode Reactions: General Remarks	2598
4.5. Pressure Effects on Electrode Kinetics in Aqueous Systems	2599
4.6. Pressure Effects on Electrode Kinetics in Nonaqueous Solvents	2602
5. Summary	2604
6. Acknowledgment	2605
7. References	2605

1. Introduction

Although the kinetics and mechanisms of electron transfer reactions in homogeneous solution have been

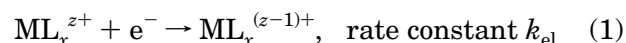
* Telephone: (403) 220-5358. Fax: (403) 289-9488. E-mail: swaddle@ucalgary.ca.



Tom Swaddle was born in Newcastle upon Tyne, U.K., and holds degrees from University College London (B.Sc. (Special, Chemistry), 1958) and the University of Leicester (Ph.D. in organo-Group 14 substitution kinetics with Colin Eaborn). After postdoctoral research with John P. Hunt (Washington State University) and Edward L. King (Universities of Wisconsin and Colorado), he joined the Chemistry Department of the University of Alberta, Calgary (now the University of Calgary), as an Assistant Professor in 1964, retiring in 2002. He now continues his research in mechanistic inorganic chemistry there as Professor Emeritus and Faculty Professor. He is a Fellow of the AAAS, the Chemical Institute of Canada, and the Royal Society of Chemistry and has been a JSPS Senior Fellow at the Tokyo Institute of Technology, a Wilsmore Fellow at the University of Melbourne, and an Alexander von Humboldt Research Award holder at the University of Erlangen-Nürnberg.

intensively studied by the inorganic reaction mechanisms community since 1945, corresponding studies of electrode reaction kinetics have largely remained the preserve of electrochemists. Thus, although electrode reaction kinetics receive some consideration in the books by Cannon¹ and Astruc^{2a} on electron transfer mechanisms, they are not mentioned at all in Lappin's otherwise excellent monograph on redox reactions^{2b} and are referred to only briefly in recent texts on redox and other inorganic reaction mechanisms.³ The present article represents an attempt to bridge the gap between the inorganic mechanistic and electrochemical traditions.

An underlying theme of this article is a simple conjecture: namely, that in the ideal case, electron transfer between a metal complex in solution and a solid electrode



may be regarded as mechanistically equivalent to the

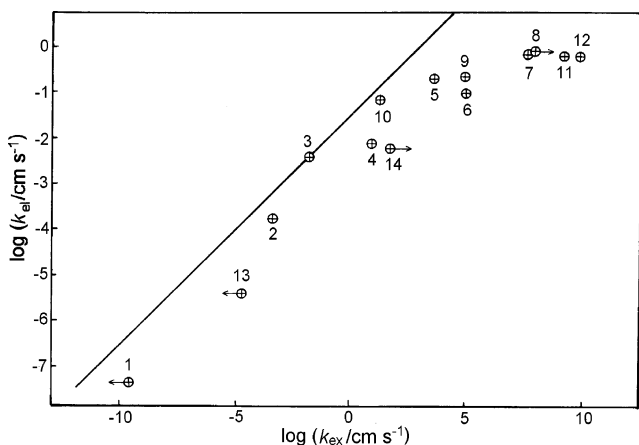
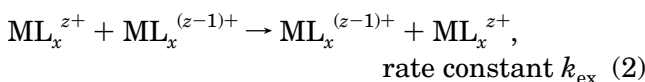


Figure 1. Log–log correlation of k_{el} with k_{ex} for some aqueous couples presented by Cannon:¹ (1) $\text{Co}(\text{NH}_3)_6^{3+/2+}$; (2) $\text{Eu}^{3+/2+}$; (3) $\text{V}^{3+/2+}$; (4) $\text{Fe}^{3+/2+}$; (5) $\text{MnO}_4^{2-/-}$; (6, 9) $\text{Fe}(\text{CN})_6^{3-/4-}$; (7) $\text{Fe}(\text{bpy})(\text{CN})_4^{-/2-}$; (8) $\text{Fe}(\text{bpy})_3^{3+/2+}$; (10) $\text{Co}(\text{phen})_3^{3+/2+}$; (11) $\text{Cr}(\text{bpy})_3^{2+/+}$; (12) perylene; (13) $\text{Cr}^{3+/2+}$; (14) $\text{UO}_2^{2+/+}$. Reproduced with permission from ref 1, p 221; Copyright 1980 Roderick D. Cannon.

corresponding self-exchange reaction in homogeneous solution



in which one of the exchanging partners is “virtual”, the electrode acting simply as a source or sink for electrons. It is implicit in this conjecture that reaction 2 is of the outer-sphere type (in which there is no formation of a M–L–M bridge to facilitate electron transfer, all M–L bonds remaining intact throughout the reaction)^{1–3} and that the electroactive species in reaction 1 is not specifically adsorbed on the electrode. Electrochemists often refer to the latter type of electrode process as “outer-sphere” also; the meaning differs from that traditionally used for homogeneous reactions, but it is convenient to say that this review is concerned with a comparison of homogeneous and heterogeneous outer-sphere electron transfer reactions from the standpoint of an inorganic chemist. In 1975, Aoyagui et al.⁴ published a correlation of $\log k_{el}$ with $\log k_{ex}$, updated in 1980 by Cannon¹ (Figure 1; see also Weaver⁵), which, as explained in section 3.1, might naïvely be expected to be linear with slope ξ of either $1/2$ or 1, depending on assumptions made regarding the electron transfer distance, σ . The fit of the data in Figure 1 suggests $\xi = 1/2$ but is not entirely convincing (k_{el} levels off just below 1 cm s^{-1} , and some k_{ex} values are given only as upper or lower limits), and much of the discussion below is concerned with the question of why this is so and whether such an approach could ever succeed quantitatively. On the other hand, it will be argued that the *pressure dependences* of k_{el} and k_{ex} can be uniquely informative in this context.

Theoretical arguments for the existence of a relationship between k_{el} and k_{ex} have been put forward by Hush, Marcus, and others,^{6–14} beginning as long ago as 1958, and the extensive experimental testing of these proposals by the late Michael J. Weaver and co-workers forms a prominent feature of this article.

In one of his last publications,¹⁵ Weaver stated that the relationship between the kinetics of electron transfer in homogeneous solution and at a solid electrode “invites a close interplay of endeavor between these two research disciplines”, in particular, because the comparison may provide a probe of the sensitivity of electron transfer kinetics to the environment of the reactants. In other words, whether or not a simple relationship actually exists between k_{el} and k_{ex} , important insights can be gained by seeking it. It is better to travel than to arrive.

The lack of interest in electrode reaction kinetics among inorganic solution chemists undoubtedly reflects the idiosyncratic experimental challenges and interpretational difficulties associated with such processes. In particular, the apparent values of the rate constants of electrode reactions often depend on the manner in which the measurements are made. Outlines of the more popular methods of measuring electrode reaction rates (section 2) and of the basic theoretical background (section 3) are therefore necessary parts of this review. Consideration will be limited to cases in which reaction 1 can be observed as a simple one-electron **E** process (i.e., as a single electrode reaction, independently of coupled chemical reactions **C** or further electrode processes **E'**—more complex mechanisms are termed **EC**, **ECE'**, etc., according to the number of successive electrochemical and chemical steps^{2a,3b,16–21}). Photoelectrochemical processes and ones in which the electroactive species are strongly adsorbed on the electrode are not directly relevant to the theme of this article and are also excluded.

2. Experimental Approaches to Electrode Kinetics

The general principles of electrochemistry and electrochemical measurements have been well covered in a wealth of recent texts^{16–31} and need not be discussed here. The techniques of electron transfer kinetics in homogeneous solution have also been amply discussed in standard texts.³ Electrode kinetics, however, although the subject of several monographs^{18,32–37} and review articles,^{38–40} as well as of detailed discussion in some comprehensive sourcebooks,^{16,19,31} present peculiar problems, both theoretical and experimental. A key point is that electrode reaction rate constants are potential-dependent; the quantity of interest in the context of this article is the *standard rate constant*, k_{el}^0 , which is the rate constant at the standard equilibrium potential, E^0 , as explained in the next section.

2.1. Butler–Volmer (Tafel) Plots

The rate R of an electrode reaction is given by $i/(nFA)$, where i is the current, n is the number of electrons transferred per mole in the reaction (for all cases considered here, $n = 1$), F is the Faraday constant ($96485 \text{ A s mol}^{-1}$), and A is the effective area of the electrode. The rate, R_f , of a reaction in the forward direction (conventionally a reduction, i.e., cathodic reaction) is given by

$$R_f = i_f/(nFA) = k_f C_O \quad (3)$$

where k_f is the forward rate constant and C_O is the concentration of the oxidized form O (ML_x^{z+}) of the electroactive species at the electrode surface. For the back (anodic) reaction (oxidation of the reduced form $R = ML_x^{(z-1)+}$), the corresponding expression is

$$R_b = i_b/(nFA) = k_b C_R \quad (4)$$

and the net current, I , at a particular applied potential, E , is $i_f - i_b$. At the standard equilibrium potential E^0 for the electrode reaction, $i_f = i_b = i_0$, the *exchange current*, and also $C_O = C_R (= C)$, so $k_f = k_b = k_{el}^0$, the standard rate constant for the reaction (conventionally reported for 25.0 °C unless otherwise stated). Thus, for these particular conditions,

$$k_{el}^0 = i_0/(FAC) \quad (5)$$

so our experimental objective is to determine i_0 . It should be noted that, if the units of C and A are mol cm^{-3} and cm^2 , respectively, then the units of k_{el}^0 will be cm s^{-1} , whereas those of the corresponding homogeneous reaction rate constant, k_{ex} , are usually $\text{L mol}^{-1} \text{s}^{-1}$; thus, the two rate constants cannot be directly compared without introducing some assumptions, as discussed in section 3.2.

At any potential E other than E^0 (often expressed as an *overpotential*, $E - E^0$), the Butler–Volmer model gives the current as

$$i = i_0 [\exp(-\alpha F(E - E^0)/(RT)) - \exp((1 - \alpha)F(E - E^0)/(RT))] \quad (6)$$

where α is the *transfer coefficient*, a factor representing the degree of symmetry between the potential responses of the forward and back reactions; for the fully symmetrical case, $\alpha = 0.5$, as is frequently observed (± 0.1). The two exponential terms represent the contributions of the forward and back reactions to the observed current i . At strongly negative (reducing) overpotentials, the first term dominates, and a plot of $\ln i$ against E (a *Tafel plot*) is a straight line of slope $-\alpha F/(RT)$. Conversely, at strongly positive overpotentials, the Tafel plot has slope $(1 - \alpha)F/(RT)$. Extrapolation of these linear segments gives an intersection at E^0 and $\ln i_0$ (Figure 2). Thus, Tafel extrapolations offer one means of determining the standard rate constant k_{el}^0 , but the procedure tends to be cumbersome, and the extrapolation is prone to rather large errors (the current scale being logarithmic). Furthermore, both the oxidized and reduced forms of the electrochemically active compound need to be stable over extended periods in the solution to complete both arms of the Tafel plot; for the cyclic voltammetric (CV) and alternating current voltammetric (ACV) techniques described below, only one form is needed in the bulk solution. Finally, high overpotentials should be avoided because they may cause nonlinearity in the Tafel plots⁴¹ (inconstancy of α) in accordance with the Gerischer–Gurney–Marcus theories discussed by Matthews.^{42,43} Matthews⁴² notes that this phenomenon could preclude observation in electrode reactions of the Marcus

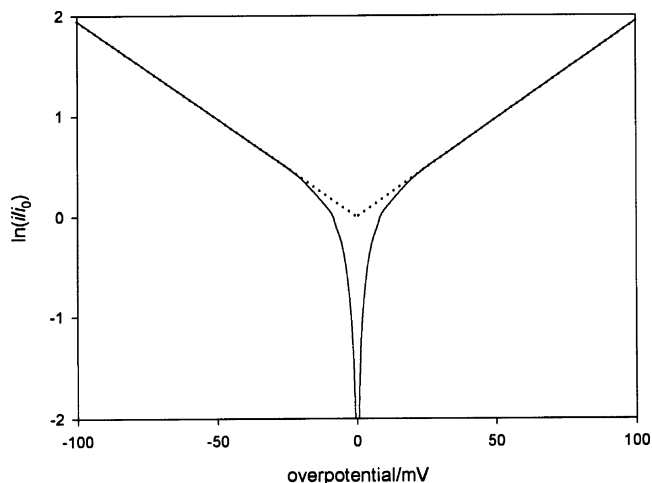


Figure 2. Generalized logarithmic Butler–Volmer plot for $\alpha = 0.50$ at 25 °C: solid curves, Butler–Volmer equation; dotted lines, Tafel extrapolation.

“inverted region” (in which rate constants for very fast electron transfer reactions in homogeneous solution may be observed to *decrease* rather than increase with increasing driving force—see, e.g., Mines et al.⁴⁴) because α becomes small at high overpotentials. Actually, the absence of a Marcus inverted region in reactions occurring at a metallic electrode reflects the existence of a continuum of electronic states on the metal, whereas homogeneous (bimolecular) electron transfer reactions involve single electronic states; thus, the nonlinearity of a Tafel plot at high overpotentials is the heterogeneous counterpart of the Marcus inverted region seen in some homogeneous reactions.

The standard conditions under which E^0 and k_{el}^0 are defined include activity coefficients of unity, implying extrapolation of the measurements to ionic strength $I = 0$ ($I = \sum_i c_i z_i^2$, where c_i and z_i are, respectively, the concentration and charge number of ions of the i th kind). In practice, electrochemical measurements must be made at nonzero values of I that may be quite high, especially where there is a need to work with an inert supporting electrolyte, and extrapolation to $I = 0$ is usually impractical. Accordingly, in this article, the equilibrium potential corresponding to E^0 , but at the prevailing I , will be represented by E^0' , and the symbol k_{el} will be used for the corresponding rate constant.

2.2. Forced Convection Methods

Equations 5 and 6 incorporate a tacit assumption that the concentrations of electroactive species at the electrode surface are the same as those in bulk solution. This implies either that the current drawn is kept very low or that the solution near the electrode surface is thoroughly stirred; otherwise, depletion of electroactive solute near the electrode surface creates a diffusion layer that increases in effective thickness δ with time, and the rate of diffusion of O or R across this layer will affect i . This phenomenon can be controlled by resorting to forced convection methods. One widely used forced convection technique uses a rotating disk electrode (RDE) or rotating ring-disk electrode (RRDE), which expels

solution outward in the plane of the rapidly spinning disk and draws fresh solution in parallel to the axis of rotation. In this way, a time-independent diffusion layer can be quickly created, and δ can be controlled by choice of the constant angular rotation speed ω of the disk electrode and evaluated with knowledge of the diffusion coefficient D_O (or D_R) of the electroactive species O (or R) and the kinematic viscosity η_K of the solvent:

$$\delta = 1.62D_O^{1/3}\omega^{-1/2}\eta_K^{1/6} \quad (7)$$

The diffusion current, i_d , is then given by $nFAC_O D_O/\delta$, and the current i_{KL} in absence of mass-transfer effects, and hence k_f , is obtainable from the Koutecký–Levich equation:

$$i_{KL} = (i^{-1} - i_d^{-1})^{-1} = k_f FAC_O \quad (8)$$

The rate of transport of O or R to the RDE is typically greater than is possible through natural diffusion. Additional advantages of the RDE method are that high precision measurements are possible and that the double-layer charging current (see below) can be disregarded once steady-state operation is achieved. From the author's standpoint, however, forced-convection methods such as RDE are unattractive because they are not easily adapted to high-pressure electrochemical measurements, which can provide significant mechanistic information that is not otherwise obtainable (sections 2.7 and 4).^{45–47}

2.3. Cyclic Voltammetry

The popularity of cyclic voltammetry,¹⁷ particularly among inorganic chemists,^{2a,21} derives primarily from its power to identify redox processes easily and to define them in terms of their relative energies ($E^{0'}$ values). In essence, the potential E applied to a working electrode, relative to a reference electrode such as Ag/AgCl/KCl(aq), is swept linearly at a constant scan rate ν , and the current is recorded; at a chosen potential, the sweep is reversed, and E is returned to its initial value. A typical cyclic voltammogram (CV) is shown in Figure 3. The half-wave potential, $E_{1/2}$, obtained by averaging the peak potentials E_{pa} and E_{pc} of the anodic (forward, in Figure 3) and cathodic (reverse) sweeps of a given redox step can be identified with $E^{0'}$ if $\alpha \approx 0.5$. In favorable cases, kinetic information can also be extracted from the peak separation, $\Delta E_p = E_{pa} - E_{pc}$. Peak currents I_a and I_c should be equal for $\alpha = 0.5$ and allow calculation of the mean reactant diffusion coefficient D . For those **E** processes that are very fast relative to diffusion of O or R across the diffusion layer (referred to as *fully reversible* reactions), $\Delta E_p = 58$ – 59 mV, but if the rate of reaction 1 is slower, $\Delta E_p > 60$ mV (*quasi-reversible reactions*), and the rate constant k_{el} can in be obtained by measuring ΔE_p over a range of scan rates, ν (Nicholson's method^{48,49}):

$$k_{el} = \psi(\pi D_O F \nu / (RT))^{1/2} (D_R / D_O)^{\omega/2} \quad (9)$$

Values of the dimensionless charge transfer parameter ψ for various ΔE_p (in mV) at 25 °C with $\alpha = 0.5$

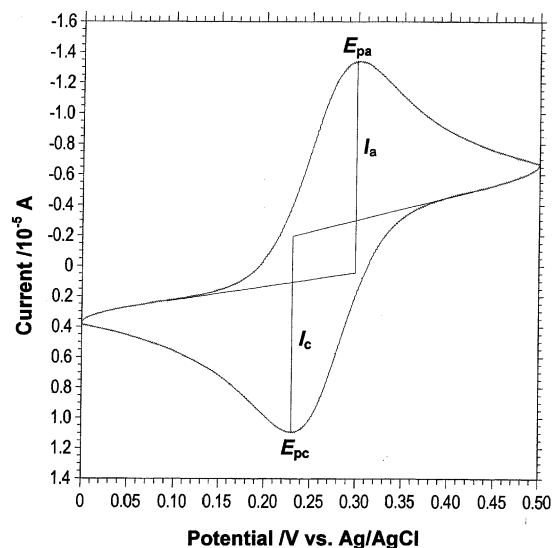


Figure 3. Cyclic voltammogram of $\text{Fe}(\text{CN})_6^{3-/4-}$ ($[\text{Fe}] = 0.004 \text{ mol L}^{-1}$) in aqueous KCl (1.0 mol L^{-1}) at 25 °C at a Pt wire electrode (0.5 mm diameter) relative to Ag/AgCl, taken by A. Czap (University of Calgary) with a CH Instruments model CHI650B electrochemical work station. Scan rate = 100 mV s^{-1} .

are tabulated by Nicholson⁴⁸ and can be represented adequately by eq 10.

$$\ln \psi = 3.69 - 1.16 \ln(\Delta E_p - 59) \quad (10)$$

Corrections may have to be applied to a CV for the distorting effect of the *uncompensated resistance*, R_u , of the electrochemical cell. For example, E_{pa} will be shifted by an amount $I_a R_u$ (Figure 3), but since I_a and R_u are typically on the order of a few microamperes and 100Ω , respectively, for conventional cells containing aqueous solutions with supporting electrolyte concentrations of a few tenths molar, the correction will be around 1 mV or less, which is within the usual experimental uncertainty. As for k_{el} , peak separation measurements will give erroneous results if R_u is significant, which is particularly the case for non-aqueous solvents. Modern potentiostats usually offer the option of correcting electronically for R_u while the measurements are being made, but the operator should be wary of possible over- or undercorrections. Furthermore, corrections for double-layer charging currents become necessary at high scan rates.

In the author's experience, ΔE_p measurements are useful only over a very limited range; for ΔE_p close to 59 mV, the percentage error in ψ becomes large, while at ΔE_p of 100 mV or more the CV peaks become so broad that the peak potentials become difficult to measure accurately (especially since the baseline is often sloping, as in Figure 3).

2.4. Alternating Current Voltammetry (AC Polarography)

If an AC signal of frequency f is superimposed upon a slowly ramped DC potential and the AC currents in-phase and 90° out-of-phase (quadrature) with the applied AC potential are recorded, it is often possible to extract quite precise rate constants from the resulting alternating current voltammogram (ACV).⁵⁰

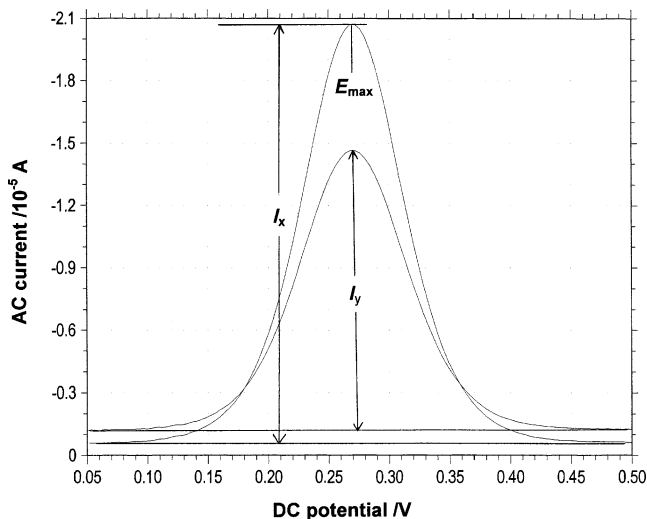


Figure 4. Alternating current voltammogram of $\text{Fe}(\text{CN})_6^{3-/4-}$: operator, conditions and equipment as for Figure 3. Imposed AC frequency $f = 25$ Hz; scan rate = 4 mV s^{-1} .

The amplitude of the impressed AC voltage is customarily kept small (around 5 mV), but important information can be obtained using larger amplitudes.^{51,52} Typical in-phase and quadrature ACVs are shown in Figure 4. The ACV technique has been less widely used in electrochemical kinetic studies than DC methods, no doubt because the mathematical complexity is greater, requiring vectorial analysis of the maximum in-phase and quadrature currents (I_x and I_y , respectively, at a corresponding DC potential E_{max}) with inclusion of corrections for the double-layer charging current and uncompensated resistance R_u . Since the maximum currents correspond to the situation $[\text{O}] = [\text{R}]$, E_{max} can be identified with E^0 and the derived rate constant is truly k_{el} .

The measurement of k_{el} by ACV has proved to be invaluable in high-pressure studies and merits detailed explanation. The mean reactant diffusion coefficient D is first obtained from the averaged peak currents of multiple CV measurements, which also give $E_{1/2}$. Then, the maximum in-phase and quadrature alternating currents of an ACV are obtained over a range of applied frequencies f (typically 15–100 Hz). Correction for the uncompensated resistance R_u can be made electronically during the measurements, but a safer procedure involves determining R_u explicitly from the cell impedance, measured at a high frequency (typically 10 kHz or more) and a potential ~ 300 mV away from $E_{1/2}$, and allowing for it specifically in the calculation of k_{el} . This allows one to see to what extent R_u affects the calculation. This is critically important because, as Weaver has stressed,^{53,54} inadequately corrected R_u effects can masquerade as electrochemical kinetics. An attractive feature of the ACV method is its ability to separate kinetic information from resistive effects even in solvents of very low permittivity such as benzene,⁵⁵ and consequently it has become the method of choice in the author's laboratory for high-pressure electrode kinetics in both aqueous and nonaqueous solutions,^{45–47,56–65} since the pressurizable cell design leads to fairly high R_u . The in-phase and quadrature

background currents, I_{bx} and I_{by} , are measured to obtain the total cell impedance, from which R_u is subtracted to give the double-layer charging impedance, Z_{dl} . This in turn can be used to recalculate I_{bx} and I_{by} (phase shift φ_Z). The faradaic peak currents, I_{fx} and I_{fy} , are obtained by subtracting the recalculated I_{bx} and I_{by} from I_x and I_y , respectively, giving a phase angle φ_f . The transfer coefficient α can be obtained from eq 11

$$E_{\text{max}} = E_{1/2} + (RT/F) \ln [\alpha/(1 - \alpha)] \quad (11)$$

whence, if φ is the corrected phase angle ($= \varphi_Z + \varphi_f$) and ω is the angular AC frequency ($= 2\pi f$),

$$\cot \varphi = 1 + (2D\omega)^{1/2}/(\alpha^{-\alpha}(1 - \alpha)^{-(1-\alpha)}k_{\text{el}}) \quad (12)$$

or, if $\alpha \approx 0.5$,

$$k_{\text{el}} = (D\omega/2)^{1/2}/(\cot \varphi - 1) \quad (13)$$

Accurate values of k_{el} can only be obtained if φ does not approach 0° or 45° too closely; as a practical guideline, this means $1.2 \leq I_x/I_y \leq 5$. Beyond this upper limit, the quadrature peak may depart from the ideal bell shape, usually because the reaction is too slow, R_u is too high, or the imposed AC frequency f is too large. For diffusion-controlled reactions, $\varphi = 45^\circ$.

Second harmonic ACV⁶⁶ offers further insights but has not seen routine use to date, presumably because of the additional complexity.

2.5. Ultramicroelectrodes

For electrode reactions with k_{el} about 1 cm s^{-1} or higher, electrodes of conventional dimensions are inadequate. The dynamic range of techniques such as CV and ACV can, however, be extended upward by use of *ultramicroelectrodes* (UMEs), which are typically disk-type electrode surfaces of diameter on the order of a few micrometers embedded in an insulating sleeve, such as gold wire in glass or glassy carbon fiber in epoxy resin.^{67–73} Besides having the obvious virtue of allowing electrochemical measurements on very small samples (e.g., in biomedical applications), UMEs permit the study of fast electrode reactions, either with ACVs^{55,74} or with CVs at scan rates up to 10^6 V s^{-1} .⁷⁵ High CV scan rates are possible because diffusion rates are very large at UMEs. For the same reason, the time constant for charging the double layer at a UME (which in any event has a very small capacitance) and hence the response time of the electrode to changes on the applied potential are very short (a few nanoseconds), allowing fast faradaic processes to be observed. Also, because the currents are so low (nanoampere range), iR_u corrections are small. Thus, UMEs can be used to measure k_{el} and D in nonaqueous solutions and other poorly conducting media: for example, Crooker and Murray⁷⁶ were able to measure k_{el} and D as low as $4 \times 10^{-12} \text{ cm s}^{-1}$ and $3 \times 10^{-17} \text{ cm}^2 \text{ s}^{-1}$, respectively, for the $\text{Co}^{\text{III/II}}$ couple in some very viscous (i.e., highly resistive) polyether hybrid bipolymer cobalt ionic liquids using microband electrodes. Finally,

because of the diminished importance of Frumkin-type diffuse double layer effects and solution conductance when UMEs are used, it is often possible to dispense with the rather high concentrations of supporting electrolytes that are typical of electrochemistry with conventional electrodes.⁷⁷ The consequences can be dramatic; thus, Lee and Anson⁷⁸ were able to demonstrate a strong “inhibition” of the $\text{Fe}(\text{CN})_6^{3-/4-}$ electrode reaction when UMEs were used in the absence of supporting electrolytes, although in retrospect the effect can be seen not so much as an inhibition as minimization of catalysis by the cations of typical supporting electrolytes (section 3.7).

An obvious disadvantage in the use of UMEs is that measurement of the very low currents requires a highly sensitive potentiostat or preamplifier and the rigorous screening of the electrochemical cell and its connections against stray electromotive forces (EMFs)—for example, from fluorescent lighting. Use of a Faraday cage is essential. The problems of low currents can be ameliorated by use of arrays of 100 or more UMEs in parallel.⁷² In addition, it is imperative to ensure that the seal between the electrode and the surrounding insulator is leakproof; this is a serious concern for high-pressure electrochemical studies, although Stevenson and White⁷⁹ report successful measurements of diffusion coefficients in acetophenone and nitrobenzene using a 12 μm Pt microdisk. The possibilities of high-pressure measurements of k_{el} with UMEs are appealing, but no such studies have been reported to date.

Fast electrode reactions can also be studied by high-speed channel⁸⁰ or microjet⁸¹ electrode techniques, but to date most work in this area has used UME methodology.

2.6. Special Constraints in Experimental Electrode Kinetics

One perennial problem in experimental electrochemical kinetics is that, despite the assumption implicit in the conjecture given at the beginning of this article, the apparent rate constant for reaction 1 can depend substantially on the nature and history of the electrode. Thus, somewhat different k_{el} values may be obtained on Pt, Au, Hg, and glassy carbon surfaces (these being the most popular electrode materials), on a given material depending on its pretreatment,⁸² or on different crystallographic planes of the same single-crystal electrodes; for example, at constant potential, the rate constant and transfer coefficient for the reduction of $\text{Fe}(\text{H}_2\text{O})_6^{3+}$ in aqueous HClO_4 increase in the order $\text{Au}(210) < \text{Au}(110) < \text{Au}(100) < \text{Au}(111)$.⁸³ For the same reaction on $\text{IrO}_2/\text{SnO}_2$ electrodes supported on Ti, De Battisti et al.⁸⁴ found that k_{el} decreased 14-fold on going from 100% IrO_2 to 95% SnO_2 . Similarly, McCreery et al.⁸⁵ found electron transfer rates for 17 aqueous inorganic couples on the basal plane of highly oriented pyrolytic graphite (HOPG) to be 2–7 orders of magnitude slower than those on glassy carbon. Such kinetic differences between different metallic electrodes or crystal planes may reflect the density of electronic states on the electrode near its Fermi level (the

topmost filled electronic energy level in the band structure of the metal, near which electron transfer to and from species in solution will occur, in the absence of overpotentials³⁰). As for pretreatment effects, possible influences on electrode reaction rates include surface roughness, specific adsorption of the reactant(s), and reduction of the available electrode surface area by the presence of adsorbed foreign atoms, ions, or molecules. In the case of the basal plane of HOPG,^{85,86} which is more like a semiconductor than a metal, the densities of edge-plane defects (which can be induced electrochemically or by laser treatment) and carriers influence the measured k_{el} , the “true” value of which may be even less than the measured $10^{-7} \text{ cm s}^{-1}$ for $\text{K}_4[\text{Fe}(\text{CN})_6]$ oxidation (cf. $\sim 0.1 \text{ cm s}^{-1}$ for edge planes). In glassy carbon, the microstructure is not directly comparable to HOPG, and the degree of oxidation of the surface will influence the reaction rate, but even if the oxides are removed by vacuum heat treatment or laser ablation, the observed k_{el} may still be influenced by the relative fractions of basal- and edge-plane-like functions, and these are likely to change in the course of electrode preparation. Similar reservations apply to the use of graphite paste^{87a} or binderless recompressed exfoliated graphite^{87b} electrodes; in the latter case, k_{el} for the oxidation of $\text{K}_4[\text{Fe}(\text{CN})_6]$ in 1 mol L^{-1} KCl was 0.0030 cm s^{-1} at a polished electrode but 0.38 cm s^{-1} at one with 400-grit roughness, although surface effects were less evident for the reactions of tris(1,10-phenanthroline)iron(II) and -cobalt(II) at the same electrodes. Worse yet, the surface properties of activated glassy carbon may change with time over the course of an experiment,⁸⁶ and indeed, this is also true for electrodes of other materials.

Electrode reactions that are fully *adiabatic* (i.e., those for which the electronic coupling of precursor and successor states via the electrode is sufficiently strong that electron transfer occurs on every reactant–electrode encounter in which the necessary reorganizational constraints are met, section 3.3) should be relatively fast and should show no dependence of k_{el} on the nature of the electrode or its surface. This is the case for the aqueous $\text{Ru}(\text{NH}_3)_6^{3+/2+}$ couple, for which a turbulent pipe flow variant of the Tafel procedure for fast reactions gave $k_{\text{el}} = 1.13 \pm 0.11 \text{ cm s}^{-1}$ on Pt, Pd, Au, Cu, and Ag electrodes (Hg gave somewhat lower, inconsistent values).⁸⁸ Essentially the same rate constant was also found for $\text{Ru}(\text{NH}_3)_6^{3+/2+}$ at Pt or Au on which adatoms of Tl have been deposited and on Pt with Pb adatoms.⁸⁹ The implication is that at least some of the variations in k_{el} with electrode properties, found for many other outer-sphere electrode reactions, may reflect varying degrees of nonadiabaticity. This is discussed further in section 3.3.

The formation of surface films on the electrode can affect k_{el} substantially. In particular, Pt has long been known^{13,90} to form films of hydrous PtO_2 at about +1.0 V vs the standard hydrogen electrode (SHE), so CV or ACV potential sweeps should avoid this region if Pt is to be used. Contamination of the electrode surface may occur by introduction of impurities into the electrochemical cell (e.g., leakage of

pressurizing fluid in high-pressure electrochemistry) or through deposition of decomposition products of the redox couple being studied. The aqueous $\text{Fe}(\text{CN})_6^{3-/4-}$ couple,^{87,90–93} for example, deposits strongly adsorbed decomposition products (mainly cyanide) on Pt(111), -(100), and -(110), resulting in surface blocking and slower electron transfer on the latter two surfaces in particular.⁹¹ Such deposits can usually be removed by potential cycling.⁵⁷ The ferricenium–ferrocene ($\text{FeCp}_2^+/\text{FeCp}_2$; $\text{Cp} = \eta^5\text{-C}_5\text{H}_5$) couple in incompletely degassed acetonitrile deposits an organic polymeric film containing hydrous Fe(III) oxide on electrodes through reaction of FeCp_2^+ with residual O_2 , leading to irreproducible electron transfer kinetics.^{61,94–96} Thus, in 1994, Fawcett and Opałło⁹⁶ listed nine reported values of k_{el} for the $\text{FeCp}_2^+/\text{FeCp}_2$ electrode reaction at Pt electrodes in acetonitrile at room temperature ranging from 0.0194 to 220 cm s^{-1} , though several values clustered near the presently accepted value of about 2 cm s^{-1} (a little too fast for techniques using conventional electrodes). Ironically, the $\text{Fe}(\text{CN})_6^{3-/4-}$ and $\text{FeCp}_2^{+/0}$ couples have traditionally been used as reference couples for aqueous and nonaqueous electrochemistry, respectively;^{2a} currently, the recommended alternatives are $\text{Ru}(\text{NH}_3)_6^{3+/2+}$ ⁹⁷ and decamethylferrocene($+/0$),^{64,98} which ordinarily do not form films on electrodes. In general, electrode kinetic measurements require the systematic and thorough cleaning of electrodes using fine alumina abrasives and ultrasound before each experiment.

Adsorbed layers can, however, modify electrode properties in a beneficial way. For example, alkanethiols form particularly stable, well-packed, reproducible, self-assembled monolayers (SAMs) on metallic electrodes such as Au and allow the study of the kinetics of electron transfer reactions that would otherwise be too fast for conventional techniques; in effect, the reaction becomes increasingly nonadiabatic, and electron tunneling phenomena become dominant.^{99,100} Conversely, the distance dependence of k_{el} for nonadiabatic reactions can be determined by selecting appropriate alkyl chain lengths to modulate electron tunneling.¹⁰¹ SAMs can be used to prevent the irreversible adsorption or denaturation of redox proteins during study of their electrode reactions; for example, the electron transfer kinetics of horse heart cytochrome *c* have recently been studied at variable pressure using a gold disk electrode treated with 4,4'-bipyridyl or 4,4'-bipyridyl-bisulfide.¹⁰²

With the exception of some studies using UMES, most electrochemical kinetic experiments have involved the use of rather high (0.1–1.0 mol L⁻¹) concentrations of a nonreacting supporting electrolyte such as an alkali metal salt in water and a quaternary ammonium (R_4N^+) salt in nonaqueous solvents. The role of the supporting electrolyte is to reduce the electrical resistance of the solution (particularly in nonaqueous systems, in which the uncompensated resistance, R_{u} , can be vexingly high) and to minimize the effect of the diffuse electrical double layer on the electrode reaction rate;¹⁰³ otherwise, the apparent k_{el} values need to be corrected (Frumkin correction,

giving $k_{\text{el}(\text{corr})}$ to the potential φ_{OCP} at the outer contact plane (OCP, the effective outer boundary of the inner Helmholtz layer, that is, the monolayer of solvent and solute molecules that coats the electrode surface) as calculated from Gouy–Chapman theory:

$$k_{\text{el}(\text{corr})} = k_{\text{el}(\text{app})} \exp[-(\alpha - z)F\varphi_{\text{OCP}}/(RT)] \quad (14)$$

where z is the charge on the oxidized reactant. High concentrations of supporting electrolytes invalidate Gouy–Chapman and other standard theoretical treatments of the diffuse double layer but fortunately render image forces on ions in the diffuse double layer negligible^{13,30} and allow the work of bringing a reactant ion up to the OCP to be disregarded to a good approximation. With high concentrations of a supporting electrolyte, anion–cation pairing with ionic reactants can be anticipated, and Savéant¹⁰⁴ has examined the likely effects on $E^{0'}$ and k_{el} . Simple electrostatic ion pairing is not expected to have large effects, but the possibility of *specific* influences of any supporting electrolyte on the reaction rate must also be considered. For instance, chloride ions, even in micromolar concentrations, have been reported to accelerate the $\text{Fe}(\text{H}_2\text{O})_6^{3+/2+}$ reaction at a Pt electrode substantially,^{105,106} presumably by promoting an inner-sphere mechanism (see, however, section 2.7). Adsorption of ions of the supporting electrolyte itself (i.e., their incorporation into the inner Helmholtz layer) may also modify the rate of electron transfer. A further effect associated with adsorbed quaternary ammonium salts in nonaqueous media is the possibility of slow desorption of these ions from the electrode, resulting in a dependence of the potential at the outer contact plane on the sweep rate and consequent distortion of voltammograms leading to false rate constants.¹⁰⁷ Finally, a strong, *specific* catalytic effect of cations on the electrode reactions of *anionic* couples is commonly encountered, for example, in cyanometalates such as $\text{Fe}(\text{CN})_6^{3-/4-}$ ^{82,91,108} and polyoxometalates such as $\text{CoW}_{12}\text{O}_{40}^{5-/6-}$,⁶³ this effect, however, is also found in the corresponding homogeneous self-exchange reactions and is not necessarily associated with the electrode as such.¹⁰⁹ This counterion catalysis phenomenon is discussed further in section 3.7.

It would seem, then, that the idiosyncrasies of electrode rate processes make for bleak prospects for a successful correlation of k_{el} with k_{ex} and that the rather loose correlation in Figure 1 may be to some degree fortuitous. It has been found, however, that *pressure effects* on k_{el} and k_{ex} are informative in this context (section 4),^{45–47,56–65} and a brief background on electrochemical measurements at elevated pressures is given next.

2.7. Electrode Kinetics at Variable Pressure and Temperature

There have been relatively few reports of measurements of k_{el} as a function of temperature, and most cover only a limited temperature range with no special practical problems or unusual results. One outstanding exception is the study by Curtiss et al.¹¹⁰

of the $\text{Fe}(\text{H}_2\text{O})_6^{3+/2+}$ reaction at a gold electrode in aqueous HClO_4 (0.5 mol L^{-1}) in a pressurizable flow-through cell. They reported strict Arrhenius behavior ($k_{\text{el}} = Z \exp(-E_a/RT)$) with $E_a = 56.8 \pm 1.5 \text{ kJ mol}^{-1}$ over the remarkably wide range $25\text{--}275 \text{ }^\circ\text{C}$ and confirmed the theoretical expectation that the transfer coefficient α at zero overpotential should be independent of temperature ($\alpha = 0.425 \pm 0.010$ over the entire range). However, besides corrosion, one perennial problem with physicochemical measurements in the hydrothermal regime is that side reactions usually interfere; here, $\text{Fe}(\text{H}_2\text{O})_6^{2+}$ is slowly oxidized by HClO_4 above about $90 \text{ }^\circ\text{C}$ ¹¹⁰ (the balance was restored electrochemically in these experiments), and $\text{Fe}(\text{H}_2\text{O})_6^{3+}$ catalyzes the otherwise negligibly slow decomposition of the acid^{111,112} with formation of chloride ion in either case. It would therefore seem, in view of the consistent Arrhenius behavior of the $\text{Fe}(\text{H}_2\text{O})_6^{3+/2+}$ electrode kinetics, $25\text{--}275 \text{ }^\circ\text{C}$, that the extreme susceptibility of this reaction to catalysis by chloride reported earlier^{105,106} may have been overestimated or misidentified.

The electrochemical kinetics of inorganic couples at variable pressure have been a special concern of the author's laboratory^{45–47,56–65} (see also Dolidze et al.¹⁰²). Typically, a three-electrode cell, machined out of virgin Teflon⁵⁷ or (better, if chemical considerations permit) stainless steel,⁶⁵ is sealed inside a thermostatable steel pressure vessel (pressure ceiling $400\text{--}500 \text{ MPa}$) and pressurized with *clean* insulating fluids such as hexanes or octanes—some leakage of traces of fluid into the cell under pressure because of differential compression of the cell components is almost inevitable, and contamination of the electrode surfaces by fluid-borne impurities is a constant concern. Necessities of the pressurizable cell design, such as free pistons to accommodate compression of the contents of the reference cell compartment and of the complete cell itself, make for cell geometries that are electrochemically less than ideal, so the aforementioned problems of uncompensated resistance (which, in nonaqueous solutions, is markedly pressure-dependent) are particularly pressing. Design problems limit the choice of electrochemical techniques to those involving static systems, notably CV and ACV measurements. Furthermore, because of the slowness of thermal reequilibration after each change of pressure (especially for a Teflon cell), a run of, say, six sets of measurements may take several hours, in which time the drift in the electrochemical response of the assembly may be substantial, whether for chemical, electrical, or mechanical reasons. It is therefore imperative that after a series of measurements at rising pressures (usually $0\text{--}200 \text{ MPa}$), the first low-pressure reading be rechecked to ensure that a drift of readings in time is not misinterpreted as a dependence upon pressure. Nevertheless, with systems that are chemically stable enough over several hours, patience will reward the experimentalist with values of the *volume of activation*, $\Delta V_{\text{el}}^\ddagger$ for the electrode reaction

$$\Delta V_{\text{el}}^\ddagger = -RT(\partial \ln k_{\text{el}}/\partial P)_T \quad (15)$$

which is almost always constant over a 200 MPa

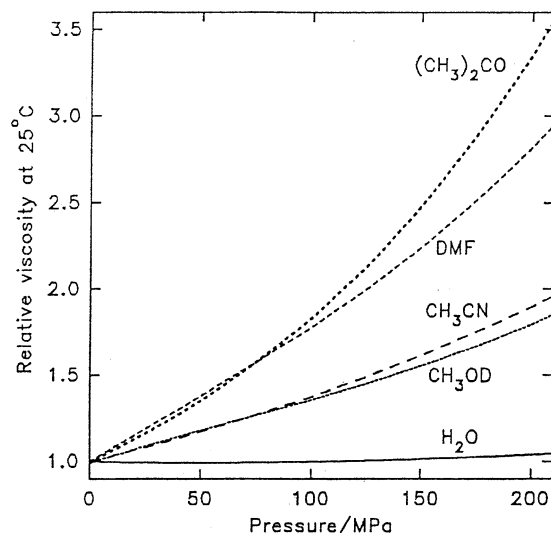


Figure 5. Dependence of viscosity η on applied pressure (relative to atmospheric pressure) for water at $25 \text{ }^\circ\text{C}$ and some common organic solvents at $30 \text{ }^\circ\text{C}$. Reprinted with permission from ref 47, p 175. Copyright 2002 Wiley-VCH.

range (despite theoretical expectations, see section 3), and consequently $\ln k_{\text{el}}$ is a linear function of the applied pressure P within experimental uncertainty:

$$\ln k_{\text{el}} = \ln k_{\text{el}}^{P=0} - P\Delta V_{\text{el}}^\ddagger/(RT) \quad (16)$$

There are two features of high-pressure electrode kinetics that offer special opportunities for mechanistic insights. First, because the nature and properties of solid electrodes and their surfaces are effectively independent of applied pressure in the range considered here ($0\text{--}200 \text{ MPa}$), the electrode-related effects that make comparisons of k_{el} with k_{ex} difficult do not apply to correlations of $\Delta V_{\text{el}}^\ddagger$ with its counterpart for homogeneous self-exchange reactions, $\Delta V_{\text{ex}}^\ddagger$ ($= -RT(\partial \ln k_{\text{ex}}/\partial P)_T$). Second, as noted in section 3.4, it transpires that solution viscosity η can be an important variable in electrode reaction kinetics, and for normal (most nonaqueous) liquids, the dependence of η on applied pressure is close to exponential in the pressure range of interest here ($0\text{--}200 \text{ MPa}$; Figure 5) and may be expressed in terms of a *volume of activation for viscous flow*, $\Delta V_{\text{visc}}^\ddagger$ that is effectively constant, $0\text{--}200 \text{ MPa}$:

$$\Delta V_{\text{visc}}^\ddagger = RT(\partial \ln \eta/\partial P)_T \quad (17)$$

For *water* at near-ambient temperatures, however, the pressure dependence of η up to 200 MPa is, for practical purposes, negligible (Figure 5). This phenomenon can be explained in terms of a simple model in which liquid water at low temperatures contains local transient ice-I-like H-bonded structures as well “free” water molecules; the low-density ice-I-like structures will be broken up by applied pressure, tending to increase the fluidity of the liquid, so that near $25 \text{ }^\circ\text{C}$ this effect fortuitously compensates very closely the “normal” contribution to the pressure dependence of η due to the free water molecules. The outcome is that, if solvent viscosity is indeed an important factor in electrode kinetics, this fact will

show up clearly in the pressure dependence of k_{el} in organic solvents relative to water, other things being equal. Conversely, $\Delta V_{\text{el}}^\ddagger$ for water near 25 °C may be said to be independent of viscosity effects, so the other factors governing $\Delta V_{\text{el}}^\ddagger$ show through more clearly.

3. Theory and Observation in Electron Transfer Reactions

The theory of outer-sphere electron transfer reactions in solution, based upon transition-state theory (TST), has been well established for half a century.^{1–3,14,30,113–123} Refinements, however, continue to appear, dealing with (for example) the asymmetry of the inner-sphere reorganization energy,¹²⁴ nonlocal effects,^{125,126} the inclusion of solute as well as solvent polarizability,^{127,128} the failure of continuum theory,¹²⁹ the effect of displacing water solvent from ML_x^{z+} and an electrode surface,¹³⁰ electron correlation effects,¹³¹ and the Duschinsky effect (changes in vibrational normal modes following electron transfer).¹³² Nevertheless, for homogeneous electron transfer between reactants of the size of typical metal complexes, the solvent can be approximated to a continuum (the smallest complexes, $\text{MnO}_4^{2-/-}$, may provide an exception¹³³), the reactants can be approximated to spheres of uniform charge distribution, and the simplest form of Marcus theory seems adequate. For electrode reactions, however, there is mounting evidence that *solvent dynamics* can be important (see, e.g., Weaver^{53,54}), leading to a failure of TST and therefore of the original Marcus-type approach—a major theme of this review.

In a very simple TST-based treatment of outer-sphere electron transfer, reaction 1 can be regarded as effectively the same as reaction 2 but with a “virtual” exchange partner. It may be assumed that the transition state for reaction 2 is symmetrical, meaning that the transfer coefficient $\alpha = 0.5$ as is indeed found for most “well-behaved” electrode reactions at their equilibrium potentials E^0 . For electron transfer to occur in reaction 2, both $\text{ML}_x^{(z+1)+}$ and ML_x^{z+} must first adjust their internal and solvational configurations to a common intermediate configuration, whereas in reaction 1 only one reactant molecule needs to reorganize to that intermediate state. Consequently, the free energy of activation, $\Delta G_{\text{el}}^\ddagger$, for reaction 1 can be expected to be just *one-half* the corresponding quantity $\Delta G_{\text{ex}}^\ddagger$ for reaction 1, as predicted by Marcus^{7,9–11} in a more rigorous fashion.

$$k_{\text{ex}} = Z_{\text{ex}} \exp(-\Delta G_{\text{ex}}^\ddagger/(RT)) \quad (18)$$

$$k_{\text{el}} = Z_{\text{el}} \exp(-\Delta G_{\text{el}}^\ddagger/(RT)) \quad (19)$$

Accordingly, one might naïvely expect that, if Z_{el} and Z_{ex} do not vary greatly between reactions, $\ln k_{\text{el}}$ should be a linear function of $\ln k_{\text{ex}}$ with slope $\xi = 1/2$. Aoyagui et al.⁴ and Cannon¹ tested this expectation for several aqueous couples (Figure 1), and it appears that it is roughly valid for k_{el} values up to about 0.2 cm s⁻¹, above which literature values of k_{el} available to these authors in 1975–1980 leveled off.

It can now be recognized that the apparent limit of ~ 1.0 cm s⁻¹ is imposed by deficiencies of the macro-electrode techniques available prior to 1980 (Tafel extrapolation, CV peak separation, RDE, etc.); in addition to problems associated with residual uncompensated resistance,¹³⁴ the techniques themselves (as distinct from the electron transfer reaction) become in effect diffusion-limited for aqueous reactions for which $k_{\text{el}} > 0.3$ cm s⁻¹. Following the discussion in section 2.6, however, it is clear that although Z_{ex} ordinarily does not differ greatly between comparable adiabatic reactions, Z_{el} and consequently k_{el} are typically affected by the nature, history, and size of the electrode surface. We also saw in section 2.6 that the rates of some ostensibly outer-sphere reactions turn out to be strongly affected by other solutes; this is particularly evident for anion–anion couples such as the much-studied $\text{Fe}(\text{CN})_6^{3-/4-}$, in which both k_{el} and k_{ex} are subject to strong catalysis by cations as discussed in section 3.7.

3.1. Free Energies of Activation

Free energies of activation, ΔG^\ddagger , and frequency factors, Z , cannot be separated experimentally through dependence of the rate constant on temperature, T , since $\Delta G^\ddagger/(RT) = \Delta H^\ddagger/(RT) - \Delta S^\ddagger/R$, so ΔS^\ddagger behaves as if it were part of Z . Furthermore, the rate constant needs to be corrected for the work, W , of bringing the reactants together (in the case of homogeneous self-exchange) or of bringing the single reactant up through the diffuse double layer to the electrode (in the case of an electrode reaction). Marcus theory provides a means of calculating ΔG^\ddagger in terms of a nuclear reorganizational energy, λ ; ΔG^\ddagger for a self-exchange reaction or an electrode reaction at zero overpotential (zero thermodynamic free energy change) is then $\lambda/4$. The reorganizational energy λ can be expressed as the sum of (i) an internal (“inner-sphere”) reorganization energy, λ_{IR} , originating in changes in M–L bond lengths and angles, etc., in going to the transition state, and (ii) a solvent or “outer-sphere” reorganizational contribution, λ_{SR} . Correspondingly, $\Delta G^\ddagger = \Delta G_{\text{IR}}^\ddagger + \Delta G_{\text{SR}}^\ddagger$, where $\Delta G_{\text{IR}}^\ddagger = \lambda_{\text{IR}}/4$ and $\Delta G_{\text{SR}}^\ddagger = \lambda_{\text{SR}}/4$. In the absence of substantial conformational changes, λ_{IR} can be estimated from the M–L force constants K_j of the j th normal coordinates of reactants 1 and 2 and is proportional to the change $(\Delta d)^2$ in the M–L bond length resulting from the change in oxidation state of M:¹⁴

$$\Delta G_{\text{IR}}^\ddagger = \lambda_{\text{IR}}/4 = (N_A/4) \sum_j [K_j^1 K_j^2 / (K_j^1 + K_j^2)] (\Delta d)^2 \quad (20)$$

For the homogeneous self-exchange reaction 2, the solvent reorganizational term depends on the optical (ϵ_{op}) and static (ϵ) dielectric constants (relative permittivities) of the solvent, the effective radii (r_1 and r_2) of the two reactant molecules, and the separation (σ) of the two M centers at the moment of electron transfer:

$$\Delta G_{\text{SR(ex)}}^{\ddagger} = (N_{\text{A}}e^2/(16\pi\epsilon_0))[(2r_1)^{-1} + (2r_2)^{-1} - \sigma^{-1}](\epsilon_{\text{op}}^{-1} - \epsilon^{-1}) \quad (21)$$

Usually, ϵ_{op} is taken to be approximately n^2 , where n is the optical refractive index of the solvent (a rather imprecise notion, because n is wavelength-dependent, see section 3.4), and σ is assumed to be $(r_1 + r_2)$ or $2r$, where r is the mean of r_1 and r_2 , these being about the same:

$$\Delta G_{\text{SR(ex)}}^{\ddagger} \approx (N_{\text{A}}e^2/(32\pi\epsilon_0r))(\epsilon_{\text{op}}^{-1} - \epsilon^{-1}) \quad (22)$$

Adaptation of eq 21 for electrode reactions has caused some controversy over the correct choice for σ . In the original Marcus theory of electrode kinetics,^{7,9–11} σ was taken as the distance from the center of the reactant to the center of its charge image inside the electrode, so $\sigma \approx 2r$ just as in homogeneous electron transfer if the thickness, δ_{H} , of the inner Helmholtz layer can be ignored (in effect, if the reactant penetrates the inner Helmholtz layer to make contact with the electrode). Equivalently, in the scenario presented in the Introduction to this review, σ would be the distance from the reactant center to the electrode and then back again to the center of the virtual reaction partner ($\sim 2r$), again assuming either that the inner Helmholtz layer is penetrated or that electron transfer takes place at its outer surface by tunneling through the layer:

$$\Delta G_{\text{SR(el)}}^{\ddagger} = \frac{1}{2}(N_{\text{A}}e^2/(16\pi\epsilon_0))(r^{-1} - \sigma^{-1})(\epsilon_{\text{op}}^{-1} - \epsilon^{-1}) \approx (N_{\text{A}}e^2/(64\pi\epsilon_0r))(\epsilon_{\text{op}}^{-1} - \epsilon^{-1}) \quad (23)$$

Neglect of the inner Helmholtz layer corresponds to the almost universal assumption that the solvation layer around the reactant molecules in *homogeneous* self-exchange reactions can be ignored in the application of eq 21; see, however, Hartnig and Koper.¹³⁰ The alternative is to concede that, in electrode reactions, electron tunneling occurs from the OCP, with likely loss of adiabaticity (section 3.3). In the Marcus treatment then,

$$\Delta G_{\text{SR(el)}}^{\ddagger} \approx \frac{1}{2}\Delta G_{\text{SR(ex)}}^{\ddagger} \quad (24)$$

$$\Delta G_{\text{el}}^{\ddagger} \approx \frac{1}{2}(\Delta G_{\text{IR(ex)}}^{\ddagger} + \Delta G_{\text{SR(ex)}}^{\ddagger}) = \frac{1}{2}\Delta G_{\text{ex}}^{\ddagger} \quad (25)$$

Marcus¹⁰ also showed that the contributions of ionic atmosphere (Debye–Hückel) effects, $\Delta G_{\text{atm(el)}}^{\ddagger}$ and $\Delta G_{\text{atm(ex)}}^{\ddagger}$, to $\Delta G_{\text{el}}^{\ddagger}$ and $\Delta G_{\text{ex}}^{\ddagger}$, respectively, should be similarly related ($\Delta G_{\text{atm(el)}}^{\ddagger} = 1/2\Delta G_{\text{atm(ex)}}^{\ddagger}$) but would be small compared to $\Delta G_{\text{SR}}^{\ddagger}$, especially in the usual case of high supporting electrolyte concentrations, which reduce the influence of double-layer effects to the point where they can be conveniently neglected.

By the same token, however, screening by high concentrations of supporting electrolyte should effectively eliminate the charge image of the reactant in the electrode. Accordingly, in the Hush theory of adiabatic electrode reactions,^{6,8,12,13,119} it is argued

that σ may be set to infinity, in which case

$$\Delta G_{\text{SR(el)}}^{\ddagger} = \frac{1}{2}(N_{\text{A}}e^2/(16\pi\epsilon_0))(r^{-1} - \sigma^{-1})(\epsilon_{\text{op}}^{-1} - \epsilon^{-1}) \approx (N_{\text{A}}e^2/(32\pi\epsilon_0r))(\epsilon_{\text{op}}^{-1} - \epsilon^{-1}) \quad (26)$$

so (contrast eq 24)

$$\Delta G_{\text{SR(el)}}^{\ddagger} \approx \Delta G_{\text{SR(ex)}}^{\ddagger} \quad (27)$$

Thus, in Hush's treatment, if Z_{el} and Z_{ex} are roughly constant for given conditions, the slope ξ of a $\ln k_{\text{el}}$ vs $\ln k_{\text{ex}}$ plot should be about 1.0. Early work by Peover^{13,135,136} on the electrochemical oxidation rates of polycyclic aromatic hydrocarbons in DMF,¹³⁷ for which $\Delta G_{\text{IR}}^{\ddagger}$ is negligible so $\Delta G_{\text{el}}^{\ddagger}$ should closely reflect $\Delta G_{\text{SR(el)}}^{\ddagger}$, gave ξ approaching 1.0 (in the present author's analysis, 0.7–0.9, depending on the corrections applied). Subsequently Kojima and Bard¹³⁸ combined these data with those for similar reactions in DMF to give $\Delta G_{\text{el}}^{\ddagger}$ values that roughly equaled $\Delta G_{\text{ex}}^{\ddagger}$ as per eq 27, although the data were rather scattered about a line with unit slope. The free energies of activation were obtained using theoretical values of Z_{el} ($= (k_{\text{B}}T/(2\pi m))^{1/2}$, where m is the molecular mass of the reactant) and Z_{ex} ($= 16r^2(\pi k_{\text{B}}T/m)^{1/2}$). These values are derived from collision theory and may not be realistic; current practice favors an encounter preequilibrium model,¹⁴ which typically gives Z_{el} values some 20-fold larger.¹³⁹ Furthermore, there is a strong possibility that the rates of electrode reactions in DMF are controlled by solvent dynamics, which could reduce Z_{el} drastically (sections 3.4 and 3.9).⁶⁴

On the other hand, eq 27 is not consistent with Figure 1 or similar plots by Aoyagui et al.,⁴ which suggest that ξ is not greater than 0.5, or with a plot of (uncorrected) $\ln k_{\text{el}}$ vs $\ln k_{\text{ex}}$ for 10 aqueous transition-metal complex couples of various charge types by Fu and Swaddle,⁵⁷ which showed severe scatter but could be taken to imply $\xi \approx 0.1$. Aoyagui et al.⁴ also showed that k_{el} for the series $\text{Fe}(\text{CN})_6^{3-/4-}$, $\text{Fe}(\text{bpy})_2(\text{CN})_2^{+/0}$, $\text{Fe}(\text{bpy})(\text{CN})_4^{-2-}$, and $\text{Fe}(\text{bpy})_3^{3+/2+}$ ¹³⁷ increased monotonically in that order, as did the limited k_{ex} data available, and the rough logarithmic correlation suggested $\xi \approx 0.2$ (see, however, the commentary in section 3.7 on cation effects on the $\text{Fe}(\text{CN})_6^{3-/4-}$ reaction rates). Endicott et al.¹⁴⁰ found a correlation between $\log k_{\text{el}}$ and $\log k_{\text{ex}}$ with slope $\xi \approx 0.5$ ($\pm 25\%$) for $\text{M}(\text{H}_2\text{O})_6^{3+/2+}$ ($\text{M} = \text{Cr}, \text{Eu}, \text{V}, \text{Fe}$), $\text{Ru}(\text{NH}_3)_6^{3+/2+}$, and $\text{Fe}(\text{CN})_6^{3+/2+}$, although $\text{Co}^{\text{III/II}}$ chelates and hexaamines deviated substantially, evidently because of large reorganizational energy barriers associated with the $\text{Co}^{\text{III/II}}$ spin-state change. Weaver^{141,142} took a different approach, using eq 25 (i.e., adopting $\xi = 0.5$ a priori) with Frumkin-corrected k_{el} values to calculate rate constants for heteronuclear (cross) redox reactions with fair success, although $\Delta G_{\text{el}}^{\ddagger}$ for aqua complexes was somewhat larger than that calculated from $\Delta G_{\text{ex}}^{\ddagger}$, whereas the reverse was true for amines. Hupp and Weaver¹⁴³ also considered whether noncontinuum (dielectric saturation) effects might contribute sub-

stantially to $\Delta G_{\text{el}}^{\ddagger}$ and $\Delta G_{\text{ex}}^{\ddagger}$ but concluded that any such contributions would only be on the order of 5 kJ mol⁻¹ so would not significantly affect predictions based on eqs 21 and 23 (or 26).

Overall, the impossibility of measuring $\Delta G_{\text{el}}^{\ddagger}$ and $\Delta G_{\text{ex}}^{\ddagger}$ without assumptions concerning the values of the preexponential factors Z_{el} and Z_{ex} prevents a simple resolution of the question of whether ξ should be 1.0 (as in the Hush approach) or 0.5 (as in Marcus theory) or some other value (if, indeed, a $\ln k_{\text{el}} - \ln k_{\text{ex}}$ correlation should exist at all). Consideration of the problem of the preexponential factors follows.

3.2. Preexponential Factors

In the currently preferred application of TST to electron transfer reactions, Z_{ex} for homogeneous self-exchange reactions (eq 1) is usually expressed as

$$Z_{\text{ex}} = K_0^{\text{ex}} \kappa_{\text{ex}} \nu_{\text{n}} \Gamma_{\text{n}} \quad (28)$$

where K_0^{ex} is the preexponential part of the formation constant of a precursor complex of the reactants formed prior to electron transfer (the exponential part being the Coulombic work correction, $\Delta G_{\text{Coul}} = Nz(z-1)e^2/(4\pi\epsilon_0\epsilon\sigma)$), κ_{ex} is the electronic transmission coefficient (= 1 for fully adiabatic electron transfer), and Γ_{n} is the nuclear tunneling factor (~ 1 for large ML_x^{z+} at near-ambient temperatures^{11,14,139,144-150}). The nuclear frequency factor, ν_{n} , can be expressed in terms of inner-sphere and solvent nuclear frequency contributions, ν_{I} and ν_{S} , respectively:

$$\nu_{\text{n}} = [(\nu_{\text{I}}^2 \Delta G_{\text{IR}}^{\ddagger} + \nu_{\text{S}}^2 \Delta G_{\text{SR}}^{\ddagger}) / (\Delta G_{\text{IR}}^{\ddagger} + \Delta G_{\text{SR}}^{\ddagger})]^{1/2} \quad (29)$$

Electron transfer by tunneling is considered to occur with significant probability (once internal and solvent reorganizational constraints are met as described in section 3.1) when the reactants approach to within a reaction zone of thickness $\delta\sigma$; thus, for SI units with k_{ex} in L mol⁻¹ s⁻¹,

$$Z_{\text{ex}} = 4000\pi N_{\text{A}} \sigma^2 \delta\sigma \kappa_{\text{ex}} \nu_{\text{n}} \quad (30)$$

For electrode reactions, Weaver and co-workers^{15,139,144-150} proposed that the precursor formation factor K_0^{el} for electrode reactions is simply the electrode reaction zone thickness, $\delta\sigma_{\text{el}}$, so for SI units with k_{el} in cm s⁻¹,

$$Z_{\text{el}} = 100\delta\sigma_{\text{el}} \kappa_{\text{el}} \nu_{\text{n}} \quad (31)$$

Although this encounter preequilibrium approach arguably gives more realistic estimates of Z_{ex} and Z_{el} than the older collision theory, it still does not offer deliverance from debatable assumptions, in particular, the choice of suitable values for $\delta\sigma$ and $\delta\sigma_{\text{el}}$ ($\delta\sigma \approx \delta\sigma_{\text{el}} \approx 100$ pm has been proposed).¹³⁹

Although k_{el} and k_{ex} as customarily presented have different dimensions and are not directly comparable, Weaver^{146,150} proposed a means of converting the work-corrected k_{el} to a form equivalent to a bimolecular rate constant so compatible with k_{ex} (work-corrected, units L mol⁻¹ s⁻¹). To achieve this, the electrode is considered to be a coreactant with zero

intrinsic barrier, infinite radius, and a continuously variable redox potential set to the potential of the coreacting couple, leading to

$$\begin{aligned} \ln(4000\pi N_{\text{A}} \sigma^2 k_{\text{el}(\text{cor})}) &= \ln k_{\text{ex}(\text{cor})} + \\ &\ln(\kappa_{\text{el}} \delta\sigma_{\text{el}} / (\kappa_{\text{ex}} \delta\sigma)) + [\Delta G_{\text{IR}}^{\ddagger} + \\ &(N_{\text{A}} e^2 / (16\pi\epsilon_0)) \{ (2r)^{-1} - \sigma^{-1} + (4\sigma_{\text{el}})^{-1} \} \times \\ &(\epsilon_{\text{op}}^{-1} - \epsilon^{-1})] / (RT) \quad (32) \end{aligned}$$

Equation 32 was intended to be applied to chemically irreversible processes, notably cross reactions. For the special case of adiabatic reactions ($\kappa_{\text{el}} = \kappa_{\text{ex}} = 1$) involving a couple $\text{ML}_x^{z+/(z-1)+}$ in which redox brings about negligible internal reorganization (i.e., no significant change in conformation or M-L bond lengths), if $\delta\sigma_{\text{el}} \approx \delta\sigma$, $\sigma \approx 2r$, and $4\sigma_{\text{el}} \gg \sigma$ (which are reasonable assumptions), eq 32 reduces to

$$4000\pi N_{\text{A}} \sigma^2 k_{\text{el}(\text{cor})} \approx k_{\text{ex}(\text{cor})} \quad (33)$$

The implication is that the relationship of k_{el} to k_{ex} resides essentially in the formation of the precursor complexes. In practice, however, the work-corrected pseudobimolecular rate constants calculated by Weaver¹⁵⁰ for a range of cross reactions at a mercury electrode exceed those for the corresponding homogeneous self-exchange reactions by up to 3 orders of magnitude (Figure 1 of ref 150)—an unsatisfactory result, given that the values ranged over about 10¹–10⁸ L mol⁻¹ s⁻¹.

3.3. Nonadiabaticity

Electron transfer becomes nonadiabatic (transmission coefficient κ_{el} or $\kappa_{\text{ex}} \ll 1$) when the off-diagonal electronic coupling matrix element, H_{12} , is substantially smaller than the thermal energy, $k_{\text{B}}T$.^{14,53,151} Intuitively, one might expect electron tunneling from a reactant to a metallic electrode to occur more readily (more adiabatically) than in the corresponding bimolecular self-exchange reaction because of stronger coupling to and the high density of electronic states within a metal surface.^{13,147,152,153} At near-equilibrium conditions (negligible overpotentials), the relevant electronic states of the reduced (filled frontier levels) and oxidized (vacant frontier levels) forms of the reactant can be expected to span the Fermi level of a metal electrode.^{30,118} In the case of nonadiabatic electron transfer, κ_{el} and hence k_{el} may be expected to depend on the distance R of the reactant center from the electrode surface (R can be adjusted with SAMs or other adsorbed layers or films) according to the approximate expression

$$\kappa_{\text{el}}(R) = \kappa_{\text{el}}^0 \exp[-S(R - R^0)] \quad (34)$$

where S is a scaling constant (on the order of 10–20 nm⁻¹⁹⁹) and κ_{el}^0 is the electronic transmission coefficient at the distance of closest approach, R^0 , in the absence of SAMs or other adsorbed layers. Then, κ_{el}^0 will depend on the density of electronic states on the electrode.¹⁵¹ Most workers have assumed electron transfer at electrode surfaces to be adiabatic ($\kappa_{\text{el}}^0 =$

1), and indeed Hush's discussions^{6,8,12,119} of electrode dynamics have focused upon adiabatic processes. Weaver and co-workers,^{144,146,148,151} however, recognized that varying degrees of nonadiabaticity could account, at least in part, for difficulties they encountered in making comparisons of electron transfer rate constants at electrodes and homogeneous solution, and in the case of the Ru(hfac)₃^{0/-} couple¹³⁷ in nonaqueous solvents, they actually concluded that the sluggishness of the electrode reaction (relative to metallocenes, for example) was attributable to nonadiabaticity despite an apparently high degree of adiabaticity in the facile homogeneous self-exchange of Ru(hfac)₃^{0/-} in the same solvents.¹⁴⁸

Although Weaver et al.¹⁵⁴ reported some success in extracting values of H_{12} (and hence κ_{ex}) from k_{ex} data for the self-exchange kinetics of some metallocene couples in various nonaqueous solvents by allowing for solvent dynamical effects (section 3.4), the estimation of κ_{el} is acknowledged to be very difficult.¹⁴⁶ As a case in point, noted in section 2.6, the lack of dependence of k_{el} on the nature of the electrode for the Ru(NH₃)₆^{3+/2+} couple^{88,89} is usually ascribed to full adiabaticity, but Gosavi and Marcus¹⁵⁵ point out that, in the case of Au vs Pt electrodes at least, the constancy of k_{el} could be consistent with nonadiabatic electron transfer despite the 7.5-fold greater density of electronic states on Pt as compared to Au. This is possible because the extra density of states in Pt is due to 5d orbitals, which couple much less strongly to reactants than do p-band states. The adiabatic interpretation of the Ru(NH₃)₆^{3+/2+} data seems more likely, inasmuch as k_{el} was the same for several other surfaces besides Au and Pt (although Hg gave a somewhat lower value).^{88,89} Nevertheless, the point is made that nonadiabaticity could be widespread among reactions at solid electrodes and would explain why the measured values of k_{el} are often very sensitive to the identity of the electrode. The degree of adiabaticity may also be influenced by the history of the electrode surface (manner of cleaning, formation of oxide films during potential sweeps, etc.), since adsorbed solvent, supporting electrolyte, or adventitious ions or molecules on the surface may reduce the effectiveness of overlap of reactant receptor orbitals with the continuum of states near the Fermi level of a metallic electrode (eq 34; cf. effect of SAMs, section 2.6).¹⁵¹

When the internal reorganization energy is small, the degree of adiabaticity for electrode reactions is intertwined with the control of the reaction rate by *solvent dynamics* (section 3.4);^{152,153} for electrode reactions in the fully adiabatic limit, the reaction rate is inevitably quite fast and is largely controlled by solvent motions, so Z_{el} becomes proportional to $\tau_{\text{L}}^{-\theta}$ (where τ_{L} is the longitudinal relaxation time of the solvent and $0 < \theta \leq 1$), whereas in the extreme nonadiabatic limit, Z_{el} is governed by κ_{el} and is independent of τ_{L} .^{53,54}

3.4. Solvent Dynamics

The original versions of the Marcus and Hush theories^{6-12,14,113-115} of both homogeneous and heterogeneous electron transfer reaction rates were cast

in terms of transition state theory, according to which the transition state at the highest point of the activation energy barrier exists in equilibrium with the initial state(s) of the reactant(s) and the reaction rate is determined by passage through the transition state at a universal rate. For thermally activated reactions in solution, ascent of the activation barrier is considered to be achieved by energy transfer to the reactant(s) from the solvent (cf. the Brownian motion). If, however, coupling to solvent motions is strong enough, solvent dynamics (solvent "friction") may actually hinder passage through the transition state, as proposed by Kramers¹⁵⁶ in 1940. With reference to eq 29, ν_{I} is much larger than ν_{S} , so when $\Delta G_{\text{IR}}^{\ddagger}$ is comparable to or greater than $\Delta G_{\text{SR}}^{\ddagger}$, ν_{n} will be dominated by ν_{I} , that is, by M-L and similar vibration frequencies, implying rapid passage through the transition state in a single vibration as assumed in TST. When $\Delta G_{\text{IR}}^{\ddagger} \ll \Delta G_{\text{SR}}^{\ddagger}$, however, implying an adiabatic reaction, $\nu_{\text{n}} \approx \nu_{\text{S}}$, which may be dominated by either rotational or collective longitudinal solvent motions. The latter ("overdamped") case results in a bottleneck due to sluggish motion back and forth through the transition state and diminution of the preexponential factor and hence the rate constant through an inverse dependence on τ_{L} . This means, in effect, the failure of TST.

In the Kramers model, further developed 40 years later by Zusman,¹⁵⁷⁻¹⁵⁹ Grote and Hynes,^{160,161} Calef and Wolynes,^{162,163} and others (for reviews germane to this article, see Weaver,^{53,54,145,151} Fawcett and Opařo,⁹⁶ Heitele,¹⁶⁴ and Galus¹⁶⁵), solvent motions and progress of the reactant over the activation barrier are treated as occurring in one dimension, that is, along the reaction coordinate. In the Kramers-Zusman (KZ) approach, for the limiting case of an adiabatic reaction in which $\Delta G_{\text{IR}}^{\ddagger}$ can be neglected so $\nu_{\text{n}} \approx \nu_{\text{S}}$ (eq 29), rate control is by solvent dynamics, and the nuclear frequency factor in eqs 30 and 31 becomes

$$\nu_{\text{n}} = \tau_{\text{L}}^{-1} (\Delta G_{\text{SR}}^{\ddagger} / (4\pi RT))^{1/2} \quad (35)$$

if the solvent behaves as a Debye liquid (i.e., one in which a solvent molecule can be approximated to a sphere rotating in a spherical cavity in a continuous dielectric). If the solvent has molar volume V_{M} , Debye relaxation time τ_{D} (obtainable from dielectric relaxation measurements), and high-frequency (microwave) dielectric constant ϵ_{∞} , τ_{L} can be estimated from eq 36,^{53,96,151,154,165-168}

$$\tau_{\text{L}}^{-1} = (\epsilon / \epsilon_{\infty}) \tau_{\text{D}}^{-1} = (\epsilon / \epsilon_{\infty}) RT / (3V_{\text{M}} \eta) \quad (36)$$

in which, on the right-hand side, τ_{D} has been replaced by a term derived from the Stokes equation containing the shear viscosity, η .^{159,165} Although η is properly the microscopic viscosity of the solvent in the vicinity of the reactant ion or molecule, it may be identified with adequate accuracy with the macroscopic shear viscosity. For unassociated Debye-type solvents, ϵ_{∞} should not be equated to ϵ_{op} , which in Galus' tabulation for common solvents¹⁶⁵ ranges from 38% to 92% of ϵ_{∞} ; however, ϵ_{op} may be a more appropriate choice

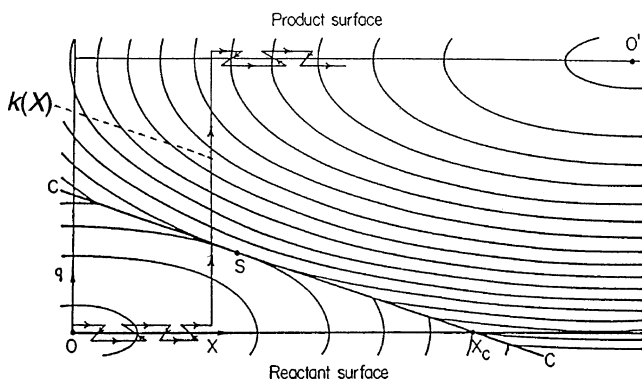


Figure 6. Adiabatic potential surface for electron transfer with an example of a reactive trajectory comprising slow solvent-driven fluctuations along the reactant and product abscissae and fast (ballistic) atomic displacements along the ordinate X , giving rate constant $k(X)$ for this trajectory. This diagram represents a general case for which the thermodynamic free energy change ΔG is nonzero; for exchange processes such as reaction 2, $\Delta G = 0$, and the reactant and product free-energy surfaces would be mirror images of each other. Reprinted with permission from ref 183b. Copyright 2001 Wiley-VCH.

when the solvation involves primarily clusters of molecules, as in the case of alcohols.^{169,170} Such associated liquids present special problems in that several solvent relaxation modes may be involved, whereas the normal application of eq 36 covers only the slowest.^{158,161,171} McManis and Weaver¹⁷² examined electron transfer kinetics in non-Debye solvents such as alcohols and concluded that the presence of higher-frequency dielectric relaxation components could lead to 5–10-fold enhancements of the reaction rates. Water exhibits uniquely fast solvation dynamics,^{173–175} and the ultrafast modes can enhance the rate of weakly adiabatic electron transfer to the extent that the rate observed is essentially that predicted by TST-based Marcus theory.^{176,177} For most nonaqueous solvents, however, the “signature” of solvent dynamical control of the reaction rate is a dependence of the rate constant on solvent fluidity (reciprocal of viscosity).^{159,165,178}

A two-dimensional alternative to the one-dimensional KZ approach, pioneered by Agmon and Hopfield^{179,180} and developed by Marcus, Sumi, and others (AHMS theory),^{181–186} regards solvent motions (horizontal axis in Figure 6) as occurring in a dimension orthogonal to the inner-sphere reorganization (vertical axis in Figure 6). Whereas motion along the vertical axis of Figure 6 is considered to be ballistic, representing in effect the TST limiting case, motion along the horizontal axis is slow and frictional. The AHMS theory has a particular advantage in that it is not restricted to cases where $\Delta G_{\text{IR}}^{\ddagger} \ll \Delta G_{\text{SR}}^{\ddagger}$. Sumi¹⁸³ showed that the observable rate constant k_s can be expressed in terms of a rate constant k_{TST} expected from transition-state theory and a rate constant k_f representing the effect of solvent fluctuations:

$$k_s^{-1} = k_{\text{TST}}^{-1} + k_f^{-1} \quad (37)$$

Thus, in the limiting case in which solvent dynamics are slow enough relative to k_{TST} to form a bottleneck,

Table 1. Values of the Standard Heterogeneous Rate Constants k_{el} and Parameter θ for Some Transition-Metal Couples in AN and DMF^a

couple	$k_{\text{el}}(\text{AN}),$ cm s^{-1}	$k_{\text{el}}(\text{DMF}),$ cm s^{-1}	θ
Co(acac) ₃ ^{0/-}	0.000 21	0.000 12	0.1
CoCp ₂ ^{0/-}	0.112	0.126	0.3
Co(dmg ₃ (BC ₄ H ₉) ₂) ⁺⁰	0.045		0.4
Co(dmg ₃ (BF) ₂) ⁺⁰	0.15		0.4
Mn(acac) ₃ ^{0/-}		0.324	0.5
Fe(acac) ₃ ^{0/-}	0.448		0.7
Cr(η^6 -C ₆ H ₆) ₂ ⁺⁰	4.0	1.2	0.7
CoCp ^{*2} ⁺⁰	3.5	1.5	0.8
CoCp ₂ ⁺⁰	3.0	1.3	1.0
FeCp ₂ ⁺⁰	2.6	0.4	1.0

^a Selected from ref 188; abbreviations as in footnote 137.

k_s is simply k_f , whereas if the fluctuations originating with the solvent are fast relative to k_{TST} , $k_s = k_{\text{TST}}$ and conventional TST can describe the kinetics. (A similar equation in which k_f represents the limiting diffusional rate constant is familiar in the context of diffusional control of reaction rates.) A key result of the AHMS approach is that when $k_f \ll k_{\text{TST}}$, k_f is predicted to be proportional to $\tau_L^{-\theta}$, where $0 \leq \theta \leq 1$. This stands in contrast to the KZ result, according to which $\theta = 1$, but had an experimental precedent in a report by McGuire and McLendon in which the rate constants for reactions of some tris(poly-pyridine)ruthenium(II) complexes with methyl viologen(2+) in glycerol were found to be proportional to $\tau_L^{-0.6}$, a result that was interpreted qualitatively in terms of a nonadiabatic process.¹⁸⁷ Fawcett and Opařo¹⁸⁸ have estimated values of θ for 18 electrode reactions in AN and DMF;¹³⁷ transition-metal complex couples selected from these are listed in Table 1 and show that the slower (arguably, the less adiabatic) the reaction, the lower is θ . The AHMS theory, however, leads to the further result that the free energy barrier may be reduced by a factor γ such that $0 < \gamma < 1$:¹⁸³

$$k_f = \tau_L^{-\theta} \nu_n^{1-\theta} \exp(-\gamma \Delta G^{\ddagger}/(RT)) \quad (38)$$

$$\gamma = \Delta G_{\text{SR}}^{\ddagger}/(\Delta G_{\text{IR}}^{\ddagger} + \Delta G_{\text{SR}}^{\ddagger}) \quad (39)$$

$$\theta = |1 - \Delta G_{\text{IR}}^{\ddagger}/\Delta G_{\text{SR}}^{\ddagger}| \quad \text{when } 0 \leq \Delta G_{\text{IR}}^{\ddagger}/\Delta G_{\text{SR}}^{\ddagger} \leq 2, \\ \text{otherwise } \theta = 1 \quad (40)$$

Equation 38 reduces to the KZ expression ($\theta = \gamma = 1$) when $\Delta G_{\text{IR}}^{\ddagger} \ll \Delta G_{\text{SR}}^{\ddagger}$, which is in effect the adiabatic limit. It may be noted that Smith and Hynes¹⁸⁴ have developed KZ theory to encompass the interplay of concurrent nonadiabaticity (“electronic friction”) and solvent friction in the near-adiabatic regime.

For the limiting case of strongly nonadiabatic electron transfer,^{96,154,182,187,188} the preexponential factor for k_{TST} is controlled by H_{12}^2 , κ_e ($= \kappa_{\text{el}}$ or κ_{ex}) becomes $\ll 1$ (in effect, $\kappa_e \nu_n$ is replaced by the electronic frequency factor ν_e), k_{TST} becomes the bottleneck according to eq 37, and solvent dynamics cease to be rate-controlling. Intermediate cases are covered by a combination of eqs 18–25, 28–31, and 35–40.

Weaver^{53,54,189} reviewed the problem of identifying solvent dynamical influences experimentally and

identified several possible pitfalls. Prominent among these, for electrode reactions, is the tendency of residual uncompensated resistance to masquerade as solvent dynamical control of chemical reaction rates, since both depend on the solvent viscosity. Furthermore, the inadequacy of solvation energy models based on dielectric continuum (Born) models may give unrealistic estimates of $\Delta G_{\text{SR}}^{\ddagger}$ (section 3.1);¹⁴³ this concern may be misplaced, however, since dielectric saturation affects ϵ but not ϵ_{op} , and it is the latter that dominates eqs 21–23 and 26. More likely sources of problems relating to solvents of lower ϵ are the work terms for assembly of the precursor state, medium effects (Debye–Hückel-type and ion pairing¹⁰⁴) on the activities of the reactants, and the tendency of tetraalkylammonium ions (widely used as supporting electrolytes in organic solvents) to form blocking layers on electrodes, decreasing the adiabaticity of the reaction¹⁸⁸ and possibly introducing dynamic artifacts through slow desorption.¹⁰⁷ Nevertheless, Weaver concluded that electrochemical reactions are typically adiabatic (while conceding that the Ru(hfac)₃^{0/−} couple in nonaqueous media could be an exception¹⁴⁸) and that their rates are at least partly controlled by overdamped solvent dynamics.

Smalley et al.,¹⁹⁰ however, have recently sounded a further cautionary note with specific reference to the interpretation of solvent effects on electrode reaction rate constants. Their study of the kinetics of the Fe(CN)₆^{3−/4−} and Ru(NH₃)₆^{3+/2+} couples in aqueous 1 mol L^{−1} KF and of dimethylferrocene(+/0) in 1 mol L^{−1} LiClO₄ in methanol at Au electrodes using the indirect laser-induced temperature jump (ILIT) method showed that all three couples adsorb on Au and that consequently their behavior departed significantly from that expected for the simple E mechanism assumed in the present article. Smalley et al.¹⁹⁰ acknowledge that not all couples necessarily adsorb on all types of electrode, but they warn that the kinetic consequences of modifying solvent properties (e.g., through changing the temperature—or implicitly the pressure as advocated here—or introducing an inert additive) may reflect changes in the extent or effects of adsorption of the redox-active couple on the electrode rather than the influences of solvent dynamics or $\Delta G_{\text{SR}}^{\ddagger}$. In the variable-pressure studies from the author's laboratory discussed below, however, evidence for adsorption effects in measurements of k_{el} was looked for but not seen except in certain metallophthalocyanine systems.^{65,191}

3.5. Reactant Size and Shape

Throughout the foregoing runs the implicit assumption that the reactants can be treated as conducting spheres with effective (e.g., van der Waals) radii r that can be estimated from standard techniques such as X-ray crystallography of solids. Indeed, Kojima and Bard¹³⁸ (for example) found for electroreduction of selected aromatic compounds in DMF that $\Delta G_{\text{el}}^{\ddagger}$ ($\approx \Delta G_{\text{SR}(\text{el})}^{\ddagger}$ because $\Delta G_{\text{IR}(\text{el})}^{\ddagger}$ is negligible) correlated with r^{-1} with values falling between the predictions of eqs 23 and 26. In fast reactions where solvent dynamics appears to be rate-controlling, a dependence of Z_{el} on a^{-1} may be anticipated,

where a is the effective hydrodynamic radius of the reactant molecule (presumably not very different from r). Compton et al.⁸⁰ used a high-speed channel electrode to study the fast oxidation of anthracene derivatives in alkyl cyanide solvents and found that the differences in rates between the different anthracenes can be accounted for quantitatively by equating r with the measured a and including it in both the Marcus $\Delta G_{\text{el}}^{\ddagger}$ and the solvent dynamical frequency factor.

Molecular dynamics calculations, however, indicate that the effective radius of an ion in solution is strongly charge-dependent because of ion–dipole interactions.^{130,192} This is supported in a qualitative way by measurements of the cell reaction volumes ($\Delta V_{\text{cell}} = -F(\partial E_{1/2}/\partial P)_T$ relative to a particular reference electrode) of the CoW₁₂O₄₀^{5−/6−} and PW₁₂O₄₀^{3−/4−} couples in acidic aqueous solution; the Born theory of ionic solvation predicts a linear dependence of ΔV_{cell} on the change in z^2/r resulting from electron transfer (Drude–Nernst relation), but although the observed dependence on z^2 is as expected, the dependence on r is the opposite.⁶³ Similarly, for the FeCp₂^{+/0} and FeCp*₂^{+/0} couples¹³⁷ in various organic solvents, although ΔV_{cell} is indeed linearly dependent upon the Drude–Nernst proportionality factor $(1/\epsilon)(\partial \ln \epsilon/\partial P)_T$ at constant $\Delta(z^2)$, the fitted values of r and also of the hydrodynamic radii a (from the Stokes–Einstein relation) cannot be reconciled with the crystallographic dimensions of the reactants.⁶⁴ Tregloan et al.^{193,194} found similar difficulties in accounting for trends in ΔV_{cell} for transition-metal complex couples in water in terms of crystallographic r data. Wherland et al.¹⁹⁵ found no clear dependence of the molar volumes of electrolytes in nonaqueous solvents on r in the Drude–Nernst context.

The spherical approximation is presumably reasonable for FeCp₂^{+/0} and FeCp*₂^{+/0} and very good for the heteropolyoxotungstates, but it is obviously unrealistic for grossly nonspherical molecules such as the roughly discoid metallophthalocyanines.⁶⁵ Grampp et al.,¹⁹⁶ in their comparison of homogeneous and heterogeneous electron transfer kinetics in the TTF^{+/0} system¹³⁷ in 10 organic solvents, treated the TTF molecule as ellipsoidal rather than spheroidal. Even for quasi-spherical reactants such as MnO₄^{−/2−} that are small enough to approach solvent molecular dimensions it may be necessary to abandon the two-sphere approach to homogeneous electron transfer and to treat the transition state as occupying an ellipsoidal cavity in the solvent (still viewed as a continuous dielectric).^{1,133} A more widely used approach that takes account of the relative sizes of reactant and solvent molecules is the mean spherical approximation (MSA) method, developed for homogeneous electron transfer kinetics by Fawcett and Blum.¹⁹⁷ The MSA treatment gave somewhat improved estimates of $\Delta G_{\text{SR}(\text{ex})}^{\ddagger}$ for the cobaltocene(+/0) self-exchange in organic solvents,¹⁹⁷ although for the Ru(hfac)₃^{0/−} self-exchange¹⁹⁸, it gave calculated $\Delta V_{\text{ex}}^{\ddagger}$ values only marginally closer to the experimental ones than did those given by a simple adaptation of Marcus theory.¹⁹⁹

The upshot of the foregoing is that the effective radii of reactants represent a significant source of possible error in calculations of $\Delta G_{\text{SR}}^{\ddagger}$, which is often the dominant factor determining k_{el} . It must also be borne in mind that many reactants are decidedly nonspherical in shape; Wherland et al.¹⁹⁵ concluded that even their clathrochelate complexes departed too far from sphericity for accurate application of Born solvation theory. Furthermore, Schwartz et al.²⁰⁰ remind us that solutes can undergo changes in shape and size in the course of reaction and show that although the response of solvent dynamics to changes in solute charge as such is linear, concomitant changes in solute size and shape may lead to a severe breakdown of linear response.

3.6. Electrolyte Effects

Both heterogeneous and homogeneous electron transfer kinetics are normally studied with concentrations of supposedly inert supporting electrolytes in the range 0.1–1.0 mol L⁻¹, in the former case to provide sufficient electrical conductivity and to minimize double-layer effects (section 2.6) and in the latter to control the activity coefficients of the reactants and the transition state through a swamping ionic strength I . Application of the extended Debye–Hückel theory to the ionic strength dependence of k_{ex} for reaction 2 gives the Brønsted–Bjerrum–Christiansen (BBC) equation,

$$\ln k_{\text{ex}}^I = \ln k_{\text{ex}}^0 + 2z(z-1)AI^{1/2}/(1 + B\hat{a}I^{1/2}) \quad (41)$$

in which A and B are constants ($A = 1.175 \text{ L}^{1/2} \text{ mol}^{-1/2}$ and $B = 3.286 \times 10^9 \text{ L}^{1/2} \text{ mol}^{-1/2} \text{ m}^{-1}$ for water at 25 °C) that one can calculate knowing only the density and static dielectric constant ϵ of the solvent at the given temperature²⁰¹ and \hat{a} represents the mean closest-approach distance of the reactants and their counterion. In principle, then, eq 41 could be solved using crystallographic or hydrodynamic data to estimate \hat{a} , but, as with r and a in section 3.5, it seems that \hat{a} is better treated as an adjustable parameter.^{64,202} The BBC equation is not expected to be valid in water for $I > 0.1 \text{ mol L}^{-1}$; some authors favor adding a term linear in supporting electrolyte concentration (cf. the well-known Davies equation²⁰³), but such approaches, including that of Pitzer,²⁰⁴ which is valid to $\sim 6 \text{ mol kg}^{-1}$ at least, introduce empirical parameters that, unlike A and B , cannot be calculated from fundamental constants and solvent properties, which is a disadvantage when one attempts to account for pressure or temperature effects on rate constants for electron transfer.²⁰¹

One likely cause of deviations from eq 41 at high electrolyte concentrations or in solvents of low dielectric constant is anion–cation pairing. The formation constant, K_{IP} , for an ion pair can be estimated reasonably well from the Fuoss equation,²⁰⁵

$$K_{\text{IP}} = (4000\pi N_A \hat{a}^3/3) \exp(|z_+z_-|e^2/(4\pi\epsilon_0\epsilon_B T\hat{a})) \quad (42)$$

which, however, depends once again on the dubious anion–cation contact parameter \hat{a} . Measurements of

K_{IP} are not necessarily better than Fuoss estimates, inasmuch as the nature of the ion pair (direct contact, solvent-separated, etc.) detected by, say, electrical conductance may be different from that giving rise to optical absorption and different again from species active (or deactivated) in electron transfer kinetics. For reaction 2, the effect of ion pairing may be to accelerate electron transfer if the ion pair is more reactive than the separate reactants or to retard it if the pair is less reactive and simply depletes the reactive pool. The former case would be characterized by a leveling-off of k_{ex} with increasing counterion concentration as ion pair formation approaches saturation. For reaction 1, the effect of ion pairing on k_{el} can be complicated¹⁰⁴ and may depend on whether ion pair breakup (assuming $|z|$ decreases on electron transfer) follows electron transfer or is concerted with it; conversely, stabilization of the product by ion pairing may cause a fast, reversible reaction to become irreversible.

Qualitatively, eq 41 predicts a leveling-off of ionic strength effects on k_{ex} in water for $0.1 < I < 1.0 \text{ mol L}^{-1}$, and this is found to be the case for cation–cation electron transfer reactions,²⁰² so the variation in k_{ex} with I at practical concentrations of supporting electrolytes turns out to be less important than might be supposed. Nevertheless, k_{ex} for reactants of like charge is certainly increased substantially relative to the “infinite dilution” value by increasing I , and this is one further complication in making comparisons between k_{ex} and k_{el} data that necessarily have been measured at different I . An obvious way of minimizing ionic strength and ion pairing effects, as well as the Coulombic work, ΔG_{Coul} , is to choose to study couples $\text{ML}_x^{z+(z-1)+}$ in which $z = 1$ or 0 , although even then some ionic atmosphere effects may be present.²⁰⁶ This requires the use of nonaqueous solvents, since metal complexes of zero charge tend to be very poorly soluble in water. Couples with a neutral partner for which both reactions 1 and 2 have been studied are¹³⁷ $\text{Ru}(\text{hfac})_3^{0/-}$,^{62,148,198,207,208} $\text{FeCp}_2^{+/0}$,^{55,61,95,96,154,209–216} $\text{CoCp}_2^{+/0}$,^{147,149,154,214,215,217,218} and $\text{FeCp}^*_{2+/0}$,^{147,210,216,219,220} and although there was a diminution of k_{ex} with increasing anion concentrations for $\text{FeCp}_2^{+/0}$ in acetonitrile, attributable to ion pairing,^{211,212} Weaver et al.²¹² considered the effect to be smaller than expected. Retardation of homogeneous electron transfer consistent with ion pairing was evident for $\text{Ru}(\text{hfac})_3^{0/-}$,^{207,208} and $\text{FeCp}^*_{2+/0}$,²¹⁹ in solvents of low polarity (chloroform and dichloromethane, respectively). Wherland²²¹ reviewed homogeneous outer-sphere electron transfer kinetics for nonaqueous systems and concluded that, in general, ion pairs were intrinsically less reactive than the free parent ions but where both reactants were of the same charge this effect could be offset by the reduction in the Coulombic work terms and by ionic strength effects as described by eq 41. Observations by Chan and Wahl²²² suggest that self-exchange in some $\text{M}(\text{polypyridine})^{3+/2+}$ couples ($\text{M} = \text{Fe}, \text{Os}$) in acetonitrile may constitute an exception to this generalization,²²¹ but as Chan and Wahl remarked,²²² such complexes may present special cases in that they depart rather far from the ideal spherical shape,

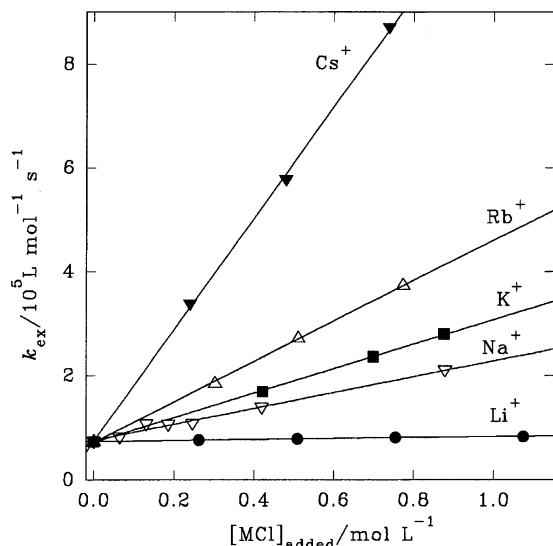


Figure 7. Effect of added alkali metal chlorides on k_{ex} for the homogeneous self-exchange of $\text{K}_4[\text{W}(\text{CN})_8]$ (0.031 mol L^{-1}) and $\text{K}_3[\text{W}(\text{CN})_8]$ (0.72 mmol L^{-1}) in D_2O at 25°C . Reprinted with permission from ref 232. Copyright 1999 American Chemical Society.

having interligand pockets that may harbor anions or solvent molecules.²²³

3.7. Specific Counterion Effects

For cationic couples, the kinetics of the self-exchange reaction 2 generally show no particular sensitivity to the nature of the counterions (anions) beyond the size and charge effects implicit in eqs 41 and 42 (the $\text{Co}(\text{phen})_3^{3+/2+}$ self-exchange is an exception, showing moderate anion effects on k_{ex}).^{221–223} For anion–anion self-exchange (z negative in eq 2), however, strong specific counterion (cation) effects on k_{ex} in aqueous media have long been noted in $\text{Fe}(\text{CN})_6^{3-/4-}$,^{108,109,224–230} and other cyanometalates^{231,232} but also in the oxoanionic couple $\text{MnO}_4^{-/2-}$,^{133,233–235} indicating that the effect is associated with the anionic nature of the reactants rather than any special characteristic of the ligands such as π -bonding (which may nevertheless play a secondary role) or the “softness” of CN vs the “hardness” of O. Typically, the heavier alkali metal cations M^+ and the smaller tetraalkylammonium ions R_4N^+ produce the greatest accelerations of anion–anion self-exchange in the sequence $\text{Li} \leq \text{Na} < \text{K} < \text{Rb} < \text{Cs}$ (Figure 7).^{133,224,225,231,232,234}

It is tempting to ascribe this trend to some consequence (such as reduction of the Coulombic work terms, $\Delta G_{\text{Coul}}^\ddagger$) of ion pairing, which follows the same qualitative pattern; for example, Nichugovskii and Shvedov²³⁶ reported the formation constants K_{IP} of the ion pairs $\{\text{M}^+, \text{Fe}(\text{CN})_6^{4-}\}$ to be 83, 83, 133, 244, and 395 L mol^{-1} for 0.05 mol L^{-1} LiCl, NaCl, KCl, RbCl, and CsCl, respectively, and Lemire and Lister²³⁷ found $K_{\text{IP}} = 12, 23, 37,$ and 51 L mol^{-1} for $\{\text{M}^+, \text{W}(\text{CN})_8^{4-}\}$ at infinite dilution ($\text{M} = \text{Na}, \text{K}, \text{Rb}, \text{Cs}$). The dependence of k_{ex} on $[\text{M}^+]_{\text{added}}$, however, is linear over the range $0–1 \text{ mol L}^{-1} \text{ M}^+$ (Figure 7, in which the common intercept is due to the pathway involving the K^+ introduced with the octacyanotungstates),^{109,133,231,232} whereas the K_{IP} data indicate that

ion pairing would show saturation over this range, even allowing for the expected decline in K_{IP} with rising ionic strength. Ion pairing apart, eq 41 predicts a decreasing slope of a plot of k_{ex} vs $[\text{M}^+]$ due to ionic strength effects.²³² For $\text{MnO}_4^{-/2-}$ in aqueous alkali in which ionic strength was held constant while $[\text{M}^+]$ was varied by adjusting a $\text{Cl}^-/\text{OH}^-/\text{SO}_4^{2-}/\text{PO}_4^{3-}$ mixture, a two-term rate law was found,

$$k_{\text{ex}} = k_{\text{ex}}^0 + k_{\text{ex}}^{\text{M}}[\text{M}^+] \quad (43)$$

in which the intercept, k_{ex}^0 , represented the rate constant for the uncatalyzed exchange pathway; the extrapolation required, however, was a long one, and the results should be viewed accordingly. In a recent reinvestigation of the homogeneous $\text{Fe}(\text{CN})_6^{3-/4-}$ exchange in which ionic strength was not constrained,¹⁰⁹ k_{ex} was nevertheless found to be a linear function of $[\text{K}^+]$ from 0 to 0.6 mol L^{-1} with no statistically significant intercept ($k_{\text{ex}}^{\text{M}} = 7 \times 10^4 \text{ L}^2 \text{ mol}^{-2} \text{ s}^{-1}$ at 25°C); in this case, the small k_{ex}^0 ($240 \text{ L mol}^{-1} \text{ s}^{-1}$) was exposed by sequestering the K^+ with 18-crown-6 or (better) crypt-2,2,2. Thus, the K^+ -dependent path would be some 300 times faster than the cation-independent path in $1.0 \text{ mol L}^{-1} \text{ K}^+$ solutions. Earlier, Wahl et al.²²⁵ had succeeded in getting an estimate of k_{ex}^0 for this reaction at low temperatures by extrapolation of radioiron tracer data in very dilute solutions; results of the two methods are in satisfactory agreement.

Several points emerge from these findings. First, the widespread use of the $\text{Fe}(\text{CN})_6^{3-/4-}$ exchange kinetics in the presence of significant concentrations of cations (usually K^+) as a benchmark for application of the Marcus cross-relation, or as a test of Marcus theory per se, is incorrect, as the rate constants used are essentially k_{ex}^{M} rather than k_{ex}^0 . In fact, the cation-independent k_{ex}^0 data extracted as described above fit the predictions of Marcus theory very well,¹⁰⁹ whereas the cation-dependent pathway is a three-body problem outside the scope of the basic theory.²²⁴ Second, the M^+ effect on k_{ex} is somewhat larger than the variation in K_{IP} noted above, although the trends are qualitatively similar; for example, for the $\text{W}(\text{CN})_8^{3-/4-}$ exchange, $k_{\text{ex}}^{\text{M}}/10^4 \text{ L}^2 \text{ mol}^{-2} \text{ s}^{-1}$ at 25°C is 0.9, 15, 24, 39, and 107 for $\text{M} = \text{Li}, \text{Na}, \text{K}, \text{Rb},$ and Cs , respectively. Arguably, the wider spread in k_{ex} relative to K_{IP} might be accommodated when the effect of ion pairing on ΔG_{Coul} is included. Certainly, some anion–cation pairing must be present and needs to be taken into account in the speciation of the reactants;^{228,232} however, the strictly linear dependence of k_{ex} on the stoichiometric concentration of M^+ is inconsistent with an ion pairing or ionic strength effect and indicates specific cation catalysis of the electron transfer process. In any event, the absence of significant counterion catalysis in cation–cation electron transfer, despite well-documented ion pairing, is an indication that the latter is not the key factor in anion–anion redox processes.

Dogonadze et al.²³⁸ and subsequently others^{45,47,57,58,133,232} have proposed that cation catalysis involves the formation of a bridge between the

two reacting anions by a cation that has been partially *dehydrated*, thereby maximizing both contact with the reacting anions and the polarizability of the bridge. Since the hydration energies of M^+ become less negative in the order $Li < Na < K < Rb < Cs$, ranging from -531 kJ mol^{-1} for Li^+ to a numerically small -283 kJ mol^{-1} for Cs^+ ,²³⁹ and polarizabilities of the naked M^+ increase in the same order, the relative efficacies of the alkali metal cations as catalysts is qualitatively explained. The catalytic effect of R_4N^+ is greatest for $R = CH_3$ (about the same as Rb or Cs) but declines as R becomes larger;^{225,232} this is consistent with the dehydration model, since R_4N^+ are not actively solvated in water²⁴⁰ (i.e., do not require dehydration to be catalytically active) and their catalytic power can be expected to fall off as their bulk and hence the anion–cation–anion span increase. Pressure effects (section 4.1) provide strong support for these views.

Electrochemists of the Moscow school have put forward theories of the mode of action of cation bridges in heterogeneous²³⁸ and homogeneous^{238,241–246} anion–anion electron transfer. Kharkats and Chonishvili²⁴⁵ presented a three-sphere model that examined the expected effect of cation bridging on $\Delta G_{SR(ex)}^\ddagger$ (cf. eq 21), but it predicts too small an increase in k_{ex} for $Fe(CN)_6^{3-/4-}$ as one goes from Li^+ to Cs^+ and a dependence on the size of R_4N^+ that is opposite to that observed.¹⁰⁹ The general problem continues to attract theoretical interest, as several biological electron transfer systems involve a third body that mediates electron transfer between the donor and acceptor centers.^{246–248} Sumi and Kakitani²⁴⁸ have presented a unified theory for electron transfer between a donor and an acceptor via a third body, linking the limiting cases of mediation by a quantum-mechanical virtual state of the bridging molecule (“superexchange”, by analogy with the related phenomenon in magnetism) and a sequential mechanism involving a real intermediate in which the electron resides in the third-body state for a time that is long compared with that of the dephasing/thermalization of phonons. For cation catalysis of anion–anion electron transfer, the superexchange process would seem more likely. Since, on simple electrostatic grounds, virtual states associating electrons with cations will be more favorable energetically than ones associating electrons with anions, the much greater importance of counterion catalysis in anion–anion exchange relative to cation–cation electron transfer can be understood.

The kinetics of anion redox at electrodes exhibit much the same kind of cation dependency as do their homogeneous analogues, at least as far as the alkali metal cations are concerned. The aqueous $Fe(CN)_6^{3-/4-}$ electrode reaction, for which an enormous literature exists, provides a convenient paradigm. Thus, Kùta and Yeager²⁴⁹ found that k_{el} for the $Fe(CN)_6^{3-/4-}$ electrode reaction on a gold RDE in aqueous MCl increased with [MCl] and with changing M in the order $Li \leq Na < K < Rb < Cs$. Peter et al. also found this sequence in fluoride, chloride, perchlorate, and nitrate media, using a gold wire electrode and current impulse^{250,251} or AC impedance spectroscopy.²⁵² Camp-

bell and Peter²⁵² showed that k_{el} for $Fe(CN)_6^{3-/4-}$ was accurately first order in [KF] from about 5×10^{-3} to 1.0 mol L^{-1} ; as noted above for K^+ effects on the corresponding homogeneous electron transfer, the absence of any falloff in k_{el} from linearity as $[K^+]$ increased shows that this effect is not due to ion pairing per se, because that would show saturation over this range (positive deviations below 5 mmol L^{-1} KF might reflect ion pairing or Debye–Hückel effects,²⁵² but the data are rather scattered).

Krulic et al.¹⁰⁸ rounded out previous observations on the electrode kinetics of $Fe(CN)_6^{3-/4-}$, finding k_{el} at a Pt disk electrode in 1.0 mol L^{-1} MCl to be 0.016, 0.030, 0.042, 0.042, 0.047, 0.068, 0.076, 0.083, and 0.11 cm s^{-1} for $M = N(C_2H_5)_4, H, Li, N(CH_3)_4, Na, K, Rb, Cs, \text{ and } NH_4$, respectively; this sequence follows that found for homogeneous self-exchange with the prominent exceptions of $M = N(CH_3)_4$ and $N(C_2H_5)_4$. Sohr et al.^{253,254} interpreted results of their studies of the $Fe(CN)_6^{3-/4-}$ electrode reaction kinetics at graphite electrodes in KCl in terms of electron transfer to or from an *adsorbed* species $\{Fe(CN)_6^{3-} \cdots K^+ \cdots Fe(CN)_6^{4-}\}$, presumably similar to that proposed as above for the analogous self-exchange in homogeneous solution. Khoshtariya and co-workers^{229,230,255–258} found near-infrared spectroscopic evidence for the existence of free species of this type (including a variety of hexa- and octacyanometalate couples and other alkali metal cations) in aqueous solution; the addition of R_4N^+ , however, caused the NIR band to disappear. At first sight, the latter observation would seem to explain why R_4N^+ are less effective than the heavier alkali metal cations in catalyzing the $Fe(CN)_6^{3-/4-}$ electrode reaction, but it fails to account for the fact that $(CH_3)_4N^+$ in particular is outstandingly efficient in catalyzing the *homogeneous* self-exchange reactions of $Fe(CN)_6^{3-/4-}$,²²⁵ $Mo(CN)_8^{3-/4-}$, and $W(CN)_8^{3-/4-}$.²³² This discrepancy between the effects of R_4N^+ relative to alkali metal cations on the rates of homogeneous and heterogeneous cyanometalate reactions can be attributed to the known tendency, noted in section 3.4, of R_4N^+ to block access to the surface of the electrode, so lowering k_{el} by removing it further from full adiabaticity¹⁸⁸ and possibly introducing dynamic artifacts through their slow desorption, the rate of which can be comparable to those of some faradaic processes.^{64,107} This is an example of the value of comparing trends in k_{el} with those in k_{ex} for a particular reaction, although here it is the *differences* that are informative rather than the anticipated similarities.

Another possible complication in seeking parallels between k_{el} and k_{ex} emerges from the observation by Bard et al.^{259,260} and subsequently Khoshtariya et al.²⁶¹ that increasing the viscosity η of an aqueous $Fe(CN)_6^{3-/4-}$ or $CrEDTA^{-2-}$ solution by addition of an inert diluent (glucose, sucrose) reduces k_{el} in a manner consistent with rate control by solvent dynamics (eqs 36 and 38–40). Further to this, Khoshtariya et al.²⁶² used alkanethiol SAMs on Au RDEs to induce varying degrees of nonadiabaticity in the aqueous $Fe(CN)_6^{3-/4-}$ electrode reaction and showed not only that there was a turnover from solvent dynamical to electronic tunneling (nona-

Table 2. Rate Constants for the $\text{Fe}(\text{CN})_6^{3-/4-}$ Electrode Reaction in 1.0 mol L⁻¹ Aqueous K⁺

medium	method	electrode	k_{el} , cm s ⁻¹	ref
KF	ILIT	Pt	1.7	190
	current impulse	Au	0.10	250, 251
	AC impedance	Au bead	0.13	252
K ₂ SO ₄	turbulent pipe flow	Pt, Au ring	0.42, 0.38	263
	turbulent pipe flow	Pt, Au ring	0.35, 0.27	263
	RDE	Pt or Au	0.02	264
	AC impedance	Pt	0.13	265
	RDE	Pt	0.07	266
KCl	fast sweep CV	Pt	0.14	267
	RDE	Au	0.07–0.10	249
	current impulse	Pt	0.028, ^a 0.24 ^b	268
	RDE	Pt, Au	0.05–0.24	264
	CV	glassy C ^c	0.14	86
	CV	HOPG basal/edge	~10 ⁻⁷ , 0.06	87a
	CV	exfoliated graphite	0.003, ^d 0.38 ^e	87b
	RDE	Pt	0.05	266
	CV	Pt	<0.010, ^f 0.18–0.23 ^g	269
	AC impedance	Pt	0.09	265
	RDE	Pt	0.068	108
	rotating cell	Pt	0.08	270
	fast scan voltammetry	Pt UME	0.1–0.25	93
fast scan voltammetry	Pt UME	0.24, 0.42, ^h 0.56 ⁱ	271	
RDE	Au, Pt	0.07–0.10, 0.078	272	

^a Oxidized Pt. ^b Reduced Pt. ^c Activated by repeated polishing with Al₂O₃ and sonication; deactivated slowly with time. ^d Polished electrode. ^e 400-grit rough finish. ^f Pt cleaned with aqua regia or anodic pulsing alone. ^g Pt cleaned by flaming or multiple methods including flaming. ^h 5 mmol L⁻¹ KCN present in electrolyte. ⁱ 5 mmol L⁻¹ KCN present in electrolyte; 10 mmol L⁻¹ KCN in alumina polishing slurry.

diabatic) control of the reaction rate as the thickness of the SAM was increased but also that the Marcus barrier was concomitantly reduced, as per eqs 36 and 38–40. There is no evidence for solvent dynamical control of the corresponding homogeneous electron transfer reaction.

A further illustration from the aqueous $\text{Fe}(\text{CN})_6^{3-/4-}$ paradigm regarding the difficulty of achieving a meaningful correlation of k_{el} with k_{ex} in the spirit of Figure 1 is the discouraging disagreement in the literature regarding k_{el} for the aqueous $\text{Fe}(\text{CN})_6^{3-/4-}$ electrode reaction. The extent of these problems can be gauged by the data given in Table 2 for the $\text{Fe}(\text{CN})_6^{3-/4-}$ electrode reaction with a particular cation concentration (1.0 mol L⁻¹ aqueous K⁺ as KF, KCl, or K₂SO₄). The lack of consistency is due partly to the tendency of reactant decomposition products (variously described as cyanides, cyanoferrates, or Prussian blue) to adsorb on the electrode, particularly when the supporting electrolyte is a Li or Na salt. This can be minimized by addition of cyanide ion^{93,271–273} or high concentrations of an appropriate supporting electrolyte such as KCl (which may stabilize the reactants in solution through ion pairing) or by careful cleaning of the electrode before each measurement (for successive measurements in the confinement of a pressurizable cell, this can be done by potential cycling to sufficiently negative potentials⁵⁷).^{82,90–93,108,251,269,271–273} The reactants themselves may also adsorb on Au electrodes.¹⁹⁰ As discussed in section 2.6, electrode properties can also affect reaction rates unless the electrode reaction is fully adiabatic at the electrode chosen. In particular, the work of Goldstein and Van De Mark²⁶⁹ highlights the importance of choosing an appropriate mode of electrode cleaning, the most consistent k_{el} values being also the fastest. These authors, while confirming the effect Li < Na < K < Rb < Cs of cations on

k_{el} for the $\text{Fe}(\text{CN})_6^{3-/4-}$ electrode reaction, also found a significant influence of supporting electrolyte anions that had been considered unimportant by previous investigators²⁴⁹ and is not apparent in Table 2; Kulesza et al.²⁷⁴ confirm the anion effect but note that it is not large.

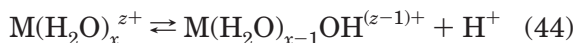
All in all, it is evident from Table 2 that the greater the pains taken to minimize these problems and the more adaptable the measurement technique is to follow fast reactions, the higher the observed value of k_{el} will be. Indeed, Galus et al.²⁷² in 1983 concluded that all k_{el} values for $\text{Fe}(\text{CN})_6^{3-/4-}$ in various media reported to that time were too low. It now seems likely that the “true” value of k_{el} for $\text{Fe}(\text{CN})_6^{3-/4-}$ in 1.0 mol L⁻¹ aqueous K⁺ media is around 2 cm s⁻¹;¹⁹⁰ this, combined with the corresponding k_{ex} of 4.3×10^4 L mol⁻¹ s⁻¹ reported recently,¹⁰⁹ gives a significantly better fit to Figure 1 than do the values used by Cannon,¹ but it should be borne in mind that the two-body Marcus theory implicit in the expectation of a linear correlation in Figure 1 may not be appropriate for the three-body $\text{Fe}(\text{CN})_6^{3-/4-}/\text{M}^+$ reaction. The essential point here is that the leveling-off in k_{el} at high k_{ex} , seen in Figure 1, probably arises because (a) most standard electrochemical kinetic techniques become mass-transport (diffusion) limited as k_{el} approaches and exceeds 1 cm s⁻¹ and (b) electrode surface effects may result in reduced rates for the electrode reaction, possibly by increasing nonadiabaticity—clearly, there are no corresponding limits on k_{ex} . In addition, solvent dynamical control of k_{el} , if present, is unlikely to be matched by corresponding constraints on k_{ex} .

Finally, Lee and Anson’s study⁷⁸ of the aqueous $\text{Fe}(\text{CN})_6^{3-/4-}$ electrode reaction rate using C or Pt UMEs with very low concentrations of hexacyanoferrate without supporting electrolyte resulted in what was termed “a very pronounced inhibition” of

the rate of reduction of $\text{Fe}(\text{CN})_6^{3-}$ with an explanation given in terms of double-layer effects. Experience with the corresponding homogeneous self-exchange reaction¹⁰⁹ indicates that this “inhibition” would be better described quite simply as an absence of the cation-catalyzed path, the cation-independent path being too slow to measure with the techniques available. An attempt,²⁷⁵ using ACV with a conventional Pt wire electrode and 0.1 mol L⁻¹ KCl supporting electrolyte, to expose the uncatalyzed $\text{Fe}(\text{CN})_6^{3-/4-}$ electrode reaction path by adding 18-crown-6 to sequester the K⁺ progressively¹⁰⁹ (so retaining some of the benefits of the supporting electrolyte while reducing the free K⁺(aq) concentration) led to a reaction rate too slow to be measured by ACV as $[\text{K}^+]_{\text{free}}$ approached zero. The point is made that none of the reported k_{el} values for the aqueous “ $\text{Fe}(\text{CN})_6^{3-/4-}$ ” electrode reaction refer to that actual couple, but rather to a pathway involving $\{\text{M}^+, \text{Fe}(\text{CN})_6^{3-/4-}\}$ at some particular $[\text{M}^+]$. It may be remarked in passing that the choice by Stevens et al.²⁷⁶ of $k_{\text{el}} = 0.04 \text{ cm s}^{-1}$ for simulation of the reduction kinetics of $\text{K}_3[\text{Fe}(\text{CN})_6]$ (0.050 mol L⁻¹) at a glassy carbon RDE both with and without added KCl (1.0 mol L⁻¹) would seem to be inappropriate.

3.8. Metal Aqua Ions in Aqueous Solution

Metal aqua ions in aqueous solution show certain traits that set them apart from other metal complexes. For example, the “hydrolysis” of metal aqua ions,



can lead to greatly enhanced rates of self-exchange in the homogeneous reaction 2 because the conjugate base complex (e.g., $\text{Fe}(\text{H}_2\text{O})_5\text{OH}^{2+}$ ^{277,278}) can engage in an inner-sphere electron transfer mechanism in which the hydroxo ligand acts as the bridge. A study⁵⁷ of the $\text{Fe}^{\text{III/II}}(\text{aq})$ electrode reaction in $\text{HClO}_4/\text{NaClO}_4$ solutions of constant ionic strength found no evidence for a pathway involving $\text{Fe}(\text{H}_2\text{O})_x\text{OH}^{2+}$ (k_{el} actually declined somewhat as $[\text{H}^+]$ was reduced, at least in part because of a minor effect of the rising $[\text{Na}^+]$), implying that conjugate base pathways are not mechanistically important in heterogeneous electron transfer. More generally, Hupp and Weaver²⁷⁹ showed that for $\text{M}(\text{aq})^{3+/2+}$ both the work-corrected k_{el} (at a Hg electrode) and k_{ex} increased in the sequence $\text{M} = \text{Cr} < \text{Eu} \leq \text{Fe} < \text{V} < \text{Ru}$ but, with the exception of $\text{M} = \text{V}$ at $\text{pH} \geq 1$, k_{el} (unlike k_{ex}) was independent of pH as long as $[\text{MOH}(\text{aq})^{2+}]$ was small compared to $[\text{M}(\text{aq})^{3+}]$.

Hupp and Weaver²⁷⁹ found that $\log k_{\text{el}}$ was a linear function of $\log k_{\text{ex}}$ for $\text{M}(\text{H}_2\text{O})_6^{3+/2+}$ with slope about 0.5, consistent with eqs 24 and 25 (cf. Figure 1) but not with eq 27; however, the case $\text{M} = \text{Fe}$ fitted the correlation only if a k_{ex} value estimated from the Marcus cross-relation were used, the directly measured value being reproducibly about 10³-fold higher.^{277,278} The discrepancy between measured and cross-relation values of k_{ex} for $\text{Fe}(\text{H}_2\text{O})_6^{3+/2+}$ has been noted by other authors and attributed to an inner-sphere mechanism for the self-exchange process,^{146,280}

but there is no relevant evidence, mechanistic or crystallographic, that an aqua ligand as such can be effective as a bridging ligand between metal ions, and Sutin et al.²⁷⁷ found no reason to invoke this unlikely scenario. The most likely explanation, supported by theoretical considerations,^{281–285} is that the $\text{Fe}(\text{H}_2\text{O})_6^{3+/2+}$ self-exchange reaction (free energy change $\Delta G^0 = 0$) is not fully adiabatic unless there is interpenetration of the first coordination spheres of the reactants, the cross-reactions being substantially less adiabatic because the mismatch between precursor and successor states increases with the increasing $|\Delta G^0|$.

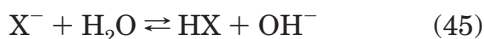
There is also much disagreement over k_{el} for $\text{Fe}(\text{H}_2\text{O})_6^{3+/2+}$ with uncorrected values in aqueous perchloric acid ranging from 7×10^{-6} to $2 \times 10^{-2} \text{ cm s}^{-1}$.^{57,83,84,105,106,110,265,279,286} The value of k_{el} at a mercury electrode ($\sim 2.5 \times 10^{-5} \text{ cm s}^{-1}$, corrected to $\sim 1 \times 10^{-4} \text{ s}^{-1}$) reported by Hupp and Weaver²⁷⁹ was estimated by Tafel extrapolation, since Hg is oxidized at the E^0 of the $\text{Fe}(\text{H}_2\text{O})_6^{3+/2+}$ couple, so a poor fit to the $\log k_{\text{el}}$ vs $\log k_{\text{ex}}$ correlation (using the true, measured k_{ex}) is perhaps to be expected. The argument^{105,106} that catalysis of the electrode reaction by traces of chloride or other potential bridging ligands in the reaction media electron transfer could cause such a wide range in k_{el} seems unrealistic and is in any case inconsistent with the observed¹¹⁰ linearity of the Arrhenius temperature dependence of the $\text{Fe}(\text{H}_2\text{O})_6^{3+/2+}$ electrode reaction kinetics in aqueous HClO_4 into temperatures at which some Fe^{III} -catalyzed decomposition of HClO_4 to Cl^- is inevitable (section 2.7). Furthermore, one of the highest k_{el} values reported for $\text{Fe}(\text{H}_2\text{O})_6^{3+/2+}$ at a Pt electrode in perchlorate media (0.020 cm s^{-1} at 25 °C) was obtained in solutions shown to contain $< 3 \text{ nmol L}^{-1} \text{ Cl}^-$.⁵⁷ Again, the most likely explanation of the wide spread in k_{el} is nonadiabaticity and consequent marked dependence on the nature of the electrode surface (section 3.3). This is shown most clearly in the study of the $\text{Fe}(\text{H}_2\text{O})_6^{3+/2+}$ electron transfer kinetics at single-crystal gold electrodes by Hromadová and Fawcett,⁸³ who found that k_{el} in 0.1 mol L⁻¹ HClO_4 ranged from $7.0 \times 10^{-6} \text{ cm s}^{-1}$ at Au(210) to $1.8 \times 10^{-3} \text{ cm s}^{-1}$ at Au(111). These authors noted that the complexity of this system is increased by the presence of a significant fraction of the Fe^{III} as $\text{Fe}(\text{aq})\text{ClO}_4^{2+}$. Nevertheless, they were able to analyze the double-layer effects in the system and located the reaction site in the diffuse layer, the distances from the Fe center to the Au surface being 786 pm for Au(210) and 641 pm for Au(111), in good agreement with the theoretical predictions of Smith and Halley²⁸⁷ of the distance dependence of k_{el} at a generic metal electrode. The transition between adiabatic and nonadiabatic electron transfer is predicted to occur at about 400 pm.²⁸⁷

Weaver^{142,150,288} noted that aqueous $\text{M}(\text{H}_2\text{O})_x^{z+/(z-1)+}$ couples in general react more slowly at an electrode than expected from their homogeneous self-exchange rates by comparison with analogous couples (e.g., metal amines $\text{M}(\text{NH}_3)_x^{z+/(z-1)+}$, with specific reference to $\text{M} = \text{Cr}$) and attributed this to the larger hydrated radii of the aqua complexes. In other words,

a second coordination sphere (solvation sheath) of water molecules is better defined in the aqua complexes than in (for example) ammines because of the greater propensity of the former to form hydrogen bonds, resulting in a very narrow (10–30 pm) reaction zone thickness, $\delta\sigma_{\text{el}}$ (eq 31). Hupp and Weaver²⁸⁸ took this to mean that electrode reactions of $\text{M}(\text{H}_2\text{O})_x^{z+(z-1)+}$ in general are marginally nonadiabatic or at least less adiabatic than those of other metal complexes. Hupp and Weaver¹⁴⁷ noted that the effect of nonadiabaticity is to oblige reacting centers to be in very close proximity for electron transfer to occur and also²⁸⁸ inferred that electron tunneling takes place over roughly comparable distances in electrode reactions as in self-exchange in bulk solution—meaning, in effect, that the Marcus model relating k_{el} to k_{ex} is to be preferred over that of Hush (section 3.1).

3.9. Nonaqueous Systems

The $\text{Fe}(\text{CN})_6^{3-/4-}$ and $\text{Fe}(\text{H}_2\text{O})_6^{3+/2+}$ paradigms were considered in some detail in sections 3.7 and 3.8 because they epitomize many of the problems encountered in measuring and interpreting the aqueous electrode kinetics of anionic and cationic couples, respectively. In section 4, difficulties specific to other aqueous couples will be noted when those couples are considered. For nonaqueous media, further obstacles emerge;^{165,289,290} some are simply matters of an increased importance of factors considered above, for example, increased uncompensated resistance and ion association, but with organic solvents there are frequently problems with persistent redox-active impurities and absorbed water.²⁹¹ Often, attempts to purify the solvent lead to fresh contamination with decomposition products. The choice of supporting electrolytes in nonaqueous media is often limited by solubility to tetraalkylammonium salts, which, as noted above, may diminish k_{el} through blockage of electrode surfaces through adsorption, the effect increasing with the alkyl chain length as expected for induced nonadiabaticity (cf. SAMs),^{188,292–294} and may introduce dynamic artifacts through slow desorption.¹⁰⁷ On the other hand, nonaqueous media can offer improved solubilities of metal complexes of low or zero charge such as metallocenes, a variety of liquid ranges, and often wide ranges of electrochemical stability (that for water is limited by H_2 and O_2 evolution). Aprotic solvents also give freedom from complications due to Brønsted acid–base phenomena—for example, metal ion (eq 44) and anion (eq 45) hydrolysis.



One major characteristic of reaction 1 in nonaqueous solutions is that fluidity-related phenomena attributable to solvent dynamical influences on k_{el} (section 3.4) become clearly evident as one goes from solvent to solvent.^{53,54,96,188,295,296} This aspect has been considered at length by Weaver's group for metallocene couples including $\text{MCp}_2^{+/0}$ and $\text{MCp}^*_{2+/0}$ ($\text{M} = \text{Fe}$ and Co),^{145,154,172,212,218,297,298} $\text{Ru}(\text{hfac})_3^{0/-}$,¹⁴⁸ the clathrochelates $\text{Co}(\text{dmg}_3(\text{BF})_2)^{+/0}$ and $\text{Co}(\text{dmg}_3-$

$(\text{BC}_4\text{H}_9)_2)^{+/0}$,²⁹⁹ and am(m)ine complexes such as $\text{Co}(\text{en})_3^{3+/2+}$, $\text{Co}(\text{NH}_3)_6^{3+/2+}$, and $\text{Ru}(\text{NH}_3)_6^{3+/2+}$.³⁰⁰ The metallocenes have the advantage that $\Delta G_{\text{IR}}^\ddagger$ is small enough to neglect, while work corrections, ion-pairing, and Debye–Hückel effects are minimal because one partner is uncharged, so ΔG^\ddagger is dominated by $\Delta G_{\text{SR}}^\ddagger$. For a given couple, the problem is then to apportion the effects of changing the solvent on k_{el} and k_{ex} between the pseudothermodynamic $\Delta G_{\text{SR}_2}^\ddagger$ which is governed by the so-called Pekar factor ($\epsilon_{\text{op}}^{-1} - \epsilon^{-1}$) (eqs 21–27), and a solvent frictional effect on the preexponential factor, governed by $\tau_{\text{L}}^{-\theta}$ or, less rigorously, $\eta^{-\theta}$ (eqs 35–40). For metallocene self-exchange reactions, Weaver et al.¹⁵⁴ used independent estimates of $\Delta G_{\text{SR}}^\ddagger$ from corresponding measurements on the optical electron transfer energy of biferrocenylacetylene to obtain a “barrier-corrected” rate constant k'_{ex} . Plots of $\log k'_{\text{ex}}$ against $\log \tau_{\text{L}}^{-1}$ for five metallocene couples in 11 solvents were somewhat scattered and not convincingly linear, but those for various cobaltocenes had slopes approaching 1.0 although for the $\text{FeCp}_2^{+/0}$ couple k'_{ex} seemed to show little if any dependence on τ_{L}^{-1} . Following a reevaluation of the $\text{FeCp}_2^{+/0}$ data, however, Weaver et al.²¹² concluded that the barrier-crossing frequency for the $\text{FeCp}_2^{+/0}$ self-exchange reaction was limited by both solvent dynamics and donor–acceptor coupling, much as for the other metallocenes studied (see, however, Zahl et al.²¹⁹ and section 4.1). Weaver et al.^{155,212} proceeded to use these results to extract electronic matrix elements H_{12} for the various self-exchange reactions. For the $\text{CoCp}_2^{+/0}$ electrode reaction in 13 solvents,²¹⁸ the observed $\log k_{\text{el}}$ data were “utterly inconsistent” with values calculated from TST-based theory (eqs 19, 23, and 31) but roughly followed the trend in theoretical values derived from the solvent dynamical model (eqs 35–40; alcohols, being non-Debye solvents, showed sharp deviations from predictions). Similarly, inclusion of solvent dynamical effects in theoretical values of k_{el} for the $\text{FeCp}^*_{2+/0}$, $\text{MnCp}^*_{2+/0}$, and $\text{Cr}(\text{C}_6\text{H}_6)_2^{+/0}$ electrode reactions gave markedly better agreement with the observed values.¹⁴⁵

Fawcett and Opałto¹⁸⁸ found evidence for various degrees of solvent dynamical control of 18 inorganic and organic electrode reactions in acetonitrile and DMF, with the exponent θ ranging from 0.1 to 1.0 (a selection is given in Table 1). The electrooxidation of $\text{Ru}(\text{phen})_3^{3+/2+}$ at Pt or Au affords an ideal case study in this context, and Fawcett et al.²⁹⁵ found the measured k_{el} to be independent of both electrode material and supporting electrolyte concentration, indicating full adiabaticity and the absence of ion pairing and double-layer effects; here again, k_{el} in seven solvents was found to depend primarily on $\tau_{\text{L}}^{-\theta}$ with $\theta \approx 0.9$ or equivalently on $\eta^{-\theta}$ with $\theta \approx 1.0$, as expected for a fully adiabatic reaction.

As proposed by Sumi and Marcus^{181,183} and Marcus and Nadler,¹⁸² solvent dynamical control of electrode reaction rates is not necessarily limited to couples with a low $\Delta G_{\text{IR}}^\ddagger$. For electron transfer between low-spin Co^{III} and high-spin Co^{II} , major internal reorganization can result from the Jahn–Teller-type distortions characteristic of both high- and low-spin Co^{II} ,

giving large $\Delta G_{\text{IR}}^{\ddagger}$ and correspondingly slow reaction rates, particularly in chelate complexes (though not in cage-type complexes where ligand reorganization is constrained).²⁰² Nielson and Weaver²⁹⁹ found large solvent dependences of k_{el} at Hg for $\text{Co}(\text{en})_3^{3+/2+}$ and $\text{Co}(\text{NH}_3)_6^{3+/2+}$ in water, formamide, AN, PC, *N*-methylformamide, DMF, and DMSO¹³⁷ that appeared to be due to differences in interfacial solvation, but for the $\text{Ru}(\text{NH}_3)_6^{3+/2+}$ electrode reaction (which is considered to be fully adiabatic, sections 2.6 and 3.3) in water, DMF, PC, and DMSO, the solvent dependence of k_{el} showed the influence of solvent dynamics. For the clathrochelates $\text{Co}(\text{dmg}_3(\text{BF})_2)^{+/0}$ and $\text{Co}(\text{dmg}_3(\text{BC}_4\text{H}_9)_2)^{+/0}$, electron transfer is accompanied by extensive internal reorganization, but again there is a marked dependence of k_{el} (through the preexponential factor Z_{el}) on the overdamped solvent relaxation dynamics.²⁹⁹ Pyati and Murray³⁰¹ found that k_{el} for $\text{Co}(\text{bpy})_3^{3+/2+}$ in dichloromethane, AN, acetone, PC, and a series of oligomeric polyether solvents (glymes) for which τ_{L} is known gave linear log–log correlations of slope 1.0 with both the solvent fluidity, η^{-1} , and τ_{L}^{-1} over a 500-fold range in these parameters and also with the reactant mean diffusion coefficient D (which, through the Stokes–Einstein law, is proportional to η^{-1}). These results indicate rate control by solvent dynamics and imply the absence of any lower limit of rate control by solvent friction. Furthermore, by attaching oligomeric polypropylene oxide chains R to the bpy ligands, Murray et al.³⁰² prepared undiluted $\text{Co}^{\text{II}}(\text{R}_2\text{bpy})_3^{2+}$ molten salts, in which log k_{el} for $\text{Co}^{\text{III/II}}$ redox was shown by CV peak separation to be linearly related to log η^{-1} and to log D with close to unit slope over 11 orders of magnitude. This approach has been extended³⁰³ to the Co^{III} self-exchange reaction in highly viscous melts of $\text{Co}(\text{bpy})_3^{2+}$ and $\text{Co}(\text{phen})_3^{2+}$ salts of hybrid polyether–sulfonates into which CO_2 was sorbed; here, k_{ex} correlates better with the diffusion coefficient for the counterion, implying a new kind of “solvent” dynamical control of electron transfer rates.

By contrast, solvent dynamical effects are difficult to identify unambiguously in water, which stands in a class by itself as a solvent. One option is to increase the viscosity of aqueous solutions progressively by addition of a presumed inert solute such as a sugar. In this way, Bard et al.²⁵⁹ showed that k_{el} for $\text{Fe}(\text{CN})_6^{3-/4-}$ at Pt in aqueous K_2SO_4 containing dextrose and for $\text{FeCp}_2^{+/0}$ in DMSO containing $[(\text{C}_4\text{H}_9)_4\text{N}][\text{BF}_4]$ and sucrose was a linear function of the fluidity, η^{-1} , of the solvent. Because these reactions were known to be far from the diffusion-controlled limit and the impact of dextrose on solution properties other than η was minimal, the viscosity effect could be confidently ascribed to solvent friction. Similarly, Bard et al.²⁶⁰ found that the electrode reaction kinetics of $\text{Cr}(\text{EDTA})^{-2-}$ in aqueous sucrose showed the expected dependence on the Pekar factor ($\epsilon_{\text{op}}^{-1} - \epsilon^{-1}$) (eq 23) only if the frequency factor Z_{el} were taken to be proportional to η^{-1} , while for ferrocenemethanol in aqueous DMSO mixtures of varying viscosities, excellent correlations of unit slope were found between $\ln k_{\text{el}}$ and $\ln \tau_{\text{L}}$ or $\ln \eta^{-1}$.³⁰⁴ Khoshtariya et al. pursued further the electrode

kinetics of $\text{Fe}(\text{CN})_6^{3-/4-}$ in aqueous glucose solutions and found evidence for solvent dynamical rate control at Pt,²⁶¹ while at Au electrodes coated with *n*-alkanethiol SAMs, there was a turnover from solvent-dynamical to nonadiabatic rate control (eqs 38–40) on lengthening the alkyl chain length in the SAM.²⁶² The kinetics at bare Au electrodes showed a reduction of the free-energy barrier by a factor of 2 in association with solvent dynamical control (eq 39). For electrode reactions in undiluted water, however, it seems that the contributions of uniquely fast solvent dynamical modes to $k_{\text{r}}^{173-177}$ result in k_{TST} becoming the bottleneck in eq 37 (section 3.4).

To summarize, there is extensive evidence for solvent dynamical rate control of *electrode* reaction rates in nonaqueous solvents and modified aqueous solutions, but none so far for *self-exchange* reactions of metal complexes with the possible exception of Co metallocenes in organic solvents.¹⁵⁴

4. Insights from Pressure Effects

It is convenient to present pressure effects on k_{ex} and k_{el} in terms of ostensibly pressure-independent volumes of activation, although the normal decrease in the compressibility β of a solvent with rising pressure (and hence in the pressure dependence of n , ϵ , etc.) predicts a corresponding decrease in $|\Delta V_{\text{ex}}^{\ddagger}|$ and $|\Delta V_{\text{el}}^{\ddagger}|$ (eqs 21 and 23). One way of avoiding this problem is to calculate theoretical rate constants over a range of pressures relative to zero applied pressure for comparison with observed values,³⁰⁵ but this turns out to be a rather severe test. In practice, plots of $\ln k_{\text{el}}$ or $\ln k_{\text{ex}}$ vs P are almost always linear to within experimental uncertainty over the customary pressure range of 0–200 MPa, and the data can be presented as a single volume of activation valid at the midrange point (100 MPa). In theoretical analyses, however, values of parameters such as ϵ and n for the midrange point should be used.

4.1. Pressure Effects on Homogeneous Electron Transfer Kinetics

The high-pressure experimental methods (NMR line widths, radioisotopic tracers, stopped-flow circular dichroism change) have been summarized elsewhere.^{199,306} Following an approach taken by Stranks,³⁰⁷ experimental $\Delta V_{\text{ex}}^{\ddagger}$ values for adiabatic self-exchange reactions can be interpreted along Marcus–Hush (TST) lines in terms of calculated values $\Delta V_{\text{ex}(\text{calcd})}^{\ddagger}$ containing contributions from internal reorganization (IR), solvent reorganization (SR), Debye–Hückel effects (DH) according to the BBC equation (eq 41), the exponential part of the Coulombic work terms (Coul), and any pressure-dependence of the preexponential term $Z_{\text{ex}(\text{pre})}$:¹⁹⁹

$$\Delta V_{\text{ex}(\text{calcd})}^{\ddagger} = \Delta V_{\text{IR}}^{\ddagger} + \Delta V_{\text{SR}}^{\ddagger} + \Delta V_{\text{DH}}^{\ddagger} + \Delta V_{\text{Coul}}^{\ddagger} + \Delta V_{\text{pre}}^{\ddagger} \quad (46)$$

These contributions can be calculated from the pressure derivatives of eqs 20–22, 28, 30, and 41. If IR is simply a matter of bond length increases in one

reactant (usually the oxidant) and compensatory decreases in the other to a common configuration for electron transfer to occur, $\Delta V_{\text{IR}}^{\ddagger}$ will be zero except for a small contribution from changes in reactant compressibilities; for typical metal complexes, Stranks³⁰⁷ estimated this to be $\sim 0.6 \text{ cm}^3 \text{ mol}^{-1}$, which is barely outside the usual experimental uncertainty in $\Delta V_{\text{ex}}^{\ddagger}$ and may be neglected in many cases. If, however, major structural reorganization is associated with electron transfer in reaction 2, then large $\Delta V_{\text{IR}}^{\ddagger}$ values may result—for example, in flexible $\text{Co}^{\text{III/II}}$ chelate complexes, where the change from low-spin $3d^6 \text{ Co}^{\text{III}}$ to high-spin $3d^7 \text{ Co}^{\text{II}}$ (possibly via Jahn–Teller-distorted low-spin Co^{II} complexes) involves large changes in geometry and consequent large negative contributions to $\Delta V_{\text{IR}}^{\ddagger}$.^{60,202}

In earlier treatments,³⁰⁵ it was supposed that the separation σ between the metal centers corresponding to the highest probability of electron transfer might exceed the hard-contact distance ($r_1 + r_2$) sufficiently that its pressure dependence (given by $\beta/3$, where β is the isothermal compressibility of the medium) should be included in calculations of $\Delta V_{\text{SR}}^{\ddagger}$ and $\Delta V_{\text{pre}}^{\ddagger}$. It transpires that the effects on $\Delta V_{\text{SR}}^{\ddagger}$ and $\Delta V_{\text{pre}}^{\ddagger}$ effectively cancel, but in any case, the reaction zone thickness, $\delta\sigma$ (eq 30), is believed to be very small compared to the almost incompressible ($r_1 + r_2$), so σ may justifiably be assumed to be pressure-independent. The same conclusion applies to the possibility of a significant pressure dependence of the electronic transmission coefficients κ_{ex} and κ_{el} (eqs 30, 31, and 34); in our recent investigation²¹⁹ of the $\text{FeCp}^{*2+/0}$ self-exchange reaction in organic solvents, calculations of the distance dependence of H_{12} by Friesner et al.³⁰⁸ were used to show that the contribution of nonadiabaticity to $\Delta V_{\text{ex}}^{\ddagger}$ would be less than $0.1 \text{ cm}^3 \text{ mol}^{-1}$, while the conclusion by Weaver (section 3.8) that nonadiabatic electron transfer requires very close approach of a reactant to its partner (or to the OCP of an electrode) indicates that the earlier expectation^{305,309} of a large negative contribution to $\Delta V_{\text{ex}}^{\ddagger}$ from nonadiabaticity was simply wrong. In short, $\Delta V_{\text{ex}}^{\ddagger}$ is indifferent to nonadiabaticity, and insofar as TST is applicable, $\Delta V_{\text{pre}}^{\ddagger}$ is negligible. Thus we have^{199,201,305,307}

$$\Delta V_{\text{SR}}^{\ddagger} = (N_{\text{A}}e^2/(16\pi\epsilon_0))[(2r_1)^{-1} + (2r_2)^{-1} - \sigma^{-1}] \times [\partial(n^{-2} - \epsilon^{-1})/\partial P]_{\text{T}} \quad (47)$$

$$\Delta V_{\text{DH}}^{\ddagger} = [RTz(z-1)AI^{1/2}/(1+B\hat{a}I^{1/2})^2] \times [(\partial \ln \epsilon/\partial P)_{\text{T}}(3 + 2B\hat{a}I^{1/2}) - \beta] \quad (48)$$

$$\Delta V_{\text{Coul}}^{\ddagger} = [N_{\text{A}}z(z-1)e^2/(4\pi\epsilon_0\sigma)](\partial\epsilon^{-1}/\partial P)_{\text{T}} \quad (49)$$

It turns out that $\Delta V_{\text{DH}}^{\ddagger}$ and $\Delta V_{\text{Coul}}^{\ddagger}$ have opposite signs and, for practical values of the ionic strength I in aqueous systems, tend to cancel, so $\Delta V_{\text{SR}}^{\ddagger}$ emerges as the dominant component of $\Delta V_{\text{ex}}^{\ddagger}$. For nonaqueous solvents of low dielectric constant ϵ , however, these two terms can become huge and their cancellation far from complete, so the calculation of $\Delta V_{\text{ex}}^{\ddagger}$

becomes numerically unstable and, because the compressibilities β of nonaqueous solvents (which ultimately govern solvent parameters such as n and ϵ ³⁰⁵) generally decrease sharply with rising pressure, highly pressure-dependent.^{199,310} In such circumstances, however, ion pairing is also likely to be important; the effect of rising pressure is to break up ion pairs through increasing ϵ (eq 42), so if ion pairing hinders electron transfer (as seems to be the case in absence of specific counterion effects, section 3.6), this will increase k_{ex} and make a negative contribution to $\Delta V_{\text{ex}}^{\ddagger}$. Unfortunately, there is at present no way to predict quantitatively the extent to which ion pairing might affect k_{ex} unless it is assumed that ion pairs are completely unreactive, which seems unrealistic, so incorporation of the pressure derivative of eq 42 into eq 46 would probably result in an overcorrection for ion pair effects. In summary, eqs 46–49 are expected to fail for solvents of low dielectric constant *except for couples in which one partner is uncharged*, in which case $\Delta V_{\text{DH}}^{\ddagger}$ and $\Delta V_{\text{Coul}}^{\ddagger}$ are by definition zero and ion pairing of the singly charged partner should be minimal. Even so, the nonlinearity of the pressure dependences of n and ϵ may cause a marked pressure dependence of the calculated $\Delta V_{\text{SR}}^{\ddagger}$, which remains as the only significant component of $\Delta V_{\text{ex}}^{\ddagger}$ (if $\Delta V_{\text{IR}}^{\ddagger}$ is small (i.e., if no major structural rearrangements accompany electron transfer)).

For aqueous systems and the more polar organic solvents, however, the measured $\Delta V_{\text{ex}}^{\ddagger}$ is satisfactorily matched by values $\Delta V_{\text{ex}}^{\ddagger(\text{calcd})}$ from eqs 46–49 for cases that we will call “well-behaved”—that is, ones in which the reaction appears to be a simple outer-sphere electron transfer process between two reactant molecules—and these are collected in Table 3. Table 4 lists cases in which $\Delta V_{\text{ex}}^{\ddagger}$ is in poor agreement with $\Delta V_{\text{ex}}^{\ddagger(\text{calcd})}$; such instances, so far from representing failures of the variable-pressure approach, give valuable insights into mechanistic aberrations. The quoted values of $\Delta V_{\text{ex}}^{\ddagger(\text{calcd})}$ in Tables 3 and 4 either are those given by the original authors or are calculated from eqs 46–49 using pressure dependences of solvent properties traceable through ref 305.

4.2. “Well-Behaved” Homogeneous Self-Exchange Reactions

The two most obvious common features of the well-behaved couples in Table 3 are, first, that they span all charge types, ranging from $5+/4+$ to $3-/4-$ (the $3-/4-$ case, however, is one in which the cations have been sequestered with a cryptand or a crown ether¹⁰⁹) and, second, that all the $\Delta V_{\text{ex}}^{\ddagger}$ and $\Delta V_{\text{ex}}^{\ddagger(\text{calcd})}$ values are *negative*. As expected for water and the more polar nonaqueous solvents, there are no significant effects attributable to ion pairing except possibly for the manganese(II/I) isonitrile couples in methanol and acetonitrile—these data, however, need to be viewed in comparison with those for the same couples in less polar solvents in Table 4. For $\text{FeCp}^{*2+/0}$, $\Delta V_{\text{ex}}^{\ddagger}$ and $\Delta V_{\text{ex}}^{\ddagger(\text{calcd})}$ match well even in CD_2Cl_2 (for which

Table 3. Volumes of Activation for Self-Exchange Reactions that Conform to Theoretical Predictions of Eqs 46–49

couple ^a	solvent	electrolyte (concn, mol L ⁻¹)	T, °C	$\Delta V_{\text{ex}}^{\ddagger}$ cm ³ mol ⁻¹	$\Delta V_{\text{ex}}^{\ddagger(\text{calcd})}$ ^b cm ³ mol ⁻¹	ref
Fe(H ₂ O) ₆ ^{3+/2+}	H ₂ O	HClO ₄ (0.5)	2	-11.1 ± 0.4	-10.4	278
Fe(phen) ₃ ^{3+/2+}	D ₂ O	D ₂ SO ₄ (0.1)	3	-2.2 ± 0.1	-2.5	311
	CD ₃ CN	anion ClO ₄ ⁻	4	-5.9 ± 0.5	-4.2 ^c	311
Fe(CN) ₆ ^{3-/4-}	H ₂ O	KCl (0.2) ^d	25	-11.3 ± 0.3	-11	109
FeCp ^{*2+/0}	(CD ₃) ₂ CO	anion PF ₆ ⁻ , BF ₄ ⁻	25	-8.7 ± 0.2	-9.5 ^e	219
	CD ₂ Cl ₂	anion PF ₆ ⁻	25	-6.4 ± 0.1	-6	219
FeCp ₂ ⁺⁰	CD ₃ CN	anion PF ₆ ⁻	0	-7 ± 2	-9.6	213, 219
Co(ttcn) ₂ ^{3+/2+}	D ₂ O	CF ₃ SO ₃ K (0.1)	25	-4.8 ± 0.2	-5.3	312
Co(sep) ^{3+/2+}	H ₂ O	NaCl (0.2)	25	-6.4 ± 0.2	-6.4	312
Co(diamsar) ^{3+/2+}	H ₂ O	CF ₃ SO ₃ K (0.1) ^f	25	-10.4 ± 0.8	-7.2	202
Co(diamsarH ₂) ^{5+/4+}	H ₂ O	CF ₃ SO ₃ H (0.4)	25	-9.6 ± 0.6	-9.7	202
Co(act) ^{3+/2+}	D ₂ O	anion ClO ₄ ⁻	25	-6.5 ± 0.5	-6.5	60
Ru(hfac) ₃ ^{0/-}	CD ₃ CN	cation (C ₄ H ₉) ₄ N ⁺	25	-5.5 ± 0.1	-5.9	198, 208
	CD ₃ OD	cation (C ₄ H ₉) ₄ N ⁺	25	-5.8 ± 0.3	-5.7	198, 208
	(CD ₃) ₂ CO	cation (C ₄ H ₉) ₄ N ⁺	25	-6.1 ± 0.3	-5.9	198, 208
Mn(CN <i>t</i> -Bu) ₆ ^{2+/+}	CH ₃ CN	anion BF ₄ ⁻	6	-12 ± 2 ^g	-16 ^h	313
	CH ₃ OH	anion BF ₄ ⁻	6	-20 ± 2 ^g	-24 ^h	313
Mn(CNchx) ₆ ^{2+/+}	CH ₃ CN	anion BF ₄ ⁻	2	-17 ± 1 ^g	-14 ^h	313
	CH ₃ OH	anion BF ₄ ⁻	2	-16 ± 2	-21	313
Cu(dmp) ₂ ^{2+/+}	(CD ₃) ₂ CO	anion CF ₃ SO ₃ ⁻	30	-7.4 ± 0.6	-6 ⁱ	314
	CD ₃ CN	anion CF ₃ SO ₃ ⁻	38	-3.4 ± 0.6	-5 ⁱ	314

^a Abbreviations as in ref 137. ^b Calculated for midrange pressure of 100 MPa except as noted. ^c Includes correction for assumed inactive ion pair according to eq 42. ^d K⁺ sequestered with Kryptofix 222. ^e At 75 MPa. ^f Plus CF₃SO₃H–morpholine buffer, pH 8.1. ^g Pressure-dependent: value given is for zero applied pressure. ^h At zero applied pressure. ⁱ At 25 °C.

Table 4. Volumes of Activation for Self-Exchange Reactions that Deviate from the Theoretical Predictions of Eqs 46–49

couple ^a	solvent	electrolyte (concn, mol L ⁻¹)	T, °C	$\Delta V_{\text{ex}}^{\ddagger}$ cm ³ mol ⁻¹	$\Delta V_{\text{ex}}^{\ddagger(\text{calcd})}$ ^a cm ³ mol ⁻¹	ref
CrOH(aq) ^{2+/Cr(aq)²⁺}	H ₂ O			+4.2 ± 1.1	-11	307
FeOH(aq) ^{2+/Fe(aq)²⁺}	H ₂ O	HClO ₄ (0.5)	2	+0.8 ± 0.9	-11	278
Fe(CN) ₆ ^{3-/4-/K⁺}	H ₂ O	KCl (1.0)	25	-2.1 ± 0.3	-11	109
	D ₂ O	KCl (1.0)	25	-0.8 ± 0.3	-11	109
Os(CN) ₆ ^{3-/4-/K⁺}	D ₂ O	cation K ⁺	25	+18.5 ± 0.8	-9	232
	D ₂ O	KCl (1.0)	25	+19.4 ± 0.9	-9	232
Mo(CN) ₈ ^{3-/4-/K⁺}	D ₂ O	cation K ⁺	25	+14.7 ± 0.6	-6	232
Mo(CN) ₈ ^{3-/4-/Et₄N⁺}	D ₂ O	cation Et ₄ N ⁺	25	-8.2 ± 0.6	-6	232
W(CN) ₈ ^{3-/4-/K⁺}	D ₂ O	cation K ⁺	25	+22.5 ± 1.1	-6	232
W(CN) ₈ ^{3-/4-/Cs⁺}	D ₂ O	CsCl (0.25) ^b	25	+16 ± 2	-6	232
W(CN) ₈ ^{3-/4-/Me₄N⁺}	D ₂ O	cation Me ₄ N ⁺	25	-7.4 ± 0.5	-6	232
Co(en) ₃ ^{3+/2+}	H ₂ O	NaClO ₄ (0.5) ^c	65	-15.5 ± 0.8 ^d	-5	309
Co(phen) ₃ ^{3+/2+}	H ₂ O	NaCl (0.1) ^e	25	-17.6 ± 0.7	-2	223
	H ₂ O	NaNO ₃ (0.1)	25	-16.0 ± 0.7	-2	223
“Co(EDTA) ₂ ”	H ₂ O	NaClO ₄ (0.5) ^f	85	-3.2 ± 0.3	+5 ^g	316
Co(dmgl ₃ (BF ₄) ₂) ⁺⁰	CH ₃ CN	anion BF ₄ ⁻	25	-15 ^h	-9	317
Ru(en) ₃ ^{3+/2+}	H ₂ O	KCl (0.4)	25	-15.1 ± 1.7 ^h	-6	60
Mn(CN <i>t</i> -Bu) ₆ ^{2+/+}	(CH ₃) ₂ CO	anion BF ₄ ⁻	6	-20 ± 2 ⁱ	-32 ^j	313
	CH ₂ Cl ₂	anion BF ₄ ⁻	0	-18 ± 2 ⁱ	-51 ^j	313
Mn(CNchx) ₆ ^{2+/+}	(CH ₃) ₂ CO	anion BF ₄ ⁻	3	-20 ± 2 ⁱ	-28 ^j	313
	CH ₂ Cl ₂	anion BF ₄ ⁻	3	-21 ± 4 ⁱ	-46 ^j	313
	C ₆ H ₅ Br	anion BF ₄ ⁻	2	-9 ± 2	-38	313
MnO ₄ ^{2-/}	50% D ₂ O	KOH etc. (1.1)	45	-17 ± 2	-9	133, 199
MnO ₄ ^{2-/K⁺}	50% D ₂ O	KOH etc. (1.1)	45	-1 ± 1	-6	133, 199
MnO ₄ ^{2-/Na⁺}	50% D ₂ O	NaOH etc. (1.1)	45	+3 ± 1	-6	133, 199

^a For bimolecular self-exchange reaction; not applicable to termolecular processes. ^b K⁺ counterion also present; >80% of reaction carried by Cs⁺ pathway. ^c Excess en present to suppress aquation of Co(en)₃²⁺. ^d Average value, 0–200 MPa; $\Delta V_{\text{ex}}^{\ddagger}$ shows some pressure dependence. ^e Excess phen present. ^f pH set to 2 with HClO₄. ^g Includes ΔV of deaquation and deprotonation of Co(HEDTA)OH₂⁻, the form of the Co^{II} complex present at pH 2. ^h From cross-reaction of Ru(en)₃²⁺ with Co(phen)₃³⁺. ⁱ Pressure-dependent: value given is for zero applied pressure. ^j At zero applied pressure. ^k From cross-reaction with FeCp₂⁺⁰.

ϵ is only 8.93 at 25 °C²⁹¹) in the absence of added electrolyte, since only one partner carries a (minimal) charge. The Co^{III/II} act, sep, and diamsar cage complexes¹³⁷ provide confirmation that $\Delta V_{\text{IR}}^{\ddagger}$ is very small if only bond length changes are involved, since $\Delta\delta$ accompanying the change between high- and low-spin states on electron transfer in these couples is

substantial²⁰² but the complexes cannot undergo major geometrical distortions. The somewhat poorer agreement between $\Delta V_{\text{ex}}^{\ddagger}$ and $\Delta V_{\text{ex}}^{\ddagger(\text{calcd})}$ for Co-(diamsar)^{3+/2+} may have originated in an unidentified interaction between the complexes and the morpholine buffer used in this one case—this couple, however, also gave an anomalously low transfer coeffi-

cient α of 0.27 in the corresponding electrode reaction at pH 9 without buffer.⁵⁷ The $\text{Co}(\text{ttn})_2^{3+/2+}$ couple is low-spin/low-spin. Inclusion of the $\text{Cu}(\text{dmp})_2^{2+/+}$ couple in Table 3 is perhaps not legitimate, because the Cu^{II} complex is far from spherical and there is a major geometrical change (nominally tetrahedral to square planar) on going from Cu^{I} to Cu^{II} , but the point is made that $\Delta V_{\text{ex}}^\ddagger$ is negative in both acetone and acetonitrile, its magnitude being roughly accounted for by the admittedly inadequate two-sphere model.

Because the effect of pressure on the viscosity η of water is fortuitously negligible over 0–200 MPa applied pressure at near-ambient temperatures (Figure 5), solvent dynamical control (section 3.6) of aqueous self-exchange reaction rates will not be revealed by variable pressure studies—in any event, the existence of fast solvent dynamical modes in undiluted water may result in k_{el} being essentially k_{TST} (sections 3.4 and 3.9 and eq 37).^{173–177} For typical organic solvents, however, η rises roughly exponentially with pressure (Figure 5), and solvent dynamics can make a substantial positive contribution $\Delta V_{\text{SD}}^\ddagger$ to $\Delta V_{\text{ex}}^\ddagger$. From eq 36, this contribution can be identified with the volume of activation, $\Delta V_{\text{visc}}^\ddagger$, for viscous flow of the solvent (eq 17), and this can in turn be equated, through the Stokes–Einstein relation for the diffusion coefficient, D ,

$$D = k_{\text{B}}T/(6\pi a\eta) \quad (50)$$

to the volume of activation, $\Delta V_{\text{diff}}^\ddagger$, for diffusion of the electroactive species. In practice, $\Delta V_{\text{diff}}^\ddagger$ is readily measurable from the pressure dependence of CV currents and is actually more appropriate than $\Delta V_{\text{visc}}^\ddagger$ for the pure solvent to the electrolyte solution conditions:

$$\Delta V_{\text{visc}}^\ddagger = RT(\partial \ln \eta / \partial P)_T = -RT(\partial \ln D / \partial P)_T = \Delta V_{\text{diff}}^\ddagger = \Delta V_{\text{SD}}^\ddagger \quad (51)$$

The very fast self-exchange of $\text{Fe}(\text{phen})_3^{3+/2+}$ in acetonitrile is one of the most likely reactions of those covered in Table 1 to exhibit solvent dynamical control, since $\Delta G_{\text{IR}}^\ddagger$ is very small in this case.¹⁷⁷ For $\text{Fe}(\text{phen})_3^{3+/2+}$ in acetonitrile (0.5 mol L⁻¹ TBAP), $\Delta V_{\text{diff}}^\ddagger$ is +8.0 cm³ mol⁻¹,⁶⁴ and the TST estimate (eqs 46–49) of $\Delta V_{\text{ex}(\text{calcd})}^\ddagger$ is -4.2 cm³ mol⁻¹, so from the pressure derivative of eq 38 with $\theta = 1$ and $\gamma = 1$ (eq 39), we have

$$\Delta V_{\text{ex}(\text{calcd},\text{SD})}^\ddagger = \Delta V_{\text{ex}(\text{calcd})}^\ddagger + \Delta V_{\text{diff}}^\ddagger \approx +4 \text{ cm}^3 \text{ mol}^{-1} \quad (52)$$

In fact, $\Delta V_{\text{ex}}^\ddagger$ is about -6 cm³ mol⁻¹, so solvent dynamical rate control can be ruled out in this case.³¹¹ In the same way, $\Delta V_{\text{ex}}^\ddagger$ for the FeCp^*_{2+0} self-exchange (for which $\Delta G_{\text{IR}}^\ddagger$ is again negligible) in acetone, dichloromethane, and (with data of limited accuracy) acetonitrile was found to be consistently negative and in good agreement with the predictions of eqs 46–49,²¹⁹ so solvent dynamical control of the kinetics can be confidently ruled out in this case too.

This conclusion is at odds with those of Weaver et al. for various metallocene couples,²¹² but it will be seen in section 4.6 that pressure effects are indeed a reliable and sensitive criterion of the presence of solvent dynamical rate control. Since $\text{Fe}(\text{phen})_3^{3+/2+}$ and FeCp^*_{2+0} are the most likely cases in Table 3 to exhibit solvent dynamical rate control because of the negligible $\Delta G_{\text{IR}}^\ddagger$, solvent dynamics can be ruled out for the other homogeneous self-exchange reactions listed in Table 3 as well. It may be noted that Drago and Ferris³¹⁵ showed that the unified solvation model, which uses a function of an empirical measure of solvent polarizability in place of the Pekar factor, can rationalize solvent effects on k_{ex} for metallocene couples without invoking solvent dynamics.

In summary, eqs 46–49 work well for uncomplicated outer-sphere self-exchange reactions of metal complexes in both aqueous and the more polar nonaqueous systems, regardless of charge-type and predict *negative* $\Delta V_{\text{ex}}^\ddagger$ values in all such cases.

4.3. “Anomalous” Homogeneous Self-Exchange Reactions

In Table 4, cases are listed in which eqs 46–49, as such, fail. For the conjugate base pathways of the $\text{Fe}(\text{aq})^{3+/2+}$ and $\text{Cr}(\text{aq})^{3+/2+}$ exchanges, the large positive departures of $\Delta V_{\text{ex}}^\ddagger$ from $\Delta V_{\text{ex}(\text{calcd})}^\ddagger$ reflect the loss of an aqua ligand from the reduced ion to allow hydroxo-bridge formation in an inner-sphere transition state²⁷⁸ (unfortunately, details of Stranks’ measurements³⁰⁷ on the Cr case have been lost). Thus, the failure of eqs 46–49 reveals a mechanism change.

For $\text{Fe}(\text{CN})_6^{3-/4-}$ in water without sequestration of the cation K^+ (Table 4), $\Delta V_{\text{ex}}^\ddagger$ exceeds that for the cation-independent path (Table 3) by about 10 cm³ mol⁻¹. A first attempt²²⁸ to measure $\Delta V_{\text{ex}}^\ddagger$ for the $\text{Fe}(\text{CN})_6^{3-/4-}/\text{K}^+$ reaction gave a seemingly reproducible but very high $\Delta V_{\text{ex}}^\ddagger$ of ~22 cm³ mol⁻¹ in repeated one-shot measurements under pressure, apparently because of a steady loss of $\text{Fe}(\text{CN})_6^{3-/4-}$ in the course of a given high-pressure experiment;¹⁰⁹ the importance of rechecking early measurements after a pressure cycle is thereby emphasized. A small solvent deuterium isotope effect may be noted. For $\text{Os}(\text{CN})_6^{3-/4-}$, $\text{Mo}(\text{CN})_8^{3-/4-}$, and $\text{W}(\text{CN})_8^{3-/4-}$, $\Delta V_{\text{ex}}^\ddagger$ values some 20–30 cm³ mol⁻¹ more positive than those calculated from eqs 46–49 were obtained with K^+ and Cs^+ as the cation, and this gives strong support to the dehydrated-cation catalysis model expounded in section 3.7. This positive excess in $\Delta V_{\text{ex}}^\ddagger$ suggests loss of some two to three waters from the first coordination sphere of the catalyzing alkali metal cation,³¹⁸ rather than complete dehydration, which would seem to be energetically unfeasible; it should be borne in mind, however, that the $\Delta V_{\text{ex}(\text{calcd})}^\ddagger$ values of Tables 3 and 4 are calculated on the basis of a two-sphere model, whereas cation catalysis is necessarily at least a three-body process. Vindication of the dehydration model comes from the observation of *negative* $\Delta V_{\text{ex}}^\ddagger$ values, similar to the two-sphere $\Delta V_{\text{ex}(\text{calcd})}^\ddagger$ estimates, for $\text{Mo}(\text{CN})_8^{3-/4-}$ and $\text{W}(\text{CN})_8^{3-/4-}$ with catalysis by tetraalkylammonium

cations, which are known²⁴⁰ not to be specifically solvated by water and so do not need to be dehydrated.

For the $\text{MnO}_4^{-/2-}$ exchange in aqueous alkali, k_{ex} can be dissected into a cation-independent term, k_{ex}^0 , and a cation-catalyzed term, k_{ex}^{M} (eq 43; cf. $\text{Fe}(\text{CN})_6^{3-/4-}$), but an effort to maintain constant ionic strength while varying $[\text{M}^+]$ forced a long extrapolation to zero $[\text{M}^+]$ to determine k_{ex}^0 . Furthermore, $\Delta V_{\text{ex}}^\ddagger$ had a noticeable pressure dependence, the value given in Table 4 being a mid-pressure-range average but, even so, much more negative than the basic two-sphere model of eqs 46–49 would predict. It was originally suggested¹³³ that the negative excess in $\Delta V_{\text{ex}}^\ddagger$ might be due partly to nonadiabaticity, as in a theoretical treatment of the $\text{MnO}_4^{-/2-}$ self-exchange kinetics by German et al.,³¹⁹ but it is now recognized (sections 3.3 and 4.1) that $\Delta V_{\text{ex}}^\ddagger$ is unlikely to be sensitive to nonadiabatic effects. It was further suggested¹³³ that the excess was due in various ways to the small sizes of the manganate and permanganate ions (the smallest transition-metal complexes), which could result in dielectric saturation, an increased importance of ion pairing (although this would account for no more than about $-2 \text{ cm}^3 \text{ mol}^{-1}$ on the Fuoss model), and failure of the two-sphere model due to the size of the reactants approaching that of the solvent molecules. This last complication was addressed by treating the transition state as two ions inside an ellipsoidal cavity in a continuous dielectric, which accounted partially for the deficit, but there is a degree of arbitrariness in choosing such procedures. As noted in section 3.5, the concept of effective radii r is imprecise, and $\Delta V_{\text{ex}}^\ddagger$ becomes very sensitive to the choice of r at this extreme end of the complex-ion size range, whether the two-sphere or the ellipsoidal-cavity model is used. What is clear, however, is that $\Delta V_{\text{ex}}^\ddagger$ for the cation-independent pathway is unusually strongly negative because of the small sizes of the MnO_4 ions, while $\Delta V_{\text{ex}}^\ddagger$ for the Na^+ - and K^+ -catalyzed pathways is at least $15 \text{ cm}^3 \text{ mol}^{-1}$ more positive. The dehydrated-cation catalysis model for the latter, as proposed in the original paper,¹³³ has gained in credibility over the past 20 years from experience with cation effects in cyanometalate self-exchange reactions.

For the aqueous $\text{Co}^{\text{III/II}}$ couples listed in Table 4, $\Delta V_{\text{ex}}^\ddagger$ is $8\text{--}15 \text{ cm}^3 \text{ mol}^{-1}$ more negative than predicted from eqs 46–49 (the “ $\text{Co}(\text{EDTA})^{-/2-}$ ” couple actually involves exchange between $\text{Co}^{\text{III}}(\text{EDTA})^-$ and $\text{Co}^{\text{II}}(\text{HEDTA})\text{OH}_2^-$ under the reaction conditions,³¹⁶ and accordingly the volume changes associated with deprotonation and deaquation of the Co^{II} complex are included in $\Delta V_{\text{ex}}^\ddagger$). The self-exchange reactions of $\text{Co}(\text{en})_3^{3+/2+}$ and “ $\text{Co}(\text{EDTA})^{-/2-}$ ” are also much slower than expected from Marcus-type calculations, and in particular are some 4 orders of magnitude slower than self-exchanges involving the Co cage complexes of Table 3 ($\text{Co}(\text{sep})^{3+}$ is essentially just $\text{Co}(\text{en})_3^{3+}$ with added bridgehead groups). All involve a spin-state change between the ground states: low-spin $3d^6$ ($^1A_{1g}$) for Co^{III} , high-spin $3d^7$ ($^4T_{1g}$) for Co^{II} . There are basically two ways in which this could

affect the kinetics: the electron transfer could be direct between the Co^{II} and Co^{III} ground states but nonadiabatic^{320–323} (Hupp and Weaver¹⁴⁶ and Geselowitz³²⁴ argued against this), or electron transfer could occur adiabatically between Co^{III} and a low-spin (2E_g) Co^{II} intermediate formed in a fast³²⁵ preequilibrium step³²⁶ with a volume change, ΔV_{spin} , of -8 to $-15 \text{ cm}^3 \text{ mol}^{-1}$ (cf. $-10 \text{ cm}^3 \text{ mol}^{-1}$ reported by Binstead and Beattie³²⁷ for the $\text{Co}(\text{terpy})_2^{2+}$ high-to-low spin state change; note, however, reservations expressed by Shalders and Swaddle²⁰²). In early publications,^{223,309} the present author, while not discounting the preequilibrium explanation, somewhat arbitrarily favored the nonadiabatic interpretation (largely because data on ΔV_{spin} and accessibility of the 2E_g state for the Co complexes of Table 4 were lacking, whereas the value of the nonadiabatic distance scaling factor required to accommodate the $\Delta V_{\text{ex}}^\ddagger$ data seemed to fall within a reasonable range). However, recognition that the cage complexes of $\text{Co}^{\text{III/II}}$ (Table 3) conformed well to the adiabatic model (eqs 18, 20, 21, 28, and 46–49) forced adoption of the preequilibrium theory,²⁰² it is inconceivable that the $\text{Co}(\text{en})_3^{3+/2+}$ exchange could be nonadiabatic if the closely related but somewhat bulkier $\text{Co}(\text{sep})_3^{3+/2+}$ couple underwent electron transfer adiabatically. Furthermore, the experimental work of Endicott and co-workers^{328–332} has shown that, although many cross reactions involving $\text{Co}^{\text{III/II}}$ a(m)mine couples with substantial ΔG s of reaction are nonadiabatic, the self-exchange reactions ($\Delta G = 0$) are close to adiabatic, as the calculations of Larsson et al.³²⁶ predict. Finally, it is now clear (section 4.1) that compression of a solution will do little to accelerate a nonadiabatic reaction; for example, for the FeCp^*_{2+} self-exchange, the distance dependence of k_{ex} is evidently too slight over the reaction zone.^{219,308} For a strongly nonadiabatic reaction, Hupp and Weaver argued that close contact between the reactants is necessary for electron transfer to occur¹⁴⁶ (section 3.9); in other words, the reaction zone thickness, $\delta\sigma$, is very narrow. This means that the separation σ between the reactant centers must consist almost entirely of the effective radii of the relatively incompressible complexes and is consequently independent of pressure within experimental uncertainty. Thus, the contribution of nonadiabaticity to $\Delta V_{\text{ex}}^\ddagger$ or $\Delta V_{\text{el}}^\ddagger$ is negligible, and our earlier assertions to the contrary^{133,199,223,278,305,309,310} are hereby retracted. The origin of the strongly negative $\Delta V_{\text{ex}}^\ddagger$ for $\text{Co}^{\text{III/II}}\text{N}_6$ chelate complexes relative to the well-behaved cage analogues can be attributed to the freedom of the former ions to distort during the progression low-spin $\text{Co}^{\text{III}} \leftrightarrow$ low-spin $\text{Co}^{\text{II}} \leftrightarrow$ high-spin Co^{II} .

It is less clear, however, why $\Delta V_{\text{ex}}^\ddagger$ for the $\text{Ru}(\text{en})_3^{3+/2+}$ self-exchange should also be so much more negative than expected; indeed, it is close to that for the $\text{Co}^{\text{III/II}}$ analogue, but the much faster low-spin $4d^5$ /low-spin $4d^6$ Ru exchange should take place without significant geometrical distortions. It might be significant that the $\text{Ru}^{\text{III/II}}$ $\Delta V_{\text{ex}}^\ddagger$ value was obtained indirectly (though reproducibly)⁶⁰ from application of the Marcus cross-reaction with $\text{Co}(\text{phen})_3^{3+/2+}$ couple, which itself has an “anomalous”

$\Delta V_{\text{ex}}^{\ddagger}$ (Table 4); direct measurement of $\Delta V_{\text{ex}}^{\ddagger}$ for $\text{Ru}(\text{en})_3^{3+/2+}$ by the most effective technique (^{13}C NMR), however, would require a high-pressure NMR probe with ^1H decoupling. However, comparison of $\Delta V_{\text{ex}}^{\ddagger}$ for $\text{Ru}(\text{en})_3^{3+/2+}$ with $\Delta V_{\text{el}}^{\ddagger}$ for the electrode reaction (section 4.5) lends credibility to the value given in Table 4.

The remaining entries in Table 4 are for nonaqueous systems studied by Wherland and co-workers.^{313,317} For the Mn^{III} isonitrile complexes, $\Delta V_{\text{ex}}^{\ddagger}$ is strongly negative but still less so than $\Delta V_{\text{ex}}^{\ddagger}(\text{calcd})$; this is unlikely to be due to ion pairing, which tends to retard electron transfer but is broken up by application of pressure, but rather reflects the failure of eq 46 for solvents of low ϵ because $\Delta V_{\text{DH}}^{\ddagger}$ and $\Delta V_{\text{Coul}}^{\ddagger}$ (eqs 48 and 49) become numerically huge and the calculation becomes unrealistic. One might expect the cage (clathrochelate) couple $\text{Co}(\text{dmg}''(\text{BF})_2)^{+/0}$ in the more polar solvent acetonitrile to be well-behaved, but its $\Delta V_{\text{ex}}^{\ddagger}$ is similar to those for $\text{Co}(\text{en})_3^{3+/2+}$ and $\text{Ru}(\text{en})_3^{3+/2+}$ in water; it may not be coincidental, however, that the anomalous $\Delta V_{\text{ex}}^{\ddagger}$ values for both $\text{Ru}(\text{en})_3^{3+/2+}$ and $\text{Co}(\text{dmg}_3(\text{BF})_2)^{+/0}$ were obtained from the cross-relation.

Wherland et al.^{333,334} have also reported extensive $\Delta V_{\text{ex}}^{\ddagger}$ data for two-electron self-exchange reactions such as $\text{RuCp}_2/\text{RuCp}_2\text{Br}^+$ in nonaqueous media; these are in effect atom transfer reactions and lie outside the scope of this article.

4.4. Pressure Effects on the Kinetics of Electrode Reactions: General Remarks

It should be evident from the foregoing considerations that attempts to correlate k_{el} for reaction 1 quantitatively with k_{ex} for reaction 2 are unlikely to succeed, and accordingly no attempt is made here to update Figure 1. The main problem is that the intuitive expectation that reactions at metal electrodes will generally be adiabatic in the absence of special features such as SAMs (or at least inherently more adiabatic than the corresponding homogeneous self-exchange reactions,¹⁴⁹ which, as noted in section 4.3, are generally close to fully adiabatic) is probably wrong. Indeed, the almost inevitable presence in the inner Helmholtz layer of adsorbed adventitious atoms, ions, molecules, or oxide layers on an electrode may be expected to reduce reactant orbital overlap (and hence κ_{el}) with the continuum of electronic states on the metal in the manner of SAMs, albeit to a lesser degree. In many cases, k_{el} for reaction 1 shows significant dependence on the nature of the metal and its surface, implying at least moderately nonadiabatic behavior and making it difficult to decide which value of k_{el} might be meaningfully compared with k_{ex} or, indeed, whether they should be compared at all if they differ in the extent of nonadiabaticity (i.e., if $\kappa_{\text{ex}} \neq \kappa_{\text{el}}$ in eqs 30 and 31). Since nonadiabaticity in an electrode reaction commonly arises from the nature of the electrode and the interaction of the reactant with the surface, an electrode process could be nonadiabatic even if the corresponding homogeneous self-exchange reaction were fully adiabatic; thus, the suspected nonadiabaticity of the unusually slow

$\text{Ru}(\text{hfac})_3^{0/-}$ electrode reaction^{62,148} is quite consistent with full adiabaticity of the rather fast homogeneous self-exchange process.^{148,198,207,208} Cases such as the aqueous $\text{Ru}(\text{NH}_3)_6^{3+/2+}$ electrode reaction^{88,89} for which k_{el} is independent of the nature of the metal electrode, suggesting full adiabaticity, are the exception rather than the rule, and even for the $\text{Ru}(\text{NH}_3)_6^{3+/2+}$ case the cautionary note sounded by Gosavi and Marcus¹⁵⁵ should be heeded. An associated experimental problem is that those electrode reactions such as $\text{Ru}(\text{NH}_3)_6^{3+/2+}$ that arguably approach full adiabaticity are by the same token somewhat faster than can be accommodated by traditional electrochemical techniques, which are typically limited by reactant diffusion rates to reactions with $k_{\text{el}} \leq 0.3 \text{ cm s}^{-1}$ (section 2), as may be seen in the leveling-off of the plot in Figure 1.

Further complications include the incompatibility of the units of k_{el} and k_{ex} ; this can in principle be circumvented by converting k_{el} to the equivalent of a bimolecular rate constant as advocated by Weaver et al.^{146,150} (section 3.2), but this involves somewhat arbitrary assumptions concerning the thickness of the reaction zone, $\delta\sigma$. Similarly, Frumkin corrections for double-layer effects in electrode kinetics (eq 14) require educated guesswork concerning the potential at the OCP; such corrections can be minimized by use of swamping concentrations of a supporting electrolyte, but this in itself can introduce fresh problems such as the formation of blocking layers on the electrode by tetraalkylammonium ions and their desorption at possibly inconvenient rates, as discussed in section 3.4.

These problems are to a large extent bypassed when one compares $\Delta V_{\text{el}}^{\ddagger}$ with $\Delta V_{\text{ex}}^{\ddagger}$. First and foremost, the nature of an electrode and its surface do not change appreciably with applied pressure over the range 0–200 MPa. As seen in eqs 15 and 16, the *absolute* value of k_{el} is immaterial to the determination of $\Delta V_{\text{el}}^{\ddagger}$; only *relative* values of k_{el} within a given pressure run are involved, and $\Delta V_{\text{el}}^{\ddagger}$ should not be affected if $k_{\text{el}}^{P=0}$ varies somewhat from run to run or from one type of electrode to another. Second, as discussed in section 4.3, it has recently become clear that neither $\Delta V_{\text{ex}}^{\ddagger}$ nor $\Delta V_{\text{el}}^{\ddagger}$ should be affected by the degree of (non)adiabaticity of either the self-exchange or the electrode reaction. Third, the units of $\Delta V_{\text{el}}^{\ddagger}$ and $\Delta V_{\text{ex}}^{\ddagger}$ are the same ($\text{cm}^3 \text{ mol}^{-1}$); no questionable conversions are needed to compare them. Fourth, for electrode reactions of transition-metal complexes in both aqueous and nonaqueous solutions, the transfer coefficient α has been found not to vary measurably with pressure (not surprisingly, since α is typically close to the ideal value of 0.50 for an **E** process at zero overpotential). Accordingly, since the inner Helmholtz layer (molecules or ions in hard contact with the electrode surface) is unlikely to be significantly affected by pressures of a few hundred megapascals, the Frumkin correction (eq 14) is effectively pressure-independent, makes no contribution to $\Delta V_{\text{el}}^{\ddagger}$, and can be ignored in variable-pressure studies. This is an important advantage in comparing $\Delta V_{\text{el}}^{\ddagger}$ with $\Delta V_{\text{ex}}^{\ddagger}$ rather than k_{el} with k_{ex} , since the

Table 5. Rate Constants $k_{\text{el}}^{P=0}$ at Zero Applied Pressure and Volumes of Activation $\Delta V_{\text{el}}^{\ddagger}$ for Electrode Reactions in Aqueous Media^a

	couple/electrode	medium (concn, mol L ⁻¹)	$k_{\text{el}}^{P=0}$, cm s ⁻¹	$\Delta V_{\text{el}}^{\ddagger}$, cm ³ mol ⁻¹	ref
A	Fe(H ₂ O) ₆ ^{3+/2+} /Pt	(H,Na)ClO ₄ (0.5)	0.021	-5.5 ± 0.2	57
B	Fe(phen) ₃ ^{3+/2+} /Pt	Na ₂ SO ₄ (0.1)	0.30	-1.6 ± 0.1	57
C	Co(phen) ₃ ^{3+/2+} /Pt	NaCl (0.1)	0.11	-9.1 ± 0.4	57
D	Co(bpy) ₃ ^{3+/2+} /Pt	NaCl (0.2)	0.17	-8.6 ± 0.4	59
E	Co(en) ₃ ^{3+/2+} /Pt ^b	KCl (0.5)	0.036	-8.3 ± 0.5	57
F	Co(act) ^{3+/2+} /GC	KCl (0.28)	0.32	-3.3 ± 0.4	60
G	Co(sep) ^{3+/2+} /Pt	KCl (0.5)	0.091	-3.0 ± 0.4	57
H	Co(diamsar) ^{3+/2+} /Au	NaClO ₄ (0.1, pH 9) ^c	0.016	-3.5 ± 0.2	57
I	Co(diamsarH ₂) ^{5+/4+} /Au	(H,Na)ClO ₄ (0.13)	0.010	-3.8 ± 0.2	57
J	Co(tacn) ₂ ^{3+/2+} /Pt	KCl (0.5)	0.075	-5.9 ± 0.9	60
K	Co(tten) ₂ ^{3+/2+} /Pt	NaClO ₄ (0.1)	0.27	-2.8 ± 0.7	57
L	Ru(en) ₃ ^{3+/2+} /GC	KCl (0.4)	0.34	-7.4 ± 0.4	60
M	Mo(CN) ₈ ^{3-/4-} /Au	NaClO ₄ (0.5)	0.053	+7.3 ± 0.7	57
N	Mo(CN) ₈ ^{3-/4-} /GC	Et ₄ NCl (0.5)	0.18	-4.2 ± 0.2	58
O	W(CN) ₈ ^{3-/4-} /Pt	KCl (0.5)	0.16	+10.8 ± 0.4	58
P	Os(CN) ₆ ^{3-/4-} /GC	KCl (0.6)	0.020	+9.4 ± 0.7	58
Q	Fe(CN) ₆ ^{3-/4-} /Au	K ₂ SO ₄ (0.5)	0.023	+1.9 ± 0.1	337
R	Fe(CN) ₆ ^{3-/4-} /Pt	KCl (0.5)	0.072	+11.9 ± 1.3	57
S	Fe(CN) ₆ ^{3-/4-} /Pt	KCl (0.2)	0.047	+10.4 ± 1.4	57
T	Fe(CN) ₆ ^{3-/4-} /Pt	KCl (0.06)	0.017	+12.0 ± 1.8	275
U	CoW ₁₂ O ₄₀ ^{5-/6-} /Pt	HClO ₄ (0.1)	0.016	+5.3 ± 0.4	63
V	CoW ₁₂ O ₄₀ ^{5-/6-} /Pt	NaClO ₄ (0.5)	0.007	+11.1 ± 0.8	63
W	CoW ₁₂ O ₄₀ ^{5-/6-} /Pt	KCl (0.1)	0.009	+15.1 ± 0.7	63
X	CoW ₁₂ O ₄₀ ^{5-/6-} /Pt	RbCl (0.1)	0.025	+13.7 ± 1.0	63
Y	CoW ₁₂ O ₄₀ ^{5-/6-} /Pt	CsCl (0.1)	0.083	+12.0 ± 0.3	63
Z	Cyt <i>c</i> / Au ^d	NaClO ₄ (0.1) ^e	0.014 ^f	+6.1 ± 0.5 ^f	102

^a Measurements by ACV at 25.0 °C, transfer coefficient $\alpha = 0.5 \pm 0.1$, except where otherwise indicated; abbreviations as in ref 137. ^b 0.2 mol L⁻¹ en present. ^c $\alpha = 0.27$. ^d With 4,4'-bipyridyl or 4,4'-bipyridyl disulfide SAM. ^e 0.02 mol L⁻¹ tris buffer (pH 7.0). ^f From fast-scan CV.

Frumkin correction to k_{el} is not well-defined, especially where multiply charged reactants are involved,³³⁵ yet it can be large.^{83,97a,142,336} Finally, as will be seen in section 4.6, pressure effects can be diagnostic of solvent dynamical control of electrode reaction rates in nonaqueous solvents and have the advantage over the traditional approach of comparing k_{el} in solvents of differing viscosities that diagnosis is achieved without changing the medium chemically.

As discussed in section 4.3, any pressure dependence of σ and $\delta\sigma$ (ν_n likewise) can be disregarded, so unless solvent dynamics are rate-controlling, Z_{el} and Z_{ex} will be unaffected by pressure (eqs 30 and 31), and since $(\partial\Delta G/\partial P)_T = \Delta V$, we have the expectation (section 3) that

$$\Delta V_{\text{el}}^{\ddagger} = \frac{1}{2}\Delta V_{\text{ex}}^{\ddagger} \quad (53)$$

For water at near-ambient temperatures, the solvent viscosity is fortuitously almost pressure-independent (sections 2.7 and 4.5 and Figure 5); consequently, we can expect eq 53 to hold for “well-behaved” electrode and homogeneous electron transfer reactions in aqueous media, whether or not solvent dynamics are important.

4.5. Pressure Effects on Electrode Kinetics in Aqueous Systems

Except for the case of cytochrome *c*, all k_{el} and $\Delta V_{\text{el}}^{\ddagger}$ data in Tables 5 and 6 were obtained by ACV, the seemingly random choices of electrode, electrolyte, and concentration being dictated by factors such

as solubility and the need for experimental conditions that would give optimum ACV performance. As noted above, k_{el} values can vary substantially with the experimental conditions, particularly the nature and history of the electrode, and are reported in Table 5 only to make the qualitative points that they lie within the capabilities of the experimental technique and follow very roughly the trend shown in Figure 1; thus, those electrode reactions that are fast (e.g., couples **B**, **D**, and **L**) generally correspond to fast self-exchange reactions. It is worth noting that the effect of alkali metal ions M⁺ on k_{el} for the anionic 12-tungstocobaltate couple (**U–Y**) follow the sequence Na < K < Rb << Cs found for anionic cyanometalate couples and MnO₄^{-/2-} (section 3.7), confirming that catalysis by the heavier alkali metal ions is a characteristic feature of electron transfer kinetics in anionic couples.

For the couples **D**, **J**, and **U–Y** in Table 5, values of $\Delta V_{\text{ex}}^{\ddagger}$ have not been reported, but for the remaining couples **A–Q**, $\Delta V_{\text{el}}^{\ddagger}$ is a linear function of $\Delta V_{\text{ex}}^{\ddagger}$ with slope 0.49 ± 0.01 and intercept 0.0 ± 0.2 cm³ mol⁻¹ (Figure 8). The validity of eq 53 is therefore proven, and it follows that Marcus' treatment of the heterogeneous–homogeneous electron transfer relationship (section 3.1, eqs 23–25) prevails over that of Hush (eqs 26 and 27), which would have given a slope of 1.0 in Figure 8. In other words, the electron transfer distance σ should be set to $2r$ rather than ∞ , and the “virtual partner” model of electron transfer at an electrode proposed in the opening paragraph of this article is appropriate. In this model (in contrast to some earlier models¹³), the virtual partner

Table 6. Rate Constants $k_{\text{el}}^{P=0}$ and Reactant Diffusion Coefficients D^0 at Zero Applied Pressure and Volumes of Activation $\Delta V_{\text{el}}^{\ddagger}$ for Electrode Reactions and $\Delta V_{\text{diff}}^{\ddagger}$ for Reactant Diffusion in Nonaqueous Media^a

couple	solvent/medium (concn, mol L ⁻¹)	$k_{\text{el}}^{P=0}$, cm s ⁻¹	D^0 , 10 ⁻⁶ cm ² s ⁻¹	$\Delta V_{\text{el}}^{\ddagger}$, cm ³ mol ⁻¹	$\Delta V_{\text{diff}}^{\ddagger}$, cm ³ mol ⁻¹	ref	
FeCp ₂ ^{+/0}	PC/TBAP (0.5)	0.037	1.77	+18.8 ± 0.9	+17.3 ± 2.1	64	
	Py/TBAP (0.5)	0.048	5.0	+12.6 ± 0.2	+13.9 ± 0.1	64	
	DCM/TBAP (0.5)	0.080	10.7	+5.0 ± 0.5	+8.3 ± 0.1	64	
	EtOH/TBAP (0.5)	0.038	4.6	+8.5 ± 0.2	+10.2 ± 0.1	64	
	BN/TBAP (0.5)	0.037	3.6	+16.5 ± 0.4	+17.2 ± 0.2	64	
	DMSO/TBAP (0.5)	0.093 ^b	3.5 ^b	+14.5 ± 0.8 ^b	+14.8 ± 0.2 ^b	64	
	DMF/TBAP (0.5)	0.122 ^b	6.9 ^b	+11.6 ± 0.6 ^b	+9.8 ± 0.2 ^b	64	
	DMF/TBAP (0.5)	0.077	6.0	+11.4 ± 0.7	+11.3 ± 1.0	64	
	DMF/TBAP (0.2)	0.053	7.4	+10.2 ± 0.3	+9.6 ± 0.1	64	
	DMF/TBAP (0.1)	0.084	9.4	+10.0 ± 0.4	+9.0 ± 0.1	64	
	DMF/TEAP (0.2)	0.057	6.4	+9.5 ± 0.2	+9.5 ± 0.2	64	
	AN/TEAP (0.2)	0.130	17.8	+7.0 ± 0.4	+6.6 ± 0.4	64	
	PC/TEAP (0.2)	0.026	1.59	+16.6 ± 0.2	+14.9 ± 0.2	64	
	DMSO/TEAP (0.2)	0.040 ^b	1.98 ^b	+13.6 ± 0.3 ^b	+11.5 ± 0.2 ^b	64	
	FeCp ₂ ^{+/0}	DMF/TBAP (0.5)	0.091	7.0	+12.2 ± 0.3	+10.9 ± 0.6	64
DMSO/TBAP (0.5)		0.048 ^b	3.7 ^b	+12.9 ± 0.1 ^b	+13.4 ± 0.1 ^b	64	
Ru(hfac) ₃ ^{0/-}	AC/TBAP (0.2)	0.024	7.2	+12.4 ± 0.7	+15.4 ± 0.7	62	
	AN/TBAP (0.2)	0.040	8.1	+8.4 ± 0.5	+12.1 ± 0.7	62	
	MeOH/TBAP (0.2)	0.041	7.3	+9.9 ± 0.4	+14.7 ± 0.7	62	
	PC/TBAP (0.2)	0.023	2.7	+11.2 ± 0.3	+18.5 ± 0.2	62	
Mn(CNchx) ₆ ^{2+/+}	AN/TBAP (0.2)	0.051	11.7	+6.7 ± 0.8	+7.3 ± 0.2	61	
	AN/TBAP (0.5)	0.043	9.3	+8.0 ± 0.5	+9.3 ± 0.4	61	
	AN/TBAHFP (0.5)	0.013	8.4	+6.4 ± 0.7	+8.9 ± 0.2	61	
	AC/TBAP (0.5)	0.039	8.2	+11.4 ± 0.6	+9.9 ± 0.3	61	
	MeOH/TBAP (0.5)	0.033	5.5	+5.8 ± 0.3	+7.5 ± 0.2	61	
Co(bpy) ₃ ^{3+/2+}	PC/TBAP (0.5)	0.0074	1.22	+20.3 ± 0.6	+17.3 ± 0.1	61	
	AN/TBAP (0.2)	0.20	10.6	+9.1 ± 0.3	+8.8 ± 0.1	59	
	AC/TBAP (0.2)	0.070	9.4	+10.2 ± 0.7	+11.1 ± 0.1	59	
	PC/TBAP (0.2)	0.016	1.4	+12.2 ± 0.9	+15.6 ± 0.4	59	
Fe(phen) ₃ ^{3+/2+}	AN/TBAP (0.1)	0.045	6.7	+16.0 ± 1.2	+6.7 ± 0.2	61	
	AN/TBAP (0.5)	0.059	5.4	+14.3 ± 1.3	+8.0 ± 0.1	61	
	DMF/TBAP (0.5)	0.051	2.7	+13.5 ± 0.6	+9.9 ± 0.3	64	
	PC/TBAP (0.5)	0.0095	0.85	+20.4 ± 0.5	+16.2 ± 0.2	64	
	DMSO/TBAP (0.5)	0.047 ^b	0.91 ^b	+16.6 ± 2.9 ^b	+11.3 ± 1.9 ^b	64	
	[Zn ^{II} (Pc ^{2-/3-})] ^{0/-}	Py/TBAP (0.2)	0.126	8.4	+12.4 ± 0.1	+11.5 ± 0.4	65
	[Zn ^{II} (Pc ^{3-/4-})] ⁻²⁻	Py/TBAP (0.2)	0.135	8.0	+13.6 ± 0.5	+11.8 ± 0.4	65
	[Zn ^{II} (Pc ^{-/2-})] ⁺⁰	DMF/TBAP (0.2)	0.098	7.1	+12.6 ± 0.3	+10.1 ± 0.5	65
	[Zn ^{II} (Pc ^{2-/3-})] ^{0/-}	DMF/TBAP (0.2)	0.155	7.0	+12.2 ± 1.8	+9.9 ± 1.2	65
	[Zn ^{II} (Pc ^{3-/4-})] ⁻²⁻	DMF/TBAP (0.2)	0.103	8.7	+12.5 ± 1.6	+9.7 ± 0.7	65
[Zn ^{II} (Pc ^{-/2-})] ⁺⁰	DMSO/TBAP (0.2)	0.086 ^b	4.5 ^b	+17.5 ± 0.7 ^b	+14.1 ± 0.2 ^b	65	
[Zn ^{II} (Pc ^{2-/3-})] ^{0/-}	DMSO/TBAP (0.2)	0.156 ^b	6.2 ^b	+15.5 ± 0.2 ^b	+14.8 ± 0.6 ^b	65	
[Zn ^{II} (Pc ^{3-/4-})] ⁻²⁻	DMSO/TBAP (0.2)	0.101 ^b	7.1 ^b	+15.2 ± 0.1 ^b	+14.7 ± 1.1 ^b	65	
[Zn ^{II} (Pc ^{-/2-})] ⁺⁰	DMA/TBAP (0.2)	0.044	2.7	+13.1 ± 0.6	+14.1 ± 0.5	65	
[Co ^{III} (TNPc ^{-/2-})] ^{2+/+}	DMF/TBAP (0.2)	0.041	1.5	+11.1 ± 1.0	+10.8 ± 0.7	65	
[Co ^{III/II} (TNPc ²⁻)] ⁺⁰	DMF/TBAP (0.2)	0.0041	1.5	+15.2 ± 0.9	+10.6 ± 0.6	65	
[Co ^{II/II} (TNPc ²⁻)] ^{0/-}	DMF/TBAP (0.2)	0.047	2.5	+21.7 ± 1.0	+10.4 ± 0.5	65	
[Co ^I (TNPc ^{2-/3-})] ⁻²⁻	DMF/TBAP (0.2)	0.046	3.2	+12.4 ± 0.9	+10.9 ± 0.4	65	
[Co ^{III} (TNPc ^{-/2-})] ^{2+/+}	DMA/TBAP (0.2)	0.032	1.3	+15.6 ± 1.7	+13.4 ± 0.9	65	
[Co ^{III/II} (TNPc ²⁻)] ⁺⁰	DMA/TBAP (0.2)	0.0042	1.3	+16.7 ± 0.8	+13.9 ± 0.5	65	
[Co ^{II/II} (TNPc ²⁻)] ^{0/-}	DMA/TBAP (0.2)	0.024	1.3	+24.6 ± 1.0	+14.9 ± 1.3	65	
[Co ^I (TNPc ^{2-/3-})] ⁻²⁻	DMA/TBAP (0.2)	0.059	2.5	+14.0 ± 0.2	+13.3 ± 0.8	65	
[Co ^{III} (TNPc ^{-/2-})] ^{2+/+}	DMSO/TBAP (0.2)	0.036 ^b	1.5 ^b	+13.4 ± 0.6 ^b	+15.8 ± 0.8 ^b	65	
[Co ^{III/II} (TNPc ²⁻)] ⁺⁰	DMSO/TBAP (0.2)	0.0041 ^b	1.5 ^b	+15.0 ± 0.7 ^b	+16.0 ± 0.5 ^b	65	
[Co ^{II/II} (TNPc ²⁻)] ^{0/-}	DMSO/TBAP (0.2)	0.030 ^b	1.4 ^b	+33.9 ± 1.0 ^b	+15.4 ± 0.5 ^b	65	
[Co ^I (TNPc ^{2-/3-})] ⁻²⁻	DMSO/TBAP (0.2)	0.031 ^b	2.6 ^b	+13.5 ± 0.3 ^b	+15.1 ± 0.4 ^b	65	
[Co ^{III/II} (Pc ²⁻)] ⁺⁰	Py/TBAP (0.2)	0.0046	5.1	+10.8 ± 1.1	+11.8 ± 0.4	65	
[Co ^I (Pc ^{2-/3-})] ⁻²⁻	Py/TBAP (0.2)	0.078	4.8	+12.5 ± 1.1	+11.7 ± 0.5	65	
[Fe ^{III/II} (Pc ²⁻)] ⁺⁰	Py/TBAP (0.2)	0.099	5.5	+10.4 ± 0.7	+11.2 ± 0.6	65	
[Fe ^{II/I} (Pc ²⁻)] ^{0/-}	Py/TBAP (0.2)	0.091	4.6	+10.6 ± 1.1	+10.8 ± 0.3	65	

^a At 25 °C with conventional Pt wire electrodes, unless otherwise stated; $\alpha = 0.5 \pm 0.1$; abbreviations as in ref 137. ^b At 45 °C.

is not conceived of as a charged image in the electrode. Such an image would be effectively erased by high concentrations of supporting electrolyte; as noted in section 2.6, the same concentrations of supporting electrolyte needed to reduce double-layer effects to insignificance would also eliminate the charge image.^{12,13,30} Rather, the virtual partner (say,

the $\text{ML}_x^{(z-1)+}$ of eq 1) is situated in the solution phase and becomes the real partner after electron transfer occurs; concomitantly, the original real partner ML_x^{z+} becomes virtual. The real/virtual couple is thus analogous to the $\text{ML}_x^{z+}/\text{ML}_x^{(z-1)+}$ couple of eq 2, and the $M_{\text{real}} - M_{\text{virtual}}$ distance via the electrode surface (or OCP, if electron transfer occurs by tunneling

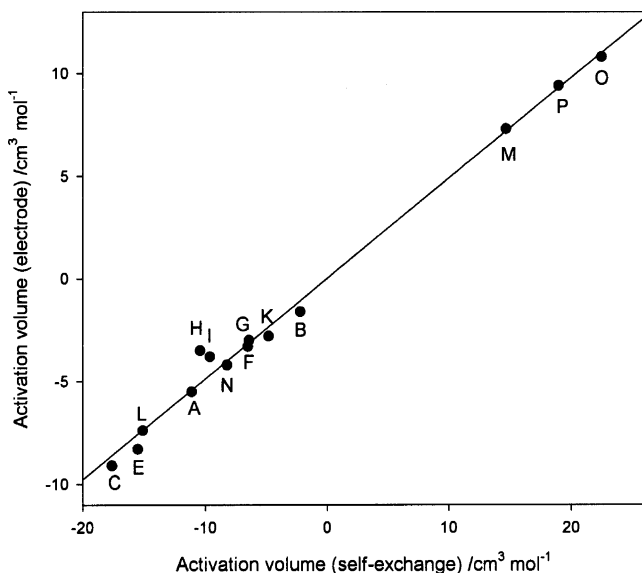


Figure 8. Relationship of $\Delta V_{\text{el}}^{\ddagger}$ to $\Delta V_{\text{ex}}^{\ddagger}$ for aqueous solutions. Letter code as in Table 5.

through the inner Helmholtz layer) is twice the mean radius of the reactants, just as in homogeneous electron transfer.

The compliance of both “well-behaved” and many “anomalous” couples (in the context of $\Delta V_{\text{ex}}^{\ddagger}$) with eq 53, as shown in Figure 8, implies that the explanations given in section 4.3 for anomalous behavior in self-exchange apply equally well to the corresponding electrode reactions. In particular, it means that the specific effects of alkali metal cations M^+ on k_{el} for electrode reactions of anionic complexes are generally attributable to catalysis by the (evidently partially dehydrated) M^+ acting on the reactant and its virtual partner, rather than to some effect of M^+ on the electrode or the double layer.

It is unfortunate (and ironic) that there is serious disagreement over values of $\Delta V_{\text{el}}^{\ddagger}$ and $\Delta V_{\text{ex}}^{\ddagger}$ for the case of the much-studied “reference” couple $\text{Fe}(\text{CN})_6^{3-/4-}$. The first published value of $\Delta V_{\text{el}}^{\ddagger}$ for any transition-metal couple was that of Conway and Currie,³³⁷ who used ACV to obtain $\Delta V_{\text{el}}^{\ddagger} = +1.9 \text{ cm}^3 \text{ mol}^{-1}$ for $\text{Fe}(\text{CN})_6^{3-/4-}$ in aqueous K_2SO_4 at a gold disk electrode. Independent ACV redeterminations of this parameter by three different researchers in the author’s laboratory, using a Pt electrode in KCl media ($0.06\text{--}1.0 \text{ mol L}^{-1}$) and cleaning the electrode between measurements by potential cycling (e.g., entries **R–T** in Table 5), have invariably given $\Delta V_{\text{el}}^{\ddagger} = +11 \pm 1 \text{ cm}^3 \text{ mol}^{-1}$. An attempt²⁷⁵ to measure k_{el} for $\text{Fe}(\text{CN})_6^{3-/4-}$ in 0.3 mol L^{-1} aqueous Et_4NCl by ACV gave no quadrature signal (i.e., the reaction rate was too slow to measure) and an in-phase current that decreased with time, implying progressive electrode surface blocking by Et_4N^+ (cf. Fawcett and Opałło¹⁸⁸). Specific problems with the $\text{Fe}(\text{CN})_6^{3-/4-}$ electrode reaction are discussed in some detail in section 3.4. Worse yet, the original attempt to measure $\Delta V_{\text{ex}}^{\ddagger}$ for the self-exchange of $(K_3/K_4)[\text{Fe}(\text{CN})_6]$ in D_2O without added electrolyte gave about $+22 \text{ cm}^3 \text{ mol}^{-1}$, which would give an excellent fit in Figure 8 with entries **R–T** from Table 5 but required confir-

mation because of reported technical difficulties.²²⁸ Accordingly, $\Delta V_{\text{ex}}^{\ddagger}$ was recently redetermined for $(K_3/K_4)[\text{Fe}(\text{CN})_6]$ under the same conditions but with a higher-field spectrometer,¹⁰⁹ and the result was very different ($-1 \text{ cm}^3 \text{ mol}^{-1}$) though still much more positive than that for the cation-independent path so that the qualitative interpretation of the cation effect was unaffected. Part of the problem with the homogeneous self-exchange results may be that $\text{Fe}(\text{CN})_6^{3-}$ is easily reduced by organic material,¹⁰⁹ perhaps leaked from hydraulic fluids used in variable-pressure work, giving an appearance of pressure dependence of k_{ex} that is actually time dependence as $[\text{Fe}(\text{CN})_6^{3-}]$ diminishes. Known aberrations associated with the $\text{Fe}(\text{CN})_6^{3-/4-}$ electrode reaction are discussed in section 2.6. Further work is needed to clarify the behavior of this recalcitrant couple; in the meantime, it has been omitted from Figure 8.

It will be seen in the next section that $\Delta V_{\text{el}}^{\ddagger}$ data for electrode reactions in *nonaqueous solvents* show correlations with the pressure dependence of solvent viscosity ($\Delta V_{\text{visc}}^{\ddagger}$) that constitute evidence for solvent dynamical rate control (as noted in section 4.2, there is no evidence for solvent dynamical control of homogeneous electron transfer rates of metal complexes). If solvent dynamics also affect k_{el} in water, as observations by Bard et al.^{259,260} and Khoshitariya et al.^{102,261,262} for water diluted with dissolved sugars suggest, then the correlation of $\Delta V_{\text{el}}^{\ddagger}$ with $\Delta V_{\text{ex}}^{\ddagger}$ in Figure 8 is serendipitously possible only because the viscosity of water is effectively independent of pressure near $25 \text{ }^\circ\text{C}$ (Figure 5) so that the contribution of solvent dynamics to $\Delta V_{\text{el}}^{\ddagger}$ for aqueous solutions is essentially nil. (In fact, as noted in sections 3.4 and 3.9, k_{el} in undiluted water may not be subject to solvent friction in any case.) A further benefit accruing from the near pressure independence of η for water is that the uncompensated resistance, R_u , in aqueous electrochemical measurements will also be effectively independent of pressure, and consequently $\Delta V_{\text{el}}^{\ddagger}$ is immune to any artifacts due to R_u that can undermine the credibility of measurements of k_{el} itself.⁵³ A possible exception to these generalizations may arise with redox reactions of metalloproteins, since it is known that “biological water” (water solvating proteins and other biological macromolecules) shows characteristic properties including additional dynamic modes that are an order of magnitude slower than those for bulk water.^{338–341} It is not known whether biological water behaves more like a normal liquid in the sense of exhibiting an increase in viscosity with pressure, but such would be a reasonable expectation.

The only biological redox couple for which kinetic data at variable pressure are currently available is the $\text{Fe}^{\text{III/II}}$ couple within aqueous cytochrome *c*, for which van Eldik et al.¹⁰² report a *positive* $\Delta V_{\text{el}}^{\ddagger}$ ($+6 \text{ cm}^3 \text{ mol}^{-1}$, entry **Z** in Table 5) that is similar in magnitude to $\Delta V_{\text{ex}}^{\ddagger}$ for the corresponding homogeneous self-exchange ($+2$ to $+7 \text{ cm}^3 \text{ mol}^{-1}$, estimated from the cross-relation³⁴²). These positive volumes of activation cannot be attributed to counterion effects such as are seen for anion–anion electron transfer

reactions in water, and the authors also argue against conformational gating effects (cf. Waldeck et al.³⁴³). Since manipulation of water viscosity with sucrose reduces the rate of the electron transfer in Cyt *c*, implying solvent dynamic control, van Eldik et al.¹⁰² propose that “solvent” dynamical control of the electrode process arises from interaction with the protein part of Cyt *c*, which acts like a droplet of viscous liquid (“molten globule” state).^{340,344} There is a long tradition³⁴⁴ of representing the internal motions of a protein as those of a viscous liquid and of connecting metalloprotein redox kinetics with Zusan-type solvent dynamics, and in this context, the interpretation of $\Delta V_{\text{el}}^{\ddagger}$ for Cyt *c* given by van Eldik et al.¹⁰² is reasonable. Caution should, however, be exercised in the interpretation of $\Delta V_{\text{el}}^{\ddagger}$ for systems as complex as solvated metalloproteins, particularly since there is no quantitative information on how the pseudoviscosity of the protein globule or the viscosity of biological water varies with pressure. Furthermore, it should be noted that the (thermodynamic) volume of reaction, ΔV , for reduction of the Cyt *c* couple, when adjusted for the contribution of the reference electrode, is about $-5 \text{ cm}^3 \text{ mol}^{-1}$,³⁴⁵ whereas a *positive* value would be expected on grounds of electrostatic solvational and bond length changes. ΔV is, of course, an equilibrium rather than a kinetic property, but it provides an indication that the solvational change accompanying electron transfer in Cyt *c* runs *opposite* to the Born model implicit in eqs 21–25, and consequently, the positive $\Delta V_{\text{el}}^{\ddagger}$ and $\Delta V_{\text{ex}}^{\ddagger}$ values reported for the Cyt *c* electrode and exchange reactions may arise from solvational factors that have nothing to do with solvent dynamics. In any event, the Cyt *c* case is evidently a mechanistic anomaly and has been excluded from Figure 8.

4.6. Pressure Effects on Electrode Kinetics in Nonaqueous Solvents

Table 6 lists rate constants ($k_{\text{el}}^{P=0}$) and reactant diffusion coefficients (D^0) at zero applied pressure, and volumes of activation ($\Delta V_{\text{el}}^{\ddagger}$ for the electrode reaction and $\Delta V_{\text{diff}}^{\ddagger}$ for reactant diffusion) at mid-range pressure, as determined by ACV for a variety of transition-metal complexes in organic solvents. Data for DMSO solutions were obtained at 45 °C to avoid freezing under pressure³⁴⁶ and should not be compared directly to other data taken at 25 °C. As in Table 5, $k_{\text{el}}^{P=0}$ data may be electrode-dependent and are included only as a rough guide. The error ranges given for the activation volumes are standard deviations of regression to eqs 16 or 54; the uncertainties in the absolute values may range up to $\pm 2 \text{ cm}^3 \text{ mol}^{-1}$.

$$\ln D = \ln D^0 - P\Delta V_{\text{diff}}^{\ddagger}/(RT) \quad (54)$$

The salient features of the data of Table 6 are as follows: (i) *all* the volumes of activation are *positive*, whereas the TST-based equations of sections 3.1 and 3.2 predict *negative* values of $\Delta V_{\text{el}}^{\ddagger}$; (ii) there is *no* correlation between $\Delta V_{\text{el}}^{\ddagger}$ and the corresponding

(negative) $\Delta V_{\text{ex}}^{\ddagger}$ values of Tables 3 and 4; (iii) $\Delta V_{\text{el}}^{\ddagger}$ correlates with (and in most cases approximately equals) $\Delta V_{\text{diff}}^{\ddagger}$; (iv) the faster electrode reactions are associated with low-viscosity solvents such as AN (k_{el} for $\text{FeCp}^{*2+/0}$ in AN and AC was actually too fast to measure by ACV) and consequently smaller values of $\Delta V_{\text{el}}^{\ddagger}$ (since $\Delta V_{\text{diff}}^{\ddagger}$ increases with increasing viscosity, a large $\Delta V_{\text{diff}}^{\ddagger}$ means that large solvent displacements are needed for viscous flow); conversely, slow reactions and large $\Delta V_{\text{el}}^{\ddagger}$ and $\Delta V_{\text{diff}}^{\ddagger}$ are found for the more viscous media such as PC.

These results indicate clearly that TST breaks down for electrode reactions in nonaqueous solvents and that reaction rates are controlled instead by solvent dynamics. This applies even to the $\text{Co}(\text{bpy})_3^{3+/2+}$ couple, which has a significant internal reorganizational barrier but was shown by Murray et al.^{301–303} through widely ranging correlations of k_{el} with η and D to be subject to rate control by solvent friction. According to eq 37, this means that the solvent-dynamical rate constant k_f , and not k_{TST} , is the rate-determining bottleneck and can be identified with k_{el} . Alternative interpretations that can be dismissed are that k_{el} is diffusion-controlled (but that would result in $\varphi = 45^\circ$ in ACVs—cf. eq 12—which was plainly not so for the couples in Table 6) or that it represents an artifact due to uncompensated resistance (but this was specifically measured and allowed for in the ACV calculations). In any event, the observed reaction rates are well below the diffusion-controlled region.²⁵⁹ In the one-dimensional KZ approach (eqs 35 and 36, section 3.4), the preexponential factor Z_{el} of eq 19 is controlled by solvent dynamics and is proportional to τ_L^{-1} and hence (to a good approximation) to η^{-1} , the pressure dependence of which contributes an amount $\Delta V_{\text{el}(\text{SD})}^{\ddagger}$ to $\Delta V_{\text{el}(\text{calcd})}^{\ddagger}$. The pressure dependence of $\Delta G_{\text{el}}^{\ddagger}$ in eq 19 may be expected to continue to contribute the same barrier-height amount to $\Delta V_{\text{el}(\text{calcd})}^{\ddagger}$ as in TST which, from eq 53, can be equated to $\frac{1}{2}\Delta V_{\text{ex}}^{\ddagger}$ where experimental $\Delta V_{\text{ex}}^{\ddagger}$ are available (or can be calculated as in section 4.1). Thus, in the KZ approach, we have

$$\Delta V_{\text{el}(\text{calcd, KZ})}^{\ddagger} = \Delta V_{\text{el}(\text{SD})}^{\ddagger} + \Delta V_{\text{el}(\text{TST})}^{\ddagger} \approx \Delta V_{\text{diff}}^{\ddagger} + \frac{1}{2}\Delta V_{\text{ex}}^{\ddagger} \quad (55)$$

In the two-dimensional AHMS approach (section 3.4), eqs 38–40, with some simplifications, lead to

$$\Delta V_{\text{el}(\text{calcd, AHMS})}^{\ddagger} = \theta\Delta V_{\text{el}(\text{SD})}^{\ddagger} + (\gamma/2)\Delta V_{\text{ex}}^{\ddagger} \approx \theta\Delta V_{\text{diff}}^{\ddagger} + (\gamma/2)\Delta V_{\text{ex}}^{\ddagger} \quad (56)$$

where $0 \leq \theta \leq 1$ and $0 \leq \gamma \leq 1$. (Some minor contributions calculated⁶² from the Sumi–Marcus–Nadler treatment^{181,182} have opposite signs and effectively cancel.) The best opportunities for testing eqs 55 and 56 would seem to lie with those couples that include one partner of zero charge, for which Coulombic work and Debye–Hückel contributions are in principle zero and ion-pairing effects should be minimal.

fold smaller than is typical for ring reductions in CoTNPc or ZnPc, as might be expected for addition of an electron to the antibonding axial $3d_{z^2}$ orbital of Co. The Co^{III} reaction does *not* show an unusually large $\Delta V_{\text{el}}^\ddagger$, however, despite the associated expulsion of an axially coordinated anion (Scheme 1); evidently, the expulsion takes place independently of the rate-determining step in this case because Co^{III} is substitution-inert,³ and the rigid N_4 environment of Co in the phthalocyanine ring will suppress significant contributions to $\Delta V_{\text{el}}^\ddagger$ from internal reorganization. Second, for the $\text{Co}^{\text{II/I}}$ couple in various solvents, $\Delta V_{\text{el}}^\ddagger$ is very much larger than $\Delta V_{\text{diff}}^\ddagger$, the value of which is entirely typical of the other cases. According to Scheme 1, the Co^{II} reduction is accompanied by loss of coordinated solvent; evidently, this coordination change precedes the rate-determining electron transfer step, resulting in an unusually large volume increase on going to the transition state. This is possible because both Co^{II} and Co^{I} are labile in ligand substitution.³ In all these cases, comparison of $\Delta V_{\text{el}}^\ddagger$ with $\Delta V_{\text{ex}}^\ddagger$ would be illuminating, but no data on the homogeneous self-exchange kinetics of metallophthalocyanines are available, not surprisingly, since their solubilities are too low for current techniques such as NMR line broadening (the NMR spectra are in any case too complex).

5. Summary

Theory suggests that a linear log–log relationship should exist between the rate constants k_{el} for heterogeneous electron transfer of transition-metal complexes at solid electrodes and k_{ex} for the corresponding self-exchange reactions in homogeneous solution, although there has been debate as to whether the slope of the relationship should be 0.5 (Marcus) or 1.0 (Hush). Attempts^{1,4,57,138–142,150,167,279,285} to correlate k_{el} with k_{ex} , however, are unlikely to succeed quantitatively, regardless of adjustments for Coulombic work, double-layer effects, and so forth, because k_{el} for the great majority of electrode reactions is influenced by the identity of the electrode and the condition of its surface. In effect, this may mean that, contrary to widespread belief, many electrode reactions are not fully adiabatic ($\kappa_{\text{el}} \ll 1$), in which case the measured k_{el} will be less than the expected adiabatic value, whereas most homogeneous self-exchange reactions seem to be essentially adiabatic. Such nonadiabaticity may result from density-of-states effects on the metal electrode or, more likely, from the presence of a layer of adsorbed matter on the electrode through which the electron must tunnel to reach the metal surface, as has been established in experiments with SAMs. Alternatively, the reactant would have to displace some of the adsorbate to make direct contact with the metal with a corresponding input of energy, but in either case, the effect will be to diminish k_{el} . Such effects apply only to electrode reactions and not to the corresponding homogeneous self-exchange reactions.

Furthermore, conventional electrochemical kinetic techniques become diffusion-limited as k_{el} approaches about 1 cm s^{-1} , so the rates of fully adiabatic

electrode reactions, which are usually somewhat faster than this, can only be measured at present by resorting to ultramicroelectrode or special forced-convection techniques. Some couples present specific complications such as decomposition and associated electrode fouling that make accurate measurement of k_{el} difficult or impossible; ironically, two of the worst offenders in this respect are the traditional reference couples $\text{Fe}(\text{CN})_6^{3-/4-}$ for aqueous solutions and $\text{FeCp}_2^{+/0}$ for nonaqueous solvents. Trace contaminants may further confuse the issue by providing alternative electrode reaction pathways to the one of interest, although the enormous catalytic effect claimed for chloride on the $\text{Fe}(\text{H}_2\text{O})_6^{3+/2+}$ couple has probably been exaggerated. Finally, the retarding effects of increased solvent longitudinal relaxation time τ_L or, equivalently, solvent viscosity on the measured k_{el} in solvents other than undiluted water provide evidence that the rates of electrode reactions are controlled by solvent dynamics, whereas those of homogeneous electron self-exchange reactions are not.

On the other hand, the corresponding volumes of activation $\Delta V_{\text{el}}^\ddagger$ and $\Delta V_{\text{ex}}^\ddagger$ for aqueous solutions do show a close correlation of slope 0.5 (consistent with the Marcus approach) and zero intercept (Figure 8). This correlation emerges because electrode properties, including electrical double layer and adsorbed (inner Helmholtz) layer effects, are not significantly affected by applied pressure over the experimental range of 0–200 MPa and because the pressure dependence of the viscosity of water is serendipitously negligible in this pressure regime at temperatures around 25 °C. Consequently, even if solvent dynamics affect k_{el} in undiluted water (and this may not be the case because the existence of very fast solvent dynamical components may leave k_{TST} as the bottleneck in eq 37), $\Delta V_{\text{el}}^\ddagger$ will not be affected. Contrary to earlier expectations, it is now recognized that $\Delta V_{\text{el}}^\ddagger$ and $\Delta V_{\text{ex}}^\ddagger$ should be unaffected by nonadiabaticity. Thus, for simple electron transfer reactions in water, calculations based on Marcus' theory predict $\Delta V_{\text{el}}^\ddagger$ and $\Delta V_{\text{ex}}^\ddagger$ quite accurately and in particular rationalize the fact that both are invariably *negative* unless special effects, such as the specific catalysis of anion–anion electron transfer (both homogeneous and heterogeneous) by cations, intervene.

In contrast, *all* $\Delta V_{\text{el}}^\ddagger$ values for electrode reactions of transition-metal complexes in *nonaqueous* solvents are *positive*, even though $\Delta V_{\text{ex}}^\ddagger$ values for the corresponding homogeneous reactions in the same solvents, where known, are invariably negative. This is because the viscosity of nonaqueous solvents increases approximately exponentially with rising pressure, and the consequence of solvent dynamical control of the electrode reactions in organic media is therefore a large positive contribution to $\Delta V_{\text{el}}^\ddagger$ that swamps the negative contributions of the effects of internal and solvent reorganization on the activation barrier height. In accordance with this phenomenon, except with highly charged couples such as $\text{Fe}(\text{phen})_3^{3+/2+}$, $\Delta V_{\text{el}}^\ddagger$ is approximately equal to $\Delta V_{\text{diff}}^\ddagger$, the mean volume of activation for diffusion of the

reactants, which is a conveniently measured equivalent of the volume of activation for viscous flow. Furthermore, high k_{el} and low (but positive) ΔV_{el}^{\ddagger} are associated with low solvent viscosity and low $\Delta V_{diff}^{\ddagger}$, as in acetonitrile, while slow rates and high ΔV_{el}^{\ddagger} and $\Delta V_{diff}^{\ddagger}$ are found with the more viscous solvents such as propylene carbonate.

Pressure effects, then, can be uniquely informative concerning electron transfer mechanisms of transition-metal complexes in solution, partly because they are very sensitive to both static and dynamic solvent effects in normal liquids but also paradoxically because they are *insensitive* to other factors such as electrode and inner Helmholtz layer properties, internal reorganization of the reactants (other than major structural changes), nonadiabaticity, and—uniquely for *aqueous* solutions at near-ambient temperatures—the viscosity of solvent water. Thus, kinetic and mechanistic phenomena that may be obscured by the plethora of influences can be revealed with greater clarity when some of those influences are hidden.

6. Acknowledgment

I thank my many collaborators, whose names appear in the references, for their contributions to our work in this field and the Natural Sciences and Engineering Research Council of Canada for consistent financial support.

7. References

- Cannon, R. D. *Electron-Transfer Reactions*; Butterworth: London, 1980.
- (a) Astruc, D. *Electron Transfer and Radical Processes in Inorganic Chemistry*; VCH: New York, 1995. (b) Lappin, A. G. *Redox Mechanisms in Inorganic Chemistry*; Ellis Horwood: New York, 1994.
- (a) Wilkins, R. G. *Kinetics and Mechanism of Reactions of Transition Metal Complexes*, 2nd ed.; VCH: New York, 1991. (b) Jordan, R. B. *Reaction Mechanisms of Inorganic and Organometallic Systems*; Oxford University Press: New York, 1998. (c) Tobe, M. L.; Burgess, J. *Inorganic Reaction Mechanisms*; Addison-Wesley Longman: New York, 1999.
- (a) Saji, T.; Yamada, T.; Aoyagui, S. *J. Electroanal. Chem. Interfacial Electrochem.* **1975**, *61*, 147. (b) Saji, T.; Maruyama, Y.; Aoyagui, S. *J. Electroanal. Chem.* **1978**, *86*, 219.
- Weaver, M. J. *J. Phys. Chem.* **1980**, *84*, 568.
- Hush, N. S. *J. Chem. Phys.* **1958**, *28*, 962.
- Marcus, R. A. *Can. J. Chem.* **1959**, *37*, 155.
- Hush, N. S. *Trans. Faraday Soc.* **1961**, *57*, 557.
- Marcus, R. A. *J. Phys. Chem.* **1963**, *67*, 853.
- Marcus, R. A. *J. Chem. Phys.* **1965**, *43*, 679.
- Marcus, R. A. *Electrochim. Acta* **1968**, *13*, 995.
- Hush, N. S. *Electrochim. Acta* **1968**, *13*, 1005.
- Hale, J. M. In *Reactions of Molecules at Electrodes*; Hush, N. S., Ed.; Wiley: New York, 1971; p 229.
- Marcus, R. A.; Sutin, N. S. *Biochim. Biophys. Acta* **1985**, *811*, 265.
- Weaver, M. J. *J. Electroanal. Chem.* **2001**, *498*, 105.
- Bard, A. J.; Faulkner, L. R. *Electrochemical Methods: Fundamentals and Applications*, 2nd ed.; Wiley: New York, 2001.
- Gosser, D. K., Jr. *Cyclic Voltammetry: Simulation and Analysis of Reaction Mechanisms*; VCH: New York, 1993.
- Fisher, A. C. *Electrode Dynamics*; Oxford University Press: Oxford, U.K., 1996.
- Bockris, J. O'M.; Reddy, A. K. N.; Gamboa-Aldeco, M. *Fundamentals of Electrode Processes*; Modern Electrochemistry, 2nd ed., Vol. 2A; Plenum Press: New York, 2000.
- Oldham, K. E.; Myland, J. C. *Fundamentals of Electrochemical Science*; Academic Press: San Diego, CA, 1994.
- Zanello, P. *Inorganic Electrochemistry*; Royal Society of Chemistry: Cambridge, U.K., 2003.
- Rieger, P. H. *Electrochemistry*, 2nd ed.; Chapman and Hall: New York, 1994.
- Christensen, P. A.; Hamnett, A. *Techniques and Mechanisms in Electrochemistry*; Blackie: New York, 1994.
- Sawyer, D. T.; Sobkowiak, A.; Roberts, J. R., Jr. *Electrochemistry for Chemists*, 2nd ed.; Wiley: New York, 1995.
- Hamann, C. H.; Hamnett, A.; Vielstich, W. *Electrochemistry*; Wiley-VCH: New York, 1998.
- Brett, C. M. A.; Brett, A. M. O. *Electrochemistry: Principles, Methods, and Applications*; Oxford University Press: Oxford, U.K., 1993.
- Koryta, J.; Dvořák, J.; Kavan, L. *Principles of Electrochemistry*; Wiley: Chichester, U.K., 1993.
- Pletcher, D. *A First Course in Electrode Processes*; Electrochemical Consultancy: Hampshire, U.K., 1991.
- Schmickler, W. *Interfacial Electrochemistry*; Oxford University Press: New York, 1996.
- Miller, R. J. D.; McLendon, G. L.; Nozik, A. J.; Schmickler, W.; Willig, F. *Surface Electron-Transfer Processes*; VCH: New York, 1995.
- Bockris, J. O'M.; Khan, S. U. M. *Surface Electrochemistry: A Molecular Level Approach*; Plenum: New York, 1993.
- Thirsk, H. R.; Harrison, J. A. *A Guide to the Study of Electrode Kinetics*; Academic Press: London, 1972.
- Albery, J. *Electrode Kinetics*; Oxford University Press: Oxford, U.K., 1975.
- Electrode Kinetics: Principles and Methodology*; Bamford, C. H., Compton, R. G., Eds.; Comprehensive Chemical Kinetics, Vol. 26; Elsevier: Amsterdam, 1986.
- Electrode Kinetics: Reactions*; Compton, R. G., Ed.; Comprehensive Chemical Kinetics, Vol. 27; Elsevier: Amsterdam, 1987.
- New Techniques for the Study of Electrodes and their Reactions*; Compton, R. G., Hamnett, A., Eds.; Comprehensive Chemical Kinetics, Vol. 29; Elsevier: Amsterdam, 1989.
- Gileadi, E. *Electrode Kinetics for Chemists, Chemical Engineers, and Materials Scientists*; VCH: New York, 1993.
- Anderson, J. L.; Bowden, E. F.; Pickup, P. G. *Anal. Chem.* **1996**, *68*, 379R.
- Anderson, J. L.; Coury, L. A., Jr.; Leddy, J. *Anal. Chem.* **1998**, *70*, 519R.
- Anderson, J. L.; Coury, L. A., Jr.; Leddy, J. *Anal. Chem.* **2000**, *72*, 4497.
- Hupp, J. T.; Weaver, M. J. *J. Phys. Chem.* **1984**, *88*, 6128.
- Matthews, D. *Aust. J. Chem.* **1994**, *47*, 2171.
- Matthews, D. *Aust. J. Chem.* **1995**, *48*, 1843.
- Mines, G. A.; Bjerrum, M. J.; Hill, M. G.; Casimiro, D. R.; Chang, I. J.; Winkler, J. R.; Gray, H. B. *J. Am. Chem. Soc.* **1996**, *118*, 1961.
- Swaddle, T. W.; Tregloan, P. A. *Coord. Chem. Rev.* **1999**, *187*, 255.
- Swaddle, T. W. In *Comprehensive Coordination Chemistry*, 2nd ed.; McCleverty, J. A., Meyer, T. J., Eds.; Elsevier: Oxford, U.K., 2003; Vol. 2, Chapter 18, pp 245–250.
- Swaddle, T. W. In *High-Pressure Chemistry: Synthetic, Mechanistic, and Supercritical Applications*; van Eldik, R., Klärner, F.-G., Eds.; Wiley-VCH: Weinheim, Germany, 2002; Chapter 5, pp 161–183.
- Nicholson, R. S. *Anal. Chem.* **1965**, *37*, 1351.
- Bard, A. J.; Faulkner, L. R. *Electrochemical Methods: Fundamentals and Applications*, 2nd ed.; Wiley: New York, 2001; p 242.
- (a) Smith, D. E. *Electroanal. Chem.* **1966**, *1*, 1. (b) Bond, A. M. *Anal. Chem.* **1972**, *44*, 315. (c) Bond, A. M. *Modern Polarographic Methods in Analytical Chemistry*; Marcel Dekker: New York, 1980; Chapter 7.
- (a) Engblom, S. O.; Myland, J. C.; Oldham, K. B. *J. Electroanal. Chem.* **2000**, *480*, 120. (b) Engblom, S. O.; Myland, J. C.; Oldham, K. B.; Taylor, A. L. *Electroanalysis* **2001**, *13*, 626.
- Gavaghan, D. J.; Bond, A. M. *J. Electroanal. Chem.* **2000**, *480*, 133.
- Weaver, M. J. *Chem. Rev.* **1992**, *92*, 463.
- Weaver, M. J. *J. Mol. Liq.* **1994**, *60*, 57.
- Baranski, A. S.; Winkler, K. *J. Electroanal. Chem.* **1998**, *453*, 29.
- Fu, Y.; Swaddle, T. W. *Chem. Commun.* **1996**, 1171.
- Fu, Y.; Swaddle, T. W. *J. Am. Chem. Soc.* **1997**, *119*, 7137.
- Fu, Y.; Swaddle, T. W. *Inorg. Chem.* **1999**, *38*, 876.
- Fu, Y.; Cole, A. S.; Swaddle, T. W. *J. Am. Chem. Soc.*, **1999**, *121*, 10410.
- Metelski, P. D.; Fu, Y.; Khan, K.; Swaddle, T. W. *Inorg. Chem.* **1999**, *38*, 3103.
- Matsumoto, M.; Lamprecht, D.; North, M. R.; Swaddle, T. W. *Can. J. Chem.* **2001**, *79*, 1864.
- Zhou, J.; Swaddle, T. W. *Can. J. Chem.* **2001**, *79*, 841.
- Matsumoto, M.; Neuman, N. I.; Swaddle, T. W. *Inorg. Chem.* **2004**, *43*, 1153.
- Matsumoto, M.; Swaddle, T. W. *Inorg. Chem.* **2004**, *43*, 2724.
- Yu, B.; Lever, A. B. P.; Swaddle, T. W. *Inorg. Chem.* **2004**, *43*, 4496.
- Bond, A. M.; O'Halloran, R. J.; Ruzic, I.; Smith, D. E. *Anal. Chem.* **1976**, *48*, 872.

- (67) Wightman, R. M. *Anal. Chem.* **1981**, *53*, 1125A.
- (68) Wightman, R. M.; Wipf, D. O. In *Electroanalytical Chemistry*; Bard, A. J., Ed.; Marcel Dekker: New York, 1989; Vol. 15, p 267.
- (69) Heinze, J. *Angew. Chem., Int. Ed. Engl.* **1993**, *32*, 1268.
- (70) Forster, R. J. *Chem. Soc. Rev.* **1994**, *23*, 289.
- (71) Robinson, J. In *New Techniques for the Study of Electrodes and their Reactions*; Compton, R. G., Hamnett, A., Eds.; Comprehensive Chemical Kinetics, Vol. 29; Elsevier: Amsterdam, 1989; Chapter 5.
- (72) Amatore, C. In *Physical Electrochemistry*; Rubenstein, I., Ed.; Marcel Dekker: New York, 1995; Chapter 4.
- (73) Pedersen, S. U.; Daasbjerg, K. In *Electron Transfer in Chemistry*; Balzani, V., Ed.; Wiley-VCH: Weinheim, Germany, 2001; Vol. 1, p 422.
- (74) Baranski, A. S. *J. Electrochem. Soc.* **1986**, *133*, 93.
- (75) Howell, J. O.; Wightman, R. M. *Anal. Chem.* **1984**, *56*, 524.
- (76) Crooker, J. C.; Murray, R. W. *Anal. Chem.* **2000**, *72*, 3245.
- (77) Ciszowska, M.; Stojek, Z. *J. Electroanal. Chem.* **1999**, *466*, 129.
- (78) Lee, C.; Anson, F. C. *J. Electroanal. Chem.* **1992**, *323*, 381.
- (79) Stevenson, K. J.; White, H. S. *J. Phys. Chem.* **1996**, *100*, 18818.
- (80) Clegg, A. D.; Rees, N. V.; Klymenko, O. V.; Coles, B. A.; Compton, R. G. *J. Am. Chem. Soc.* **2004**, *126*, 6185 and references therein.
- (81) Macpherson, J. V.; Beeston, M. A.; Unwin, P. R. *J. Chem. Soc., Faraday Trans.* **1995**, *91*, 899.
- (82) McCreery, R. L. In *Electroanalytical Chemistry*; Bard, A. J., Ed.; Marcel Dekker: New York, 1991; Vol. 17, p 221.
- (83) Hromadová, M.; Fawcett, W. R. *J. Phys. Chem. A* **2001**, *105*, 104.
- (84) Ferro, S.; Urgeghe, C.; De Battisti, A. *J. Phys. Chem. B* **2004**, *108*, 6398.
- (85) (a) Cline, K. K.; McDermott, M. T.; McCreery, R. L. *J. Phys. Chem.* **1994**, *98*, 5314. (b) Rice, R. J.; McCreery, R. L. *Anal. Chem.* **1989**, *61*, 1637. (c) Chen, P.; McCreery, R. L. *Anal. Chem.* **1996**, *68*, 3958.
- (86) Hu, I.-F.; Karweik, D. H.; Kuwana, T. *J. Electroanal. Chem.* **1985**, *188*, 59.
- (87) (a) Rice, M. E.; Galus, Z.; Adams, R. N. *J. Electroanal. Interfacial Electrochem.* **1983**, *143*, 89. (b) Ramesh, P.; Sampath, S. *Anal. Chem.* **2003**, *75*, 6949.
- (88) Iwasita, T.; Schmickler, W.; Schultze, J. W. *Ber. Bunsen-Ges. Phys. Chem.* **1985**, *89*, 138.
- (89) Iwasita, T.; Schmickler, W.; Schultze, J. W. *J. Electroanal. Chem.* **1985**, *194*, 355.
- (90) Anson, F. C. *Anal. Chem.* **1961**, *33*, 934.
- (91) Kitamura, F.; Nanbu, N.; Ohsaka, T.; Tokuda, K. *J. Electroanal. Chem.* **1998**, *456*, 113.
- (92) Winkler, K. *J. Electroanal. Chem.* **1995**, *388*, 151.
- (93) Beriet, C.; Pletcher, D. *J. Electroanal. Chem.* **1993**, *361*, 93.
- (94) Zotti, G.; Schiavon, G.; Zecchin, S.; Favretto, D. *J. Electroanal. Chem.*, **1998**, *456*, 217.
- (95) Mahlendorf, F.; Heinze, J. *J. Electroanal. Chem.* **1993**, *352*, 119.
- (96) Fawcett, W. R.; Opařo, M. *Angew. Chem., Int. Ed. Engl.* **1994**, *33*, 2131.
- (97) (a) Gennett, T.; Weaver, M. J. *Anal. Chem.* **1984**, *56*, 1444. (b) Wilke, N.; Baruzzi, A. M. *J. Electroanal. Chem.* **2002**, *537*, 67.
- (98) Noviadri, I.; Brown, K. N.; Fleming, D. S.; Gulyas, P. T.; Lay, P. A.; Masters, A. F.; Phillips, L. *J. Phys. Chem. B* **1999**, *103*, 6713.
- (99) Finklea, H. O. In *Electroanalytical Chemistry*; Bard, A. J., Rubenstein, I., Eds.; Marcel Dekker: New York, 1996; Vol. 19, p 109.
- (100) Xing, Y. F.; O'Shea, S. J.; Li, S. F. Y. *J. Electroanal. Chem.* **2003**, *542*, 7.
- (101) Wold, D. J.; Haag, R.; Rampi, M. A.; Frisbie, C. D. *J. Phys. Chem. B* **2002**, *106*, 2813.
- (102) Dolidze, T. D.; Khoshtariya, D. E.; Waldeck, D. H.; Macyk, J.; van Eldik, R. *J. Phys. Chem. B* **2003**, *107*, 7172.
- (103) Gavaghan, D. J.; Feldberg, S. W. *J. Electroanal. Chem.* **2000**, *491*, 103.
- (104) Savéant, J.-M. *J. Phys. Chem. B* **2001**, *105*, 8995.
- (105) Johnson, D. C.; Resnick, E. W. *Anal. Chem.* **1977**, *49*, 1918.
- (106) Hung, N. C.; Nagy, Z. *J. Electrochem. Soc.* **1987**, *134*, 2215.
- (107) Abbott, A. P.; Harper, J. C.; Stimson, G. *J. Electroanal. Chem.* **2002**, *520*, 6.
- (108) Krulic, D.; Fatouros, N.; Khoshtariya, D. E. *J. Chim. Phys.* **1998**, *95*, 497.
- (109) Zahl, A.; van Eldik, R.; Swaddle, T. W. *Inorg. Chem.* **2002**, *41*, 757.
- (110) Curtiss, L. A.; Halley, J. W.; Hautman, J.; Hung, N. C.; Nagy, Z.; Rhee, Y.-J.; Yonco, R. M. *J. Electrochem. Soc.* **1991**, *138*, 2032.
- (111) Henderson, M. P.; Miasek, V. I.; Swaddle, T. W. *Can. J. Chem.* **1971**, *49*, 317.
- (112) Fabes, L.; Swaddle, T. W. *Can. J. Chem.* **1975**, *53*, 3053.
- (113) Marcus, R. A. *J. Chem. Phys.* **1956**, *24*, 966.
- (114) Marcus, R. A. *J. Chem. Phys.* **1956**, *24*, 979.
- (115) Sutin, N. *Adv. Chem. Phys.* **1999**, *106*, 7.
- (116) *Electron Transfer in Chemistry*; Balzani, V., Ed.; Wiley-VCH: New York, 2001; Vol. 1, Part 1, Chapters 1–10.
- (117) Schmickler, W.; Frank, S. In *Interfacial Kinetics and Mass Transport*; Bard, A. J., Calvo, E. J., Eds.; Encyclopedia of Electrochemistry, Vol. 2; Wiley-VCH: Weinheim, Germany, 2003; p 31.
- (118) Miller, C. J. In *Physical Electrochemistry*; Rubenstein, I., Ed.; Marcel Dekker: New York, 1995; Chapter 2.
- (119) Hush, N. S. *J. Electroanal. Chem.* **1999**, *460*, 5.
- (120) (a) Newton, M. D. *Chem. Rev.* **1991**, *91*, 767. (b) Newton, M. D. *Coord. Chem. Rev.* **2003**, *238/239*, 167.
- (121) Barbara, P. F.; Meyer, T. J.; Ratner, M. A. *J. Phys. Chem.* **1996**, *100*, 13148.
- (122) Levich, V. G. *Adv. Electrochem. Electrochem. Eng.* **1966**, *4*, 249.
- (123) Dogonadze, R. R. In *Reactions of Molecules at Electrodes*; Hush, N. S., Ed.; Wiley: New York, 1971; p 135.
- (124) Tsirlina, G. A.; Kharkats, Yu. I.; Nazmutdinov, R. R.; Petrii, O. A. *J. Electroanal. Chem.* **1998**, *450*, 63.
- (125) Medvedev, I. G. *J. Electroanal. Chem.* **2000**, *481*, 215.
- (126) Medvedev, I. G. *J. Electroanal. Chem.* **2001**, *517*, 1.
- (127) Gupta, G.; Matyushov, D. V. *J. Phys. Chem. A* **2004**, *108*, 2087.
- (128) Small, D. W.; Matyushov, D. V.; Voth, G. A. *J. Am. Chem. Soc.* **2003**, *125*, 7470.
- (129) Vath, P.; Zimmt, M. B.; Matyushov, D. V.; Voth, G. A. *J. Phys. Chem. B* **1999**, *103*, 9130.
- (130) Hartnig, C.; Koper, M. T. M. *J. Am. Chem. Soc.* **2003**, *125*, 9840.
- (131) Kuznetsov, A. M.; Medvedev, I. G. *J. Electroanal. Chem.* **2001**, *502*, 15.
- (132) Sando, G. M.; Spears, K. G.; Hupp, J. T.; Ruhoff, P. T. *J. Phys. Chem. A* **2001**, *105*, 5317.
- (133) (a) Spiccia, L.; Swaddle, T. W. *Inorg. Chem.* **1987**, *26*, 2265. (b) Spiccia, L.; Swaddle, T. W. *Inorg. Chem.* **1988**, *27*, 4080 (correction).
- (134) Milner, D.; Weaver, M. J. *J. Electroanal. Chem.* **1985**, *191*, 411.
- (135) Peover, M. E. In *Reactions of Molecules at Electrodes*; Hush, N. S., Ed.; Wiley: New York, 1971; p 259.
- (136) Forno, A. E. J.; Peover, M. E.; Wilson, R. *Trans. Faraday Soc.* **1970**, *66*, 1322.
- (137) Abbreviations: AC = acetone; AN = acetonitrile; BN = benzonitrile; DCM = dichloromethane; DMA = *N,N*-dimethylacetamide; DMF = *N,N*-dimethylformamide; DMSO = dimethyl sulfoxide; PC = propylene carbonate; Py = pyridine; TBAP = tetra-*n*-butylammonium perchlorate; TBAHFP = tetra-*n*-butylammonium hexafluorophosphate; TEAP = tetraethylammonium perchlorate; GC = glassy carbon; bpy = 2,2'-bipyridine; hfac⁻ = hexafluoroacetylacetonate; Cp^{*} = η⁵-C₅H₅; Cp^{*} = η⁵-C₅(CH₃)₅; TST = transition-state theory; TTF = tetrathiafulvalene; acac⁻ = acetylacetonate; dmg²⁻ = doubly deprotonated dimethylglyoxime; EDTA⁴⁻ = ethylenediaminetetraacetate; en = 1,2-diaminoethane; phen = 1,10-phenanthroline; tacn = 1,4,7-triazacyclononane; ttcn = 1,4,7-trithiacyclononane; sep = sepulchrate = 1,3,6,8,10,13,16,19-octaazabicyclo[6.6.6]eicosane; diamsar = diaminosarcophagine = 1,8-diamino-3,6,10,13,16,19-hexaazabicyclo[6.6.6]eicosane; act = azacaptan = 8-methyl-1,3,13,16-tetraaza-6,10,19-trithiabicyclo[6.6.6]eicosane; Me = methyl; Et = ethyl; Bu = butyl; chx = cyclohexyl; dmp = 2,9-dimethyl-1,10-phenanthroline; terpy = 2,2':6,2''-terpyridine; Cyt c = horse-heart cytochrome c; Pc = phthalocyanine; TNPc = tetraeneoptoxyphthalocyanine.
- (138) Kojima, H.; Bard, A. J. *J. Am. Chem. Soc.* **1975**, *97*, 6317.
- (139) Hupp, J. T.; Weaver, M. J. *J. Electroanal. Chem.* **1983**, *152*, 1.
- (140) Endicott, J. F.; Schroeder, R. R.; Chidester, D. H.; Ferrier, D. R. *J. Phys. Chem.* **1973**, *77*, 2579.
- (141) Weaver, M. J. *Inorg. Chem.* **1976**, *15*, 1733.
- (142) Weaver, M. J. *J. Phys. Chem.* **1980**, *84*, 568.
- (143) Hupp, J. T.; Weaver, M. J. *J. Phys. Chem.* **1985**, *89*, 1601.
- (144) Hupp, J. T.; Liu, H. Y.; Farmer, J. K.; Gennett, T.; Weaver, M. J. *J. Electroanal. Chem.* **1984**, *168*, 313.
- (145) Gennett, T.; Milner, D. F.; Weaver, M. J. *J. Phys. Chem.* **1985**, *89*, 2787.
- (146) Hupp, J. T.; Weaver, M. J. *J. Phys. Chem.* **1985**, *89*, 2795.
- (147) Nielson, R. M.; Golovin, M. N.; McManis, G. E.; Weaver, M. J. *J. Am. Chem. Soc.* **1988**, *110*, 1745.
- (148) Weaver, M. J.; Phelps, D. K.; Nielson, R. M.; Golovin, M. N.; McManis, G. E. *J. Phys. Chem.* **1990**, *94*, 2949.
- (149) Phelps, D. K.; Kornyshev, A. A.; Weaver, M. J. *J. Phys. Chem.* **1990**, *94*, 1454.
- (150) Weaver, M. J. *J. Phys. Chem.* **1990**, *94*, 8608.
- (151) Weaver, M. J. In *Electrode Kinetics: Reactions*; Compton, R. G., Ed.; Comprehensive Chemical Kinetics, Vol. 27; Elsevier: Amsterdam, 1987; p 1.
- (152) Morgan, J. D.; Wolynes, P. G. *J. Phys. Chem.* **1987**, *91*, 874.
- (153) Zusman, L. D. *Chem. Phys.* **1987**, *112*, 53.
- (154) McManis, G. E.; Nielson, R. M.; Gochev, A.; Weaver, M. J. *J. Am. Chem. Soc.* **1989**, *111*, 5533.
- (155) Gosavi, S.; Marcus, R. A. *J. Phys. Chem. B* **2000**, *104*, 2067.
- (156) Kramers, H. A. *Physica (Amsterdam)* **1940**, *7*, 284.
- (157) Zusman, L. D. *Chem. Phys.* **1980**, *49*, 295.
- (158) Zusman, L. D. *Chem. Phys.* **1990**, *144*, 1.
- (159) Zusman, L. D. *J. Phys. Chem.* **1994**, *186*, 1.
- (160) Grote, R. F.; Hynes, J. T. *J. Chem. Phys.* **1980**, *73*, 2715.

- (161) Hynes, J. T. *J. Phys. Chem.* **1986**, *90*, 3701.
- (162) Calef, D. F.; Wolynes, P. G. *J. Phys. Chem.* **1983**, *87*, 3387.
- (163) Calef, D. F.; Wolynes, P. G. *J. Chem. Phys.* **1983**, *78*, 470.
- (164) Heitele, H. *Angew. Chem., Int. Ed. Engl.* **1993**, *32*, 359.
- (165) Galus, Z. *Adv. Electrochem. Sci. Eng.* **1995**, *4*, 217.
- (166) Kivelson, D.; Friedman, H. *J. Phys. Chem.* **1989**, *93*, 7026.
- (167) Fawcett, W. R.; Foss, C. A., Jr. *J. Electroanal. Chem.* **1989**, *270*, 103.
- (168) Grampp, G.; Harrer, W.; Jaenicke, W. *J. Chem. Soc., Faraday Trans. 1* **1987**, *83*, 161.
- (169) Sumi, H.; Marcus, R. A. *J. Chem. Phys.* **1986**, *84*, 4272.
- (170) Marcus, R. A.; Sumi, H. *J. Electroanal. Chem.* **1986**, *204*, 59.
- (171) Sparpaglione, M.; Mukamel, S. *J. Phys. Chem.* **1987**, *91*, 3938.
- (172) McManis, G. E.; Weaver, M. J. *J. Chem. Phys.* **1989**, *90*, 912.
- (173) Jimenez, R.; Fleming, G. R.; Kumar, P. V.; Maroncelli, M. *Nature* **1994**, *369*, 471.
- (174) Agmon, N. *J. Phys. Chem.* **1996**, *100*, 1072.
- (175) Nitzan, A. *Nature* **1999**, *402*, 472.
- (176) Roy, S.; Bagchi, B. *J. Phys. Chem.* **1994**, *98*, 9207.
- (177) Ovchinnikova, M. Ya. *Theor. Exp. Chem.* **1981**, *17*, 507.
- (178) Winkler, K.; McKnight, N.; Fawcett, W. R. *J. Phys. Chem. B* **2000**, *104*, 3575.
- (179) Agmon, N.; Hopfield, J. J. *J. Chem. Phys.* **1983**, *78*, 6947.
- (180) Agmon, N.; Hopfield, J. J. *J. Chem. Phys.* **1983**, *79*, 2042.
- (181) Sumi, H.; Marcus, R. A. *J. Chem. Phys.* **1986**, *84*, 4894.
- (182) Marcus, R. A.; Nadler, W. J. *J. Chem. Phys.* **1987**, *86*, 3906.
- (183) (a) Sumi, H. *J. Phys. Chem.* **1991**, *95*, 3334. (b) Sumi, H. In *Electron Transfer in Chemistry*; V. Balzani, Ed.; Wiley-VCH: New York, 2001; Vol. 1, p 64.
- (184) Smith, B. B.; Hynes, J. T. *J. Chem. Phys.* **1993**, *99*, 6517.
- (185) Basilevsky, M. V.; Ryaboy, V. M.; Weinberg, N. N. *J. Phys. Chem.* **1990**, *94*, 8734.
- (186) Basilevsky, M. V.; Ryaboy, V. M.; Weinberg, N. N. *J. Phys. Chem.* **1991**, *95*, 5533.
- (187) McGuire, M.; McLendon, G. *J. Phys. Chem.* **1986**, *90*, 2549.
- (188) Fawcett, W. R.; Opařto, M. *J. Electroanal. Chem.* **1993**, *349*, 273.
- (189) Weaver, M. J.; McManis, G. E., III *Acc. Chem. Res.* **1990**, *23*, 294.
- (190) Smalley, J. F.; Geng, L.; Chen, A.; Feldberg, S. W.; Lewis, N. S.; Cali, G. *J. Electroanal. Chem.* **2003**, *549*, 13.
- (191) Yu, B.; Swaddle, T. W. Unpublished work.
- (192) Hartnig, C.; Koper, M. T. M. *J. Chem. Phys.* **2001**, *115*, 8540.
- (193) Sachinidis, J. I.; Shalders, R. D.; Tregloan, P. A. *Inorg. Chem.* **1994**, *33*, 6180.
- (194) Bajaj, H. C.; Tregloan, P. A.; van Eldik, R. *Inorg. Chem.* **2004**, *43*, 1429.
- (195) Tran, D.; Hunt, J. P.; Wherland, S. *Inorg. Chem.* **1992**, *31*, 2460.
- (196) Grampp, G.; Kapturkiewicz, A.; Jaenicke, W. *Ber. Bunsen-Ges. Phys. Chem.* **1990**, *94*, 439.
- (197) Fawcett, W. R.; Blum, L. *J. Chem. Phys. Lett.* **1991**, *187*, 173.
- (198) Takagi, H. D.; Swaddle, T. W. *J. Chem. Phys. Lett.* **1996**, *248*, 207.
- (199) Swaddle, T. W. *Can. J. Chem.* **1996**, *74*, 631.
- (200) Aherne, D.; Tran, V.; Schwartz, B. J. *J. Phys. Chem. B* **2000**, *104*, 5382.
- (201) Wherland, S. *Inorg. Chem.* **1983**, *22*, 2349. Note the following corrections: the first term on the right of eq 7 should be negative; for water at 25 °C ($\partial \ln \epsilon/\partial P$)_T = 4.71 × 10⁻¹⁰ Pa⁻¹ and B = 3.284 × 10⁹ kg^{1/2} mol^{-1/2} m⁻¹.
- (202) Shalders, R. D.; Swaddle, T. W. *Inorg. Chem.* **1995**, *34*, 4815.
- (203) Davies, C. W. *Prog. React. Kinet.* **1961**, *1*, 161.
- (204) (a) Pitzer, K. S. *J. Phys. Chem.* **1973**, *77*, 268. (b) Pitzer, K. S. In *Activity Coefficients in Electrolyte Solutions*; Pytkowicz, R. M., Ed.; CRC Press: Boca Raton, FL, 1979; Vol. 1, pp 157–208.
- (205) Fuoss, R. M. *J. Am. Chem. Soc.* **1958**, *80*, 5059.
- (206) Kuznetsov, A. M.; Phelps, D. K.; Weaver, M. J. *Int. J. Chem. Kinet.* **1990**, *22*, 815.
- (207) Chan, M.-S.; Wahl, A. C. *J. Phys. Chem.* **1982**, *86*, 126.
- (208) Doine, H.; Swaddle, T. W. *Inorg. Chem.* **1988**, *27*, 665.
- (209) Karpinski, Z. J.; Osteryoung, R. A. *J. Electroanal. Chem.* **1993**, *349*, 285.
- (210) Yang, E. S.; Chan, M.-S.; Wahl, A. C. *J. Phys. Chem.* **1975**, *79*, 2049.
- (211) Yang, E. S.; Chan, M.-S.; Wahl, A. C. *J. Phys. Chem.* **1980**, *84*, 3094.
- (212) Nielson, R. M.; McManis, G. E.; Safford, L. K.; Weaver, M. J. *J. Phys. Chem.* **1989**, *93*, 2152.
- (213) Kirchner, K.; Dang, S.-Q.; Stebler, M.; Dodgen, H. W.; Wherland, S.; Hunt, J. P. *Inorg. Chem.* **1989**, *28*, 3604.
- (214) Weaver, M. J.; Gennett, T. *J. Chem. Phys. Lett.* **1985**, *113*, 213.
- (215) Gennett, T.; Weaver, M. J. *J. Electroanal. Chem.* **1985**, *186*, 179.
- (216) Safford, L. K.; Weaver, M. J. *J. Electroanal. Chem.* **1992**, *331*, 857.
- (217) Nielson, R. M.; McManis, G. E.; Golovin, M. N.; Weaver, M. J. *J. Phys. Chem.* **1988**, *92*, 3441.
- (218) McManis, G. E.; Golovin, M. N.; Weaver, M. J. *J. Phys. Chem.* **1986**, *90*, 6563.
- (219) Zahl, A.; van Eldik, R.; Swaddle, T. W. *Inorg. Chem.* **2003**, *42*, 3718.
- (220) Richardson, J. N.; Harvey, J.; Murray, R. W. *J. Phys. Chem.* **1994**, *98*, 13396.
- (221) Wherland, S. *Coord. Chem. Rev.* **1993**, *123*, 169.
- (222) Chan, M.-S.; Wahl, A. C. *J. Phys. Chem.* **1978**, *82*, 2542.
- (223) Grace, M. R.; Swaddle, T. W. *Inorg. Chem.* **1993**, *32*, 5597.
- (224) Shporer, M.; Ron, G.; Loewenstein, A.; Navon, G. *Inorg. Chem.* **1965**, *4*, 361.
- (225) Campion, R. J.; Deck, C. F.; King, P., Jr.; Wahl, A. C. *Inorg. Chem.* **1967**, *6*, 672.
- (226) Loewenstein, A.; Ron, G. *Inorg. Chem.* **1967**, *6*, 1604.
- (227) Kurland, R. J.; Winkler, M. E. *J. Biochem. Biophys. Methods* **1981**, *4*, 215.
- (228) Takagi, H.; Swaddle, T. W. *Inorg. Chem.* **1992**, *31*, 4669.
- (229) Khoshtariya, D. E.; Kjaer, A. M.; Marsagishvili, T. A.; Ulstrup, J. **1992**, *96*, 4154.
- (230) Khoshtariya, D. E.; Dolidze, T. D.; Neubrand, A.; van Eldik, R. *J. Mol. Liq.* **2000**, *89*, 127.
- (231) Macartney, D. H. *Inorg. Chem.* **1991**, *30*, 3337.
- (232) Metelski, P. D.; Swaddle, T. W. *Inorg. Chem.* **1999**, *38*, 301.
- (233) Sheppard, J. C.; Wahl, A. C. *J. Am. Chem. Soc.* **1957**, *79*, 1020.
- (234) Gjertsen, L.; Wahl, A. C. *J. Am. Chem. Soc.* **1959**, *81*, 1572.
- (235) Myers, O. E.; Sheppard, J. C. *J. Am. Chem. Soc.* **1961**, *83*, 4739.
- (236) Nichugovskii, G. F.; Shvedov, V. P. *Zh. Neorg. Khim.* **1969**, *14*, 299.
- (237) Lemire, R. J.; Lister, M. W. *J. Solution Chem.* **1976**, *5*, 171.
- (238) Dogonadze, R. R.; Ulstrup, J.; Kharkats, Yu. I. *Electroanal. Chem. Interfacial Electrochem.* **1972**, *39*, 47.
- (239) Marcus, Y. *Ion Properties*; Marcel Dekker: New York, 1997; p 121.
- (240) Symons, M. C. R. *J. Phys. Chem. Chem. Phys.* **1999**, *1*, 113.
- (241) Vol'kenshtein, M. V.; Dogonadze, R. R.; Madumarov, A. K.; Kharkats, Yu. I. *Dokl. Akad. Nauk SSSR* **1971**, *199*, 124.
- (242) Levich, V. G.; Madumarov, A. K.; Kharkats, Yu. I. *Dokl. Akad. Nauk SSSR* **1972**, *203*, 1351.
- (243) Kharkats, Yu. I. *Sov. Electrochem.* **1972**, *8*, 1266.
- (244) Kharkats, Yu. I. *Sov. Electrochem.* **1973**, *9*, 845.
- (245) Kharkats, Yu. I.; Chonishvili, G. M. *Sov. Electrochem.* **1975**, *11*, 164.
- (246) Kharkats, Yu. I.; Kuznetsov, A. M.; Ulstrup, J. *J. Phys. Chem.* **1995**, *99*, 13545.
- (247) Bixon, M.; Jortner, J. *Adv. Chem. Phys.* **1999**, *106*, 35.
- (248) Sumi, H.; Kakitani, T. *J. Phys. Chem. B* **2001**, *105*, 9603.
- (249) Křta, J.; Yeager, E. *Electroanal. Chem. Interfacial Electrochem.* **1975**, *59*, 110.
- (250) Bindra, P.; Gerischer, H.; Peter, L. M. *J. Electroanal. Chem.* **1974**, *57*, 435.
- (251) Peter, L. M.; Dřrr, W.; Bindra, P.; Gerischer, H. *J. Electroanal. Chem.* **1976**, *71*, 31.
- (252) Campbell, S. A.; Peter, L. M. *J. Electroanal. Chem.* **1994**, *364*, 257.
- (253) Sohr, R.; Mřller, L.; Landsberg, R. *J. Electroanal. Interfacial Electrochem.* **1974**, *50*, 55.
- (254) Sohr, R.; Mřller, L. *Electrochim. Acta* **1975**, *20*, 451.
- (255) Khoshtariya, D. E.; Kjaer, A. M.; Marsagishvili, T.; Ulstrup, J. *J. Phys. Chem.* **1991**, *95*, 8797.
- (256) Billing, R.; Khoshtariya, D. E. *Inorg. Chem.* **1994**, *33*, 4038.
- (257) Khoshtariya, D. E.; Meusinger, R.; Billing, R. *J. Phys. Chem.* **1995**, *99*, 3592.
- (258) Khoshtariya, D. E.; Billing, R.; Ackermann, M.; van Eldik, R. *J. Chem. Soc., Faraday Trans.* **1995**, *91*, 1625.
- (259) Zhang, X.; Leddy, J.; Bard, A. J. *J. Am. Chem. Soc.* **1985**, *107*, 3719.
- (260) Zhang, X.; Yang, H.; Bard, A. J. *J. Am. Chem. Soc.* **1987**, *109*, 1916.
- (261) Khoshtariya, D. E.; Dolidze, T. D.; Krulic, D.; Fatouros, N.; Devilliers, D. *J. Phys. Chem. B* **1998**, *102*, 7800.
- (262) Khoshtariya, D. E.; Dolidze, T. D.; Zusman, L. D.; Waldeck, D. H. *J. Phys. Chem. A* **2001**, *105*, 1818.
- (263) Iwasita, T.; Schmickler, W.; Herrmann, J.; Vogel, U. *J. Electrochem. Soc.* **1983**, *130*, 2026.
- (264) Angell, D. H.; Dickinson, T. *J. Electroanal. Chem. Interfacial Electrochem.* **1972**, *35*, 55.
- (265) Randles, J. E. B.; Somerton, K. W. *Trans. Faraday Soc.* **1952**, *48*, 937.
- (266) Jahn, D.; Vielstich, W. *J. Electrochem. Soc.* **1962**, *109*, 849.
- (267) Dus, B. *Pol. J. Chem.* **1979**, *53*, 1117.
- (268) Daum, P. H.; Enke, C. G. *Anal. Chem.* **1969**, *41*, 653.
- (269) Goldstein, E. L.; Van De Mark, M. R. *Electrochim. Acta* **1982**, *27*, 1079.
- (270) (a) Jordan, J. *Anal. Chem.* **1955**, *27*, 1708. (b) Jordan, J.; Javick, R. A. *Electrochim. Acta* **1962**, *6*, 23.
- (271) Huang, W.; McCreery, R. *J. Electroanal. Chem.* **1992**, *326*, 1.
- (272) Kawiak, J.; Jedral, T.; Galus, Z. *J. Electroanal. Chem.* **1983**, *145*, 163.
- (273) Kawiak, J.; Kulesza, P. J.; Galus, Z. *J. Electroanal. Chem.* **1987**, *226*, 305.
- (274) Kulesza, P.; Jedral, T.; Galus, Z. *J. Electroanal. Chem.* **1980**, *109*, 141.
- (275) Matsumoto, M.; Swaddle, T. W. Unpublished observations.

- (276) Stevens, N. P. C.; Rooney, M. B.; Bond, A. M.; Feldberg, S. W. *J. Phys. Chem. A* **2001**, *105*, 9085.
- (277) Brunschwig, B. S.; Creutz, C.; Macartney, D. H.; Sham, T. K.; Sutin, N. S. *Faraday Discuss. Chem. Soc.* **1982**, *74*, 113.
- (278) Jolley, W. H.; Stranks, D. R.; Swaddle, T. W. *Inorg. Chem.* **1990**, *29*, 1948.
- (279) Hupp, J. T.; Weaver, M. J. *Inorg. Chem.* **1983**, *22*, 2557.
- (280) Bernhard, P.; Sargeson, A. M. *Inorg. Chem.* **1987**, *26*, 4122.
- (281) Newton, M. D. In *Mechanistic Aspects of Inorganic Reactions*; Rorabacher, D. B., Endicott, J. F., Eds.; ACS Symposium Series 198; American Chemical Society: Washington, DC, 1982; p 255.
- (282) Friedman, H. L.; Newton, M. D. *Faraday Discuss. Chem. Soc.* **1982**, *74*, 73.
- (283) Tembe, B. L.; Friedman, H. L.; Newton, M. D. *J. Chem. Phys.* **1982**, *76*, 1490.
- (284) Logan, J.; Newton, M. D. *J. Chem. Phys.* **1983**, *78*, 4086.
- (285) Kuharski, R. A.; Bader, J. S.; Chandler, D.; Sprik, M.; Klein, M. L.; Impey, R. W. *J. Chem. Phys.* **1988**, *89*, 3248.
- (286) Anson, F. C. *Anal. Chem.* **1961**, *33*, 939.
- (287) Smith, B. B.; Halley, J. W. *J. Chem. Phys.* **1994**, *101*, 10915.
- (288) Hupp, J. T.; Weaver, M. J. *J. Phys. Chem.* **1984**, *88*, 1463.
- (289) Izutsu, K. *Electrochemistry in Nonaqueous Solutions*; Wiley-VCH: Weinheim, Germany, 2002.
- (290) Abbott, A. P. *Chem. Soc. Rev.* **1993**, *22*, 435.
- (291) Riddick, J. A.; Bunger, W. B.; Sakano, T. K. *Organic Solvents: Physical Properties and Methods of Purification*, 4th ed.; Wiley-Interscience: New York, 1986.
- (292) Petersen, R. A.; Evans, D. H. *J. Electroanal. Chem.* **1987**, *222*, 129.
- (293) Evans, D. H.; Gilicinski, A. G. *J. Phys. Chem.* **1992**, *96*, 2528.
- (294) Fawcett, W. R.; Fedurco, M.; Opallo, M. *J. Phys. Chem.* **1992**, *96*, 9959.
- (295) Winkler, K.; McKnight, N.; Fawcett, W. R. *J. Phys. Chem. B* **2000**, *104*, 3575.
- (296) Kapturkiewicz, A.; Behr, B. *J. Electroanal. Chem.* **1984**, *179*, 187.
- (297) Nielson, R. M.; McManis, G. E.; Weaver, M. J. *J. Phys. Chem.* **1989**, *93*, 4703.
- (298) Weaver, M. J.; McManis, G. E.; Jarzeba, W.; Barbara, P. F. *J. Phys. Chem.* **1990**, *94*, 1715.
- (299) Nielson, R. M.; Weaver, M. J. *J. Electroanal. Chem.* **1989**, *260*, 15.
- (300) Farmer, J. K.; Gennett, T.; Weaver, M. J. *J. Electroanal. Chem.* **1985**, *191*, 357.
- (301) Pyati, R.; Murray, R. W. *J. Am. Chem. Soc.* **1996**, *118*, 1743.
- (302) Williams, M. E.; Crooker, J. C.; Pyati, R.; Lyons, L. E.; Murray, R. W. *J. Am. Chem. Soc.* **1997**, *119*, 10249.
- (303) Lee, D.; Harper, A. S.; DeSimone, J. M.; Murray, R. W. *J. Am. Chem. Soc.* **2003**, *125*, 1096.
- (304) Miao, W.; Ding, Z.; Bard, A. J. *J. Phys. Chem. B* **2002**, *106*, 1392.
- (305) Swaddle, T. W. *Inorg. Chem.* **1990**, *29*, 5017.
- (306) Swaddle, T. W. *Can. J. Phys.* **1995**, *73*, 258.
- (307) Stranks, D. R. *Pure Appl. Chem.* **1974**, *38*, 303.
- (308) Baik, M.-H.; Crystal, J. B.; Friesner, R. A. *Inorg. Chem.* **2002**, *41*, 5926.
- (309) Jolley, W. H.; Stranks, D. R.; Swaddle, T. W. *Inorg. Chem.* **1990**, *29*, 385.
- (310) Swaddle, T. W. *J. Mol. Liq.* **1995**, *65/66*, 237.
- (311) Doine, H.; Swaddle, T. W. *Can. J. Chem.* **1988**, *66*, 2763.
- (312) Doine, H.; Swaddle, T. W. *Inorg. Chem.* **1991**, *30*, 1858.
- (313) Stebler, M.; Nielson, R. M.; Siems, W. F.; Hunt, J. P.; Dodgen, H. W.; Wherland, S. *Inorg. Chem.* **1988**, *27*, 2893.
- (314) Doine, H.; Yano, Y.; Swaddle, T. W. *Inorg. Chem.* **1989**, *28*, 2319.
- (315) Drago, R. S.; Ferris, D. C. *J. Phys. Chem.* **1995**, *99*, 6563.
- (316) Jolley, W. H.; Stranks, D. R.; Swaddle, T. W. *Inorg. Chem.* **1992**, *31*, 507.
- (317) Murguia, M. A.; Wherland, S. *Inorg. Chem.* **1991**, *30*, 139.
- (318) (a) Swaddle, T. W.; Mak, M. K. S. *Can. J. Chem.* **1983**, *61*, 473. (b) Swaddle, T. W. *Inorg. Chem.* **1983**, *22*, 2663.
- (319) Dolin, S. P.; Dogonadze, R. R.; German, E. D. *J. Chem. Soc., Faraday Trans. 1*, **1977**, *73*, 648.
- (320) Most theoretical discussions of the spin-state change effect on kinetics have considered the extremely slow $\text{Co}(\text{NH}_3)_6^{3+/2+}$ self-exchange but similar arguments apply to $\text{Co}(\text{en})_3^{3+/2+}$, for which k_{ex} is only about 100-fold larger: Hammershøi, A.; Geselowitz, D.; Taube, H. *Inorg. Chem.* **1984**, *23*, 979.
- (321) Buhks, E.; Bixon, M.; Jortner, J.; Navon, G. *Inorg. Chem.* **1979**, *18*, 2014.
- (322) Sutin, N. *Prog. Inorg. Chem.* **1983**, *30*, 441.
- (323) Newton, M. D. *J. Phys. Chem.* **1991**, *95*, 30.
- (324) Geselowitz, D. *Inorg. Chim. Acta* **1988**, *154*, 225.
- (325) Beattie, J. K. *Adv. Inorg. Chem.* **1988**, *32*, 2.
- (326) Larsson, S.; Ståhl, K.; Zerner, M. C. *Inorg. Chem.* **1986**, *25*, 3033.
- (327) Binstead, R. A.; Beattie, J. K. *Inorg. Chem.* **1986**, *25*, 1481.
- (328) Endicott, J. F.; Ramasami, T. *J. Am. Chem. Soc.* **1982**, *104*, 5252.
- (329) Endicott, J. F.; Ramasami, T.; Gaswick, D. C.; Tamilarasan, R.; Heeg, M. J.; Brubaker, G. R.; Pyke, S. C. *J. Am. Chem. Soc.* **1983**, *105*, 5301.
- (330) Ramasami, T.; Endicott, J. F. *Inorg. Chem.* **1984**, *23*, 3324.
- (331) Ramasami, T.; Endicott, J. F. *J. Am. Chem. Soc.* **1985**, *107*, 389.
- (332) Endicott, J. F.; Ramasami, T. *J. Phys. Chem.* **1986**, *90*, 3740.
- (333) Anderson, K.; Wherland, S. *Inorg. Chem.* **1991**, *30*, 624.
- (334) Anderson, K. A.; Kirchner, K.; Dodgen, H. W.; Hunt, J. P.; Wherland, S. *Inorg. Chem.* **1992**, *31*, 2605.
- (335) Fawcett, W. R.; Markušová, K. *Can. J. Chem.* **1983**, *61*, 2821.
- (336) Sahami, S.; Weaver, M. J. *J. Electroanal. Chem.* **1981**, *124*, 35.
- (337) Conway, B. E.; Currie, J. C. *J. Electrochem. Soc.* **1978**, *125*, 257.
- (338) Nandi, N.; Bhattacharyya, K.; Bagchi, B. *Chem. Rev.* **2000**, *100*, 2013.
- (339) Bhattacharyya, S. M.; Wang, Z.-G.; Zewail, A. H. *J. Phys. Chem. B* **2003**, *107*, 13218.
- (340) Sen, P.; Mukherjee, S.; Dutta, P.; Halder, A.; Mandal, D.; Banerjee, R.; Roy, S.; Bhattacharyya, K. *J. Phys. Chem. B* **2003**, *107*, 14563.
- (341) Pal, S. K.; Zewail, A. H. *Chem. Rev.* **2004**, *104*, 2099.
- (342) Meier, M.; van Eldik, R. *Inorg. Chim. Acta* **1996**, *242*, 185.
- (343) Khoshitariya, D. E.; Wei, J.; Liu, H.; Yue, H.; Waldeck, D. H. *J. Am. Chem. Soc.* **2003**, *125*, 7704.
- (344) (a) Beece, D.; Eisenstein, L.; Frauenfelder, H.; Good, D.; Marden, H. C.; Reinisch, L.; Reynolds, A. H.; Sorensen, L. B.; Yue, Y. T. *Biochemistry* **1980**, *19*, 5147. (b) Bashkin, J. S.; McLendon, G.; Mukamel, S.; Marohn, J. *J. Phys. Chem.* **1990**, *94*, 4757. (c) Ansari, A.; Jones, C. M.; Henry, E. R.; Hofrichter, J.; Eaton, W. *Biochemistry* **1994**, *33*, 5128. (d) Shibata, Y.; Takahashi, H.; Kaneko, R.; Kurita, A.; Kushida, T. *Biochemistry* **1999**, *38*, 1802. (e) Sagnella, D. E.; Straub, J. E.; Thirumalai, D. *J. Chem. Phys.* **2000**, *113*, 7702. (f) Rector, K. D.; Jiang, J.; Berg, M. A.; Fayer, M. D. *J. Phys. Chem. B* **2001**, *105*, 1081.
- (345) Sun, J.; Wishart, J. F.; van Eldik, R.; Shalders, R. D.; Swaddle, T. W. *J. Am. Chem. Soc.* **1995**, *117*, 2600.
- (346) Fuchs, A. H.; Ghelfenstein, M.; Szwarc, H. *J. Chem. Eng. Data* **1980**, *25*, 206.
- (347) Lever, A. B. P.; Milaeva, E. R.; Speier, G. In *Phthalocyanines: Properties and Applications*; Leznoff, C. C., Lever, A. B. P., Eds.; VCH: New York, 1993; Vol. 3, Chapter 1.
- (348) Nevin, W. A.; Hempstead, M. R.; Liu, W.; Leznoff, C. C.; Lever, A. B. P. *Inorg. Chem.* **1987**, *26*, 570.

CR030727G